Screening Tests of Composites for use in Tidal Energy Devices

Anderson Ogg

A thesis

submitted in partial fulfillment of the

requirements for the degree of

Master of Science in Engineering

University of Washington

2011

Program Authorized to Offer Degree:

Mechanical Engineering

University of Washington

Graduate School

This is to certify that I have examined this copy of a master's thesis by

Anderson Ogg

and have found that it is complete and satisfactory in all respects,
and that any and all revisions required by the final
examining committee have been made.

Committee Members:

_____

Mark Tuttle

_____

Brian Fabien

_____

Brian Polagye

Date:_____

University of Washington

Abstract

Screening Tests of Composites for use in Tidal Energy Devices

Anderson Ogg

Chair of the Supervisory Committee:
Professor Mark Tuttle
Mechanical Engineering

Four different composite material systems are subjected to nine months of in situ exposure at a potential tidal energy site. These four systems are fiberglass/epoxy, carbon fiber/epoxy, fiberglass/vinylester, and carbon fiber pre impregnated with epoxy. The loss of shear modulus due to this exposure is observed and these values are compared to unexposed samples of these same material systems. The four systems have a loss of shear modulus of 66%, 26%, 13% and 7% respectively. In addition, three panels of the fiberglass/vinylester system are exposed to accelerated testing in the laboratory and the change in shear modulus due to this exposure is also calculated and compared. These panels lose 38%, 33% and 33% due to 30 days of exposure at 30℃, 40° C and 50℃ respectively. It is concluded that tidal energy device developers interested in using composites should focus on fiberglass/vinylester and pre impregnated systems. It is also concluded that changes in the accelerated testing procedures are required to better mimic the nine months of in situ exposure.

TABLE OF CONTENTS

Table of Tables

Table of Figures

Acknowledgments

I would like to thank my wife for her seemingly boundless support and encouragement. I would also like to thank Bill Kuykendall, the UWME Department's lab technician for all of his help, especially that which was given on short notice. I also greatly appreciate the guidance of my committee and teachers, and the frequent and willing help of my fellow graduate students.

Dedication

To Mariette and Oakland

1 Introduction

1.1 Purpose

The purpose of this study is to explore the use of composite materials that will likely be used in the development of tidal energy devices. The differences in shear strength and stiffness losses experienced by these different composites in the marine environment are examined. The loss of stiffness and strength experienced by the different grades of composites are compared so that device developers can have more information with regards to cost and quality tradeoffs provided by the different composite systems. This study is characterized as a screening test because a few different composite systems are examined and only one type of test was completed. It is expected that the results from this screening test would be used for more in-depth work in the future.

Additionally, this study seeks to determine whether accelerated exposure performed in the laboratory environment can accurately reflect the in situ conditions experienced by one of the composite systems. If accelerated exposure can be used to test composite systems, than device developers can more easily run their own tests on their own composite systems and gain a better understanding of how these systems might perform over the long-term.

1.2 Background

There are many ways to extract energy from the movement of water. The most common method currently in use to produce electricity from the flow of water is with conventional hydroelectric dams. With this method rivers are dammed to create a head pressure and then that water is control released to create electricity as needed. The second most common method is run-of-the-river systems where the head pressure created by the natural elevation change of a river is used to power a hydroelectric device. Some of the other methods currently being developed are wave energy devices, tidal energy devices (including barrage and in-stream), ocean current devices and ocean thermal energy conversion devices [1].

As the search for ways to produce electricity from sustainable, renewable, environmentally low impact and carbon dioxide neutral sources continues, one of the major challenges is to find sources that can provide the same type of base load power currently provided by conventional and nuclear power plants. Tidal energy devices offer the possibility of supplying a highly predictable amount of electricity not susceptible to the disruptions faced by other technologies such as solar or wind. The height and time of the ocean tides and therefore the velocity and time of the currents produced by those tides can be accurately predicted years in advance [2]. If a utility knows how much electricity is produced by an array of tidal energy devices at a given water velocity, than the utility can broadly predict how much electricity will be produced years into the future.

There is currently a large variation in the way hydrokinetic devices extract energy from the tides [3]. Some devices use a low solidity propeller similar to that seen in a modern wind turbine, while others use a high solidity blade. Some designs use a "cross flow" type design such as might be seen in a vertical axis wind turbine. Some involve mass based gravity anchors while others may use pylons or positive buoyancy and multiple anchor chains. Some have drivetrains that can be removed for servicing, while others are designed to be lifted entirely out of the water for maintenance. For most devices, lift generated over rotor blades results in rotational motion that is than converted into usable electricity via a generator. Because of the limited water depth at prospective tidal energy sites (e.g., <80 m), relative to the depth of the atmospheric boundary layer, these rotor blades will be smaller than wind turbine blades and will rotate at lower speeds to keep blade tip velocities below cavitation onset [4]. These devices will still be large though, some designs have used blades as large as ten meters in diameter. Because of their large size, strength and weight will be important factors to consider so that structural failure is prevented while keeping the loads required to be supported by the drivetrain to a minimum. The heavier these blades are for their size, in general, the less efficient they will be. Figure 1-1 shows some of the tidal energy device designs currently being developed and deployed.

Clockwise from Top Left – Verdent Power's RITE Turbine, Open Hydro's Open-Centre Turbine, Ocean Renewable Power Company's TidGen Power System, and Marine Current Turbine's SeaGen.
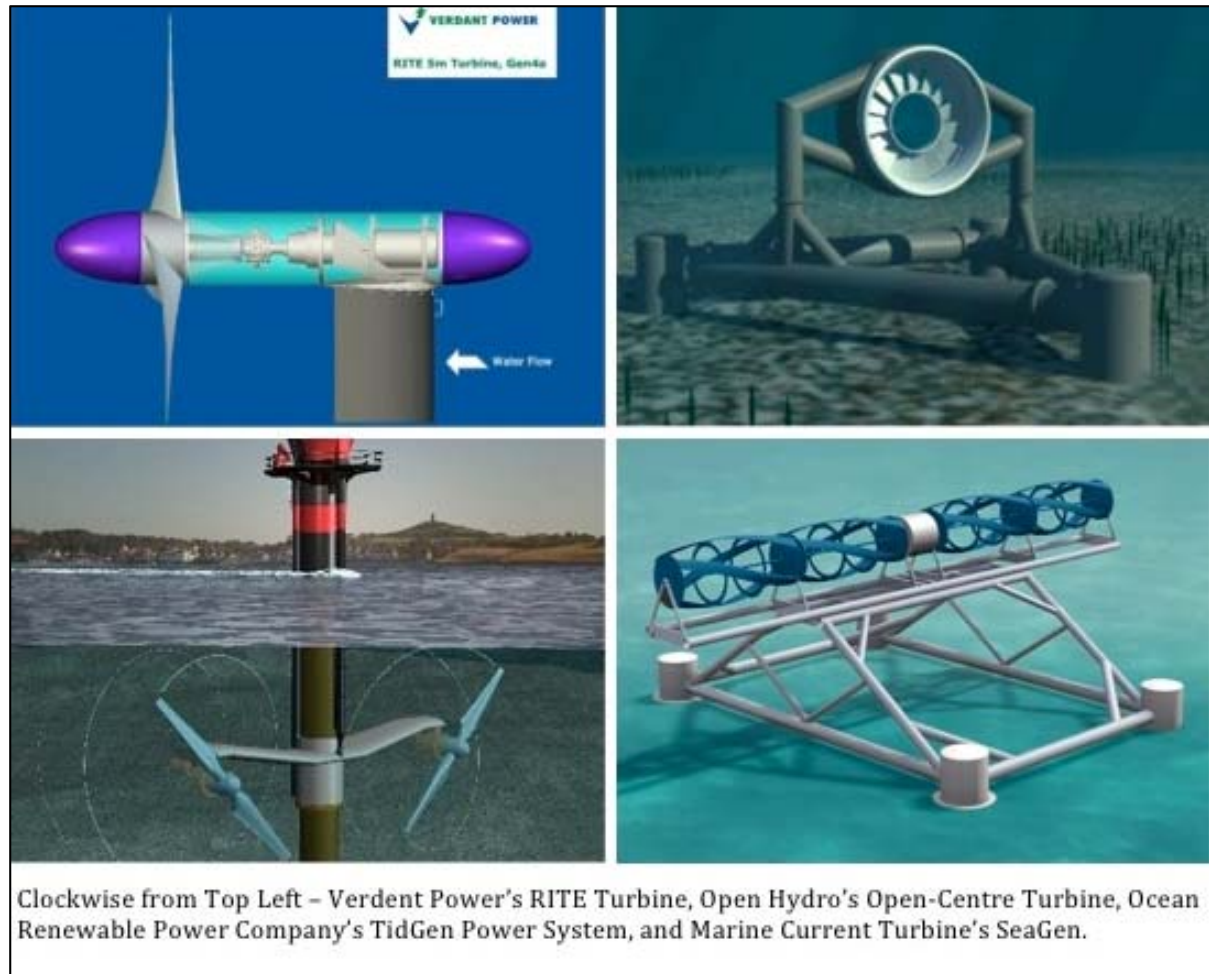
Figure 1-1: Four Different Turbine Designs Currently Being Developed

These tidal energy devices will also typically operate in fairly extreme environments because they will almost always be in a highly corrosive marine environment and subject to continually variable water velocities in the range from 0 to 2.5 meters per second or more [**4**]. Some characteristics of these high flow marine environments include high sediment transfer, scoured ocean bottoms, narrow channels where other marine traffic will be operating and a large variation in the amount of marine life present. Some of these devices will operate below the photic zone, while others may not. Most likely, many of these devices will operate in high latitudes because this is generally where the largest tidal ranges occur, some of these areas my be remote and difficult to access when maintenance is required.

With their typically high strength to weight ratios, high corrosion resistance, potential for decreased maintenance and ability to be formed into complex shapes, fiber reinforced polymer composite systems will likely be desirable materials to be considered by hydrokinetic turbine developers. Marine Current Turbines, the Ocean Renewable Power Company and OpenHydro have all incorporated fiber reinforced polymer composites into their device designs. Composites may offer the additional advantage of not needing the same level of coatings and preservation that many metals would need; this could make them even lighter and more easily maintainable.

1.3   Problem Statement

There have been studies conducted in the past that examine the effects of salt water on composites but there is a lack of information in the public domain regarding how composites may react in the high flow, extreme environment experienced by a tidal energy device. Because of this lack of information, device developers are not able to evaluate the tradeoffs associated with using lower quality, cheaper composites or higher quality, more expensive composites.

The results of this study provide device developers in the tidal energy industry with information regarding how various fiber reinforced polymer composites will perform in the high flow marine environment experienced by hydrokinetic turbines.

2   Operational Definition of Terms

Absorption – The movement of bulk (as apposed to molecular) water across the interface between a dry composite panel and the surrounding water it is submerged in. This type of moisture has little affect on the material properties of the composite.

As-Produced – This describes the panels that were made but were not subjected to exposure before they were tested.

Autoclave – Equipment that allows for pressure, temperature and vacuum to be applied to a material system so that cure can be achieved. This is typically necessary for pre impregnated material systems.

Base Load Power – This is the power that is typically required by a utility to meet the demands of customers at some minimal level. As power demands exceed this base load, other forms of power generation must be brought online, such as gas generators.

Diffusion – The movement of water on a molecular level across the moisture gradient between a composite panel and the surrounding water it is submerged in. This type of moisture has an affect on the strength and stiffness properties of composite because of the changes at the molecular level.

Fiber Reinforced Polymer – This is the general description for plastic composite material systems. The polymer refers to the matrix that is used to provide structure for the fibers. Polymers are broadly classified as either thermoplastics or thermosets. A thermoplastic polymer is one that can be melted and reformed, whereas a thermoset polymer cannot. Fiber-reinforced polymers based on thermoplastics or thermosets are commercially available. Some common fiber materials are aramid, glass and carbon fibers. There are many different names used in literature to describe this class of composites.

Hydrokinetic – Harnessing of the energy in a moving body of water.

Marine Environment – The physical environment associated with potential tidal energy sites.

Matrix – The general name for the material in which a reinforcing material(s) is embedded to form a composite material.

Photic Zone – The depth in a body of water where enough light reaches such that photosynthesis can occur.

Pre-Preg – Fibers which are pre impregnated with an epoxy that is kept in a "B-stage" by being kept in a freezer and which only fully cure once they have been brought to an elevated temperature. This curing process is typically completed in an autoclave.

Sea Spider –The platform developed by the Northwest National Marine Renewable Energy Center to characterize the physical and biological characteristics of tidal energy sites. The platform with the composite panels is deployed on the floor of Puget Sound in northern Admiralty Inlet at the site proposed for the installation of an array of tidal energy devices.

Solidity – The ratio of the area occluded by the blades of a turbine to the area that is not occluded when viewing the swept area created by the rotating blades from straight on.

Tidal Energy Device – A device that converts the kinetic energy in tidal currents to a form of usable energy such as electricity.

Tow – An untwisted bundle of continuous fibers, typically used in reference to carbon and glass fibers.

Wet Layup – The process of placing plies of woven fiber down and brushing each ply with a coat of liquid matrix and stacking all plies as desired before the matrix begins to gel or harden. Unlike Pre-Preg, the curing of the composite is usually completed at room temperature. Also this process can be completed with or without a vacuum being applied. If a vacuum is applied the finished product generally has fewer defects, such as voids, and a higher fiber volume fraction.

3   Theoretical Rationale

3.1   Material Selection

Two main criteria were used to select the material systems used in this study; the body of knowledge currently in the public domain and the likelihood of tidal device developers being interested in using the materials.

The first step driving the material selection process was determining what area of the device to focus on. The possible categories included the supporting structure/gravity bases, the rotating components such as the blades, the various fasteners and the mechanical components such as bearings, shafts and axels. Gravity bases and supporting structure can be constructed from a combination of, steel, cement, and low-cost aggregate or lead. The rotating components can be made from bronze, stainless steels, aluminum, or fiber reinforced plastics. Fastener materials include marine-grade stainless steel (e.g., 316) and titanium. Bearings may consist of phenolics, metals, nylon and PTFE coated materials. Shafts and axles can be fabricated from steel or stainless steel, but can also be made from fiber reinforced composites or a combination of the two. From studying the literature available in the public domain, it appeared that fiber reinforced plastic composites had the least amount of research conducted on how they would perform in the marine environment (see section 4). Additionally, because most tidal devices undergoing prototype testing incorporate composite blades, a decision was made to focus this study on composites. Focusing on composites offered the added advantage that the results may be useful for those that are currently designing composite ship propellers that can be engineered to change shape at different speeds to optimize their efficiency [5,6]. This same technique can possibly also be used in tidal energy devices, even though their rotational speeds are much lower.

After deciding to focus on composites, the specific material systems were chosen. Due to the volume of material required for by ASTM D3518 standard and space constraints on the Sea Spider, it was only possible to examine a limited number of material systems. It was determined that because of the rather large coupon sizes needed that a total of eight panels could be mounted on the Sea Spider. This limited number of panels required that a tradeoff be made between the different types of systems tested and the amount of time each panel spent immersed at the project site. After some deliberation, it was determined that it would be more important to examine the effects of the marine environment over a longer period of time than across a large number of different systems. In light of this it was decided that a total of four different material systems would be tested and each system would have two panels on the sea spider. The first of

these two panels would be removed at nine months, while the second set would be removed at 18 months.

It was decided that the materials chosen should at a minimum include a higher quality autoclaved-cure aerospace grade material, to represent the expensive high-performance end of the spectrum, and a wet-lay-up marine pleasure craft grade material to represent the less expensive end of the spectrum. This left two other material systems which needed to be chosen and it was concluded that these two systems should be commonly available and should possibly be used in other similar applications such as wind turbines. Given all these considerations, it was decided that the highest grade material would be a carbon fiber pre impregnated with epoxy. A Hexel product called HexPly M46JB was chosen. This product was typical of the aerospace grade products in this class because it needed to be stored in a freezer until used and must be cured in an autoclave. From this point forward in this study, these are referred to as "Pre-Preg". For the cheaper material, a fiberglass vinylester wet layup system was used. This material system is often used in the pleasure boat industry for smaller craft. This is a commonly available system and is workable into complex shapes with a minimum amount of equipment. The fiberglass and vinylester were sourced from a local company, Fiberlay. This system was referred to as Glass Fiber Reinforced Vinlyester (GFRV).

For the two other systems it was decided to again use two commonly available systems. The first system chosen was a Glass Fiber Reinforced Epoxy (GFRE) and the second was a Carbon Fiber Reinforced Epoxy (CFRE). Both of these systems were produced using the wet layup process and cured at room temperature because this is likely how they would be used in the construction of a tidal energy device. The same epoxy was used for both systems so that a possible comparison could be made between systems with regards to how the fiber-matrix interface affected the shear properties. These systems were also chosen because they were considered to be a higher grade than vinylester based systems, yet did not require the complicated autoclave equipment required by pre-pregs. There is a likelihood that for reasons of overall system efficiency, the rotating

components on tidal energy devices will be large, for example the blades on Marine Current Turbines' SeaGen are designed to be between seven and ten meters [**7**]. Autoclaves of this size are not common, making it likely that composite fabrication will involve room temperature cures. Figure 3-1 shows the four different systems chosen.
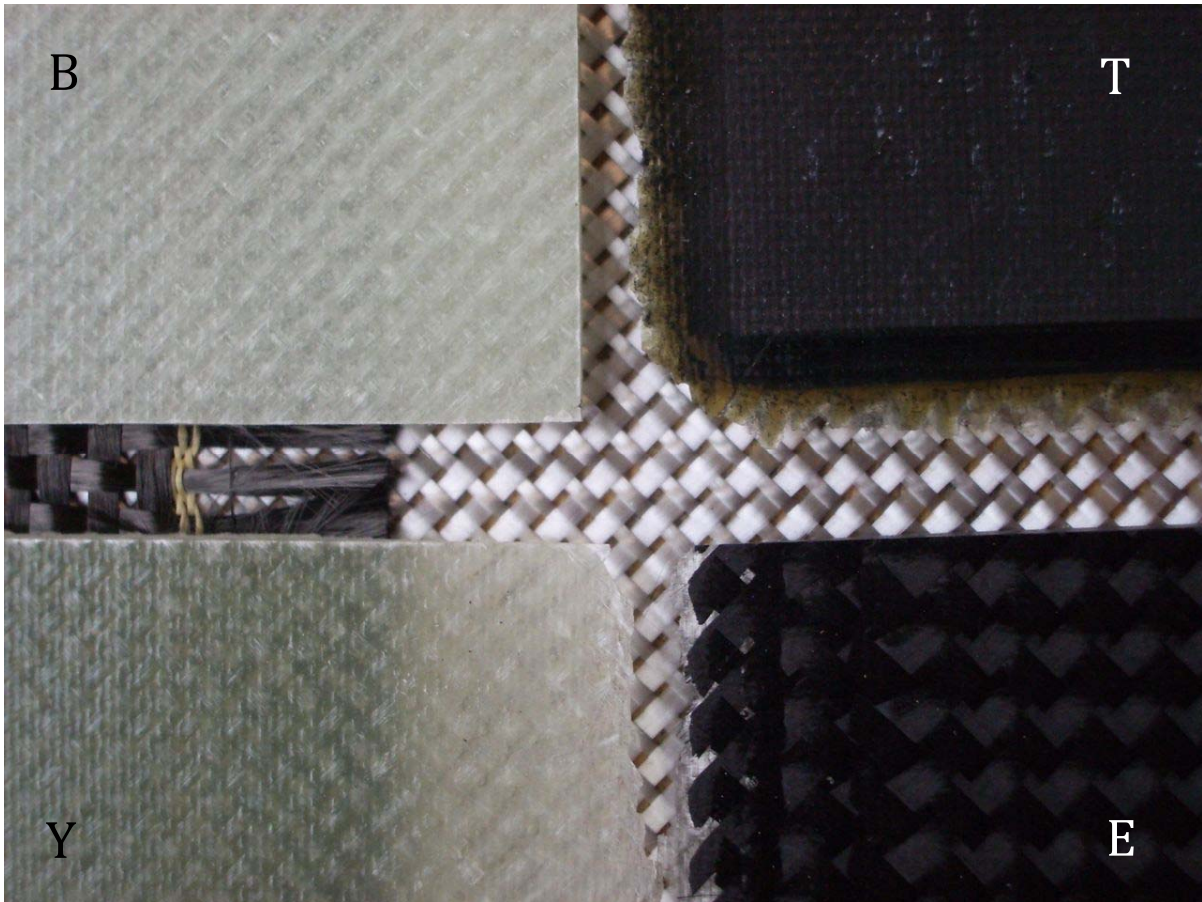
Figure 3-1: All Four Types of Systems Tested. Clockwise from the Upper Left; Panel B - Fiberglass/Epoxy (GFRE), Panel T - Pre-Preg, Panel E - Carbon Fiber/Epoxy (CFRE), Panel Y - Fiberglass/Vinylester (GFRV).

There was also interest in determining if the any degradation experienced by the material systems in-situ over long times could be simulated in the lab under accelerated conditions. If accelerated tests can accurately predict long-term degradation, than device developers could test materials that they are interested in on an accelerated timeline and gain an understanding how the material will perform over longer times. It is likely that these tidal energy devices will need to be kept operational for 20 years or

more to be economical, so it will be important to know how materials will perform over this long period.

There have been different ways accelerated testing has been studied for composite materials in the past [**8**,**9**,**10**,**11**,**12**,**13**,**14**]. Given the time and budget available for testing, only one material system was able to be tested with accelerated exposure. The GFRV system was chosen because it was the least costly of the systems and previous studies suggested that it would exhibit the most dramatic changes due to exposure. The accelerated exposure was completed by placing three panels of the GFRV in heated water baths for a 30-day exposure. The water used in the baths was an artificial salt water created in the lab to be similar to the water in Puget Sound. Each of the panels was held at a different temperature for the 30 day period. After the 30 days the panels were tested in the same manner as the as-produced panels and the panels retrieved from the Puget Sound.

3.2   Method

Both qualitative and quantitative data collection techniques were used in this study. Quantitative techniques included measuring the strain and loads applied to the various composite systems and using these to calculate the shear and tensile moduli and stresses experienced by these composites. Other quantitative techniques included dimensional analysis of all specimens and measuring the weight gain experienced by the different systems.

The qualitative techniques employed in this study included comparing the microstructure of the different composites using optical microscopy, comparing the amount of biofouling experienced by the different systems and comparing the failure modes observed in the different systems during testing. To a lesser extent the noises produced by each specimen during testing were also observed, particularly the noises leading up to failure of the composite during destructive shear tests.

The in-plane shear response was used to characterize the changes to the composites with immersion in the marine environment because it provided a reasonable proxy for

the general strength properties of the composites. It was also a matrix-dominated property and the long-term loss of strength observed in these composites was expected to be principally caused by changes in the matrix, rather than to changes in the fibers. For the purposes of material screening, the in-plane shear response also provided a relatively inexpensive and quick way to classify how the different material systems perform [15]. The ASTM method D3518 Standard Test Method for In-Plane Shear Response of Polymer Matrix Composite Materials by Tensile Test of a ±45° Laminate [16], was used as a guide during testing and was followed closely when feasible. The shear response of each system was measured in the as-produced condition and an exposed condition. These measurements were then compared to each other. Although some comparisons were made between different material systems, most of the analysis focused on the changes observed within each material system.

To calculate the shear modulus of the different specimens, the shear strain and shear stress were calculated in each specimen while they were loaded to failure. These values were plotted against each other so that the slope of the linear portion of the curve could be used to determine the shear modulus. The shear stress was given by

$$\tau_{12} = \frac{P}{2A} \qquad \textbf{Equation 3–1}$$

where τ_{12} was the shear stress in the 1-2 coordinate system (defined as the fiber direction), P was the load applied and A was the initial cross sectional area of the specimen where the strain gage was located. Figure 3-2: Fiber Orientation shows the coordinate system used.
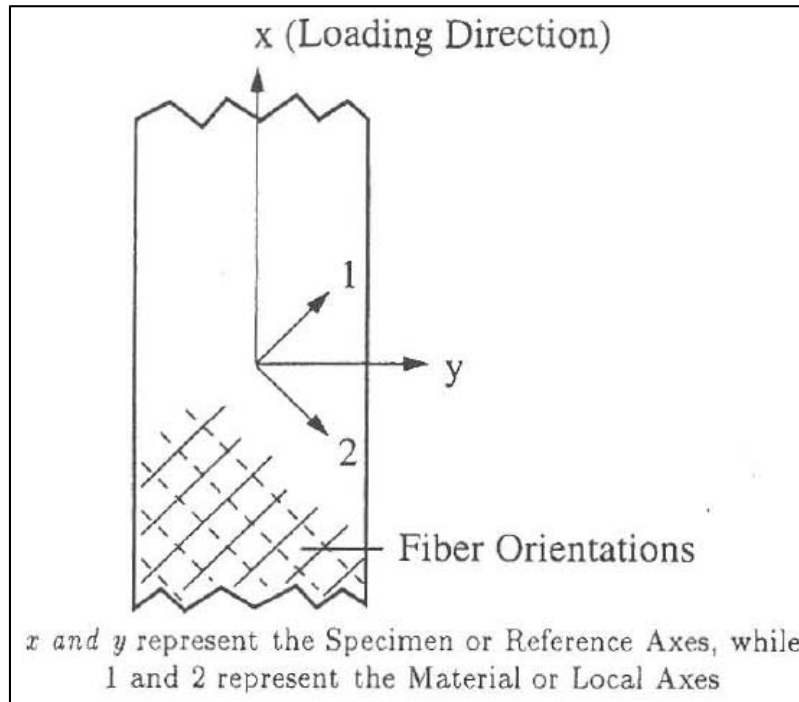
Figure 3-2: Fiber Orientation [16**]**

The shear strain in the fiber direction was given as

$$\gamma_{12} = \varepsilon_x - \varepsilon_y \qquad\qquad \textbf{Equation 3–2}$$

where γ_{12} was the shear strain in the fiber plane ε_x was the strain in the axial direction and ε_y was the strain in the longitudinal or transverse directions. The basis for Equation 3–1 and Equation 3–2 was provided by the ASTM 3518 standard [**16**].

The results of this screening test can be used to complete a more in-depth analysis in the future where additional tests can be used to better characterize the properties of a selected composite material system. Some of these potential tests are described in the following ASTM standards;

- D3039 Tensile Properties of Polymer Matrix Composite Material – Would provide a good indication of the changes in the properties due to the fiber in the 0° orientation and the changes in the matrix in the 90° direction.

- D5379 Shear Properties of Composite Materials by the V-Notched Beam Method – Would provide another indication of the pure shear properties of the composites which may be comparable to that determined by D3518.

- D3410 Compressive Properties of Polymer Matrix Composite Materials with Unsupported Gage Section by Shear Loading

- E1640 Assignment of the Glass Transition Temperature By Dynamic Mechanical Analysis

- E1356 Assignment of the Glass Transition Temperatures by Differential Scanning Calorimetry. – The glass transition tests could provide useful information about the changes in the molecular structure of the matrices of the composites.

4   Literature Review

There have been a number of studies completed on how fiber reinforced polymer composites are affected by environmental effects such as moisture absorption, but very little scientific literature exists for how these composites actually perform in a real life application. George S. Springer and his colleagues [8] wrote much of the early literature that focused on the effects of environmental exposure on the physical properties of composites. Springer compiled much of the literature published between the late 1960s and mid 1980s in book titled "Environmental Effects on Composite Materials." This book is in three volumes and covers the literature in which the changes in physical, chemical and electrical properties of composites were examined due to environmental effects such as moisture absorption, elevated temperatures and load cycling.

Moisture absorption in composites has been determined to initially follow Fick's law of diffusion for most high humidity and immersed environments. Fick's law of diffusion is a method to characterize the moisture uptake behavior of a material. It is calculated by

$$M = \left[1 - \frac{8}{\pi^2} \exp\left(-\pi^2 \frac{Dt}{h^2}\right)\right] M_\infty \qquad \text{\textbf{Equation 4–1 [9]}}$$

where M is the moisture content at time t, h is the thickness, D is the diffusion coefficient for a given material and M_∞ is the maximum moisture content of the material.

Loos and Springer [**17**] exposed three different types of fiberglass reinforced polyester composites to high humidity air, saltwater and distilled water at different temperatures and determined that;

- Fick's law could be used to approximate the weight gain of these composites until a maximum moisture content was reached.

- The maximum moisture content depended heavily upon the type of material and exposure but not the different exposure temperatures used in these tests. The maximum weight gain experienced by the three composite systems varied from about 2.5% to 4% when placed in distilled water and 0.25% to 3% when placed in salt water.

- The apparent diffusivity was heavily dependent on the type of material, the environment and the temperature. The rate at which the three systems reached their maximum moisture content varied from 4 days to 200 days depending on these different factors.

- At some point, the maximum moisture absorption and diffusivity of the composites no longer matched that which was predicted by Fick's law. In some cases the composite systems actually begin to lose weight, which was likely caused by matrix material beginning to deteriorate and be lost after a certain amount of time.

The absorption of water has been shown to have negative affects on the strengths and moduli of composite systems. Springer, Sanders and Tung [**18**] exposed a glass fiber reinforced vinylester composite to saturated salt water for six months at 23°C and 93°C.

They performed tensile and three point bending tests to determine changes in the strength and moduli of the tension and shear values due to this exposure. For the specimens at 23℃ it was observed that the material lost about 25% of its tensile strength, 10% of its shear strength, 20% of its tensile modulus and 10% of its shear modulus after six months exposure. For the specimens at 93℃ it was observed that the material lost about 50% of its tensile strength, 30% of its shear strength, 20% of its tensile modulus and 10% of its shear modulus after six months exposure. It was also observed that the specimens gained approximately 1% in weight at both temperatures, but that it took about 120 days for the specimens in the 23℃ saltwater to reach this while it only required about 10 days for the specimens in the 93℃ saltwater.

Kootsookos and Mouritz [9] exposed glass and carbon fiber reinforced vinylester and polyester composites to 30℃ saltwater for two years and monitored their weight gain, flexural modulus and inter-laminar fracture toughness at certain time intervals. They found that the polyester based composites initially gained between 0.3% and 0.5% weight but after about 15 days the weights began to decrease and after about a year and a half they started to drop below their initial values. By comparison the vinylester based composites gained approximately 0.5% weight but this was achieved over a longer period of time and the weight gain leveled off after about a year and never decreased in the two years. They also observed that the fiberglass based systems generally absorbed more water than the carbon fiber based systems. The researchers calculated between a 10% and 20% decrease in flexural modulus of the polyester composites and a 30% decrease for the vinylester composites and in both cases the carbon fiber and fiberglass reinforced systems performed about the same. They note that the reasons for the vinylester composites performing more poorly than the polyester based systems were not clear, especially since the vinylester was more chemically stable in saltwater than the polyester, which they determined via leaching experiments. The researchers found no correlation between fracture toughness and immersion time in any of the composite systems.

Davies, Mazéas and Casari [10] conducted an extensive study in which the effects of 18 months of immersion in distilled and saltwater were monitored in four composite systems. All the systems used the same fiberglass reinforcement but had orthophthalic polyester, isophthalic polyester, vinylester and epoxy matrices. The composites were immersed in three different conditions, 20°C saltwater, 50°C saltwater, and 50°C distilled water. The weight gain experienced by the different systems was monitored over the 18 months and various tests were conducted, including the ASTM D3518 in-plane shear response test. The researchers found that the vinylester based system gained about 0.5% weight in 20°C saltwater, and 0.6% weight in 50°C saltwater, and distilled water, while the epoxy based system gained about 2.5% and 3% in these same conditions. The researchers also found that the vinylester based systems lost about 12% of their shear modulus in 20°C saltwater 16% in 50°C saltwater and 18% in 50°C distilled water, while the epoxy based systems lost about 8%, 20% and 22% in these respective conditions.

Miller [11] completed an extensive study that focused on a particular fiberglass and polyester composite system and one of the tests he used was also the ASTM D3518 method. The batch of specimens that were kept in room temperature (~25°C) tap water for 15 months showed a weight gain of approximately 2% and a loss in shear modulus of approximately 11%.

Narasimha Murthy, et al. [12] completed a number of tests on four different composite systems that included, fiberglass reinforced vinylester and epoxy and carbon fiber reinforced vinylester and epoxy. The composites were submerged in artificial seawater that was kept at room temperature. Specimens were removed from the water at various intervals and tested, with the maximum length of submersion being 450 days. The composites were tested for weight gain, flexural strength, interlaminar shear strength and tensile strength. The authors concluded that:

> "The flexural strength and ultimate tensile strength (UTS) dropped by about 35% and 27% for glass/epoxy, 22% and 15% for glass/vinyl ester, 48% and 34% for carbon/epoxy 28%, and 21% carbon/vinyl ester

composites respectively. The water uptake behavior of epoxy-based composites was inferior to that of the vinyl system."

The authors found that the fiberglass and carbon fiber reinforced vinylester systems showed a weight gain of about 0.4% and 0.5% respectively whereas the fiberglass and carbon fiber reinforced epoxy systems gained about 0.7% and 0.9% respectively. All the systems appeared to reach their maximum weight gain after about 250 days, at which point they plateaued. The researchers used scanning electron microscopy to determine that the moisture absorption caused debonding in the fiber/matrix interface, which weakened the systems.

While extensive research has been conducted on how prepreg composites perform in aerospace [13], it was difficult to find studies in which prepreg laminate systems were submerged in seawater. A possible explanation for this is that most researchers assume that prepegs will not be used for marine applications in the near future because of cost. Rege and Lakkand [14] studied carbon and fiberglass reinforced epoxy specimens made using the filament winding process, which is another high quality way of manufacturing composite systems. In this study the researchers exposed the composite systems to distilled water and saltwater for 120 hours at 40, 60 and 80 degrees Celsius. After exposure the specimens were tested for weight gain and compressive, flexural and interlaminar shear strengths. The fiberglass reinforced specimens experienced approximately 0.3%, 0.4% and 0.7% weight gain in their respective 40, 60 and 80 degree saltwater baths, while the carbon fiber reinforced systems experienced approximately 0.3%, 0.5% and 0.7% weight gain with the same exposure. These same fiberglass reinforced specimens lost approximately 49%, 55% and 64% of their flexural strength while the carbon fiber specimens lost approximately 28%, 41% and 54% of theirs. This study showed that even short-term exposure to moisture under elevated temperatures could have large effects on the properties of composites. The authors also conclude that the losses due to exposure in saltwater were much higher than those due to distilled water and that results from tests done in distilled water could not be used for composites that were going to be used in saltwater.

Even though there has probably been a large amount of research performed by various private companies and the world's navies that has not been made publicly available, there is still evidence that the US Navy is still interested in learning how composites will perform in the marine environment. In a recent contracted study that was completed for the Office of Naval Research [**19**], researchers examined different ways in which composites were affected by exposure to the marine environment. The study included many applied projects, but also some more basic research that, for example, examined the degradation of epoxy and vinylester matrices both with and without carbon fiber reinforcements. This research in particular determined that the vinylester matrix absorbed more water when there was carbon fiber reinforcement present, but the opposite results were true for the epoxy matrix.

The review of the literature verified that there was a need for research to be conducted into how composite materials performed in the actual marine environment and not just in the lab.

Based on the literature review, an expected range of values were created that the author expected find as the result of nine months of in situ exposure. Table 4-1 shows these expected values for the materials tested in this study.

Table 4-1: Expected Property Changes Determined from the Literature Review

System	Expected Loss in Shear Modulus	Expected Weight Gain
GFRE	15%	2.50%
CFRE	unsure	0.60%
GFRV	20%	0.50%
Pre-Preg	Least	Least

There was not enough literature found on the change in shear modulus in Carbon/Epoxy systems to make an educated estimate of the expected loss for the CFRE system. There was also not enough literature found to develop values for the changes in the Pre-Preg system, but it was decided that because the Pre-Preg had the highest quality manufacturing process, it would experience the lowest change.

5 Method For In Situ Experiment and As-produced Panels

5.1 Procedure

5.1.1 Panel Manufacturing

The panels were manufactured by the author at the University of Washington throughout 2011. All wet layup material systems were manufactured with a vacuum bagging system and the prepreg panels were manufactured with an autoclave. Table 5-1 gives an overview of all panel information including dates of manufacture.

Table 5-1: Panel Production and Exposure Information

Material System	Panel Letter	Date Produced	Exposure Type	Exposure Start	Exposure End	Date Tested
GFRE	B	9-Apr-10	9 Months	6-May-10	10-Feb-11**	19-Feb-11
	C	12-Apr-10	18 Months	6-May-10	Ongoing	N/A
	D	14-Apr-10	None	N/A	N/A	28-Jan-11
CFRE	E	16-Apr-10	9 Months	6-May-10	10-Feb-11**	19-Feb-11
	F	19-Apr-10	18 Months	6-May-10	Ongoing	N/A
	G	20-Apr-10	None	N/A	N/A	28-Jan-11
Pre Preg	T	9-Aug-10	None	N/A	N/A	7-Feb-11
	U	9-Aug-10	9 Months	17-Aug-10	10-Feb-11**	18-Feb-11
	V	9-Aug-10	18 Months	17-Aug-10	Ongoing	N/A
GFRV	M	3-May-10	9 Months	6-May-10	10-Feb-11**	19-Feb-11
	N	3-May-10	18 Months	6-May-10	Ongoing	N/A
	Q	29-Jun-10	30 Days @ 30°C	7-Jan-11	6-Feb-11	7-Feb-11
	R	29-Jun-10	30 Days @ 40°C	10-Jan-11	9-Feb-11	10-Feb-11
	X	1-Feb-11	30 Days @ 50°C	14-Feb-11	16-Mar-11	17-Mar-11
	Y	1-Feb-11	None	N/A	N/A	7-Feb-11

** Although these panels were removed from the Puget Sound on 10 February, they were kept at ambient temperture in seawater for transport back to the lab. They were not removed from the seawater until 18 February.

The GFRE panels made from the epoxy and fiberglass system used a Fiberlay (www.fiberlay.com) 6oz plain weave e-glass fiberglass (part # 152640), which had a sizing of silane type 3733. This fiberglass was 0.21mm thick and had a thread count of 72 per 100 cm. The epoxy was Fiberlay's Orca 1300 (part # 100120210) cured with their Orca 4:1 medium curing agent (part # 100220108). In accordance with ASTM D3518 these panels used a stacking sequence of [45/-45]3s for a total thickness of 12

plies. Since these were plainly woven plies, symmetry occurred naturally when using a 45/-45 stacking sequence. These panels were made to be 250 mm by 250 mm square.

The CFRE panels made from the epoxy and carbon fiber system used Fiberlay's 5.7 oz plain weave cloth (part # 1725750) made from Toray's T-300 fiber with 3000 fibers per tow. This cloth had a thickness of 0.31mm and a thread count of 50 per 100 cm. The epoxy was the same Orca 1300 used in the fiberglass panels. These panels used a stacking sequence of [45/-45]2s for a total thickness of eight plies. These panels were also made to be 250 mm by 250 mm square. Figure 5-1 shows the wet layup procedure for one of the CFRE panels.

The four figures show the wet layup process with a CFRE panel. Figure (a) shows the cutting of the plies on the 45° angle. Figure (b) shows the laying of the plies on top of the non-porous release ply and coating each ply with epoxy. Figure (c) shows all eight plies laid up with the porous release ply and breather cloth on top. Figure (d) shows the panel under vacuum and the epoxy being drawn into the vacuum trap.

Figure 5-1: Wet Layup Panel Manufacturing Process

The Pre-Preg autoclave cured panels were made with Hexcel's HexPly M46JB 12K/M71;35%;145AW unidirectional pre impregnated carbon fiber. In accordance with ASTM D3518 these panels used a stacking sequence of [45/-45]4s for a total thickness of 16 plies. Since these plies were unidirectional, symmetry did not occur naturally. The first set of four panels were not made correctly and had to be discarded because they were not symmetric and were only 12 plies each. All of the Pre-Preg panels were made to be 300 mm by 300 mm square because the roll of pre impregnated carbon fiber was 1.2 meters wide.

The GFRV panels made from the vinylester and fiberglass system used the same Fiberlay fiberglass cloth as the GFRE panels. The vinylester is Fiberlay's Orca 555 (part # 055555G) with a 1% Methal Ethal Keytone Peroxide (MEKP) catalyst. In accordance with ASTM D3518 these panels used a stacking sequence of [45/-45]3s for a total thickness of 12 plies. These panels were also made to be 250 mm by 250 mm square

For all the panels an aluminum cull plate was used during manufacturing. The sequence for the manufacturing process was first the cull plate, then a nonporous Airtech release ply (Release Ease 234TFNP) followed by the panel plies, followed by a porous Airtech release ply (Release Ease 234TFP), followed by breather cloth and then topped with the bagging material sealed with General Sealants Inc. yellow sealant tape. After curing for all the panels was completed, the side that was against the cull plate was noticeably smoother than the side that was against the breather cloth. It was decided to call the rougher side "side A" and the smother side "side B". All the panels in Figure 3-1 show side B.

5.1.2 Panel Mounting Procedures

The panels that were mounted on the sea spider were first cut down to 235 mm long by 185 mm wide. This was done so that the panels would not interfere with the other instruments on the sea spider while still allowing for at least five, 25 mm wide specimens to be cut from each panel after exposure. This sizing also allowed for the specimens to be in the 200 to 300 mm length range needed as per ASTM D3518 [16]. The panels were cut to size using either a wet tile saw or a K.O. Lee surface grinder (Figure 5-2) with a diamond grinding wheel that was 0.89 mm thick. The surface grinder was the better tool to use, providing for very straight, clean, repeatable and accurate cuts.

Figure 5-2: K.O. Lee Surface Grinder in the Process of Cutting a Pre-Preg Panel

Once the panels were cut to size, two holes were drilled in each panel to create attachment points. The holes were drilled offset from the width's centerline by 8 mm so that there were more mounting options and to decrease the likelihood of interfering with other instruments on the Sea Spider (Figure 5-3). This also ensured that at least three 25 mm specimens could be cut from the wider side and at least two could be cut from the narrower side.
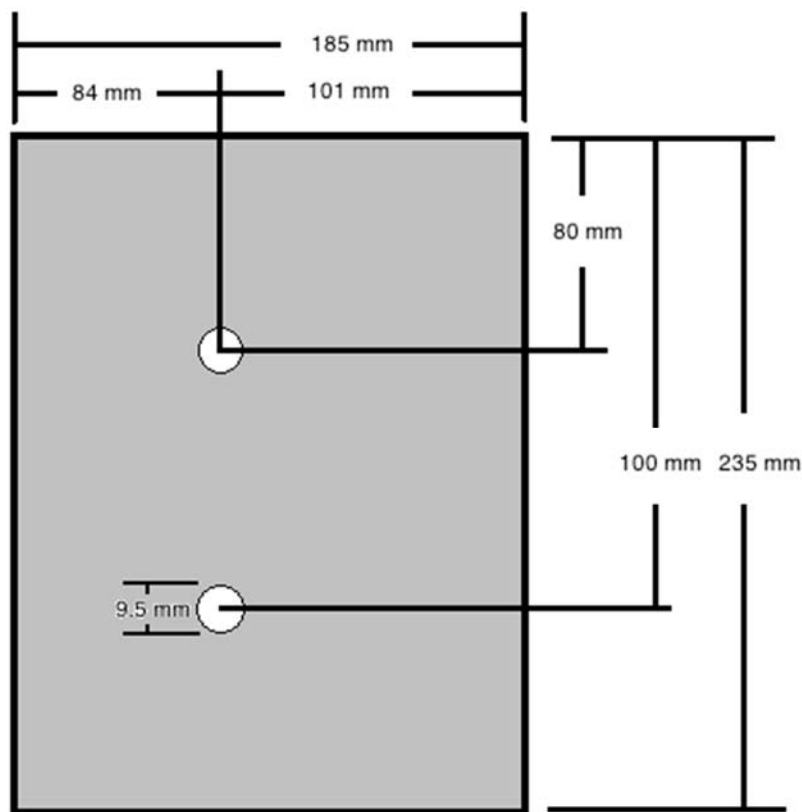
Figure 5-3: Panel Dimension and Hole Location for Mounting on the Sea Spider

After the holes were drilled, each panel was wiped with a paper towel and placed in an oven at 50°C for 30 minutes and then weighed. The reason for placing the panels in the oven before weighing them was to create a repeatable method for preparing the panels to be weighed.

The panels were mounted to the Sea Spider with 316 stainless steel bolts and with ¾ inch long ½ inch inner diameter PVC pipe spacers between each panel. The expectation was that the ¾ inch of space between the panels would allow for adequate water flow around all of the panels so that some panels did not experience more water absorption and diffusion than others. It had also been seen on other Sea Spider deployments that marine life was more likely to grow in crevices, the standard ¾ of space made it so that there wasn't an increased chance of marine life growing in-between some panels and not others. All bolt and nut connections used lock washers and marine grease because there had been previous experiences where the use of Nylock style self locking nuts caused the 316 stainless steel to corrode very quickly where the nylon and stainless

steel threads interfaced. The panels were mounted in two stacks of four panels each, for a total of eight panels. Figure 5-4 shows all of the panels mounted on the sea spider prior to their initial deployment.

Figure 5-4: Panels Mounted on Sea Spider Prior to Initial Deployment

The panels that were designated as those that would not be subjected to exposure (as-produced) were stored in a laboratory within the UW ME building to await future testing. These panels were kept out of direct sunlight and were protected from physical damage such as scratching. These panels were not cut or drilled.

5.1.3 Panel Submersion

Two of each type of panel were initially placed on the Sea Spider for in situ exposure. Panels B and C (GFRE), E and F (CFRE), I and J (Pre-Preg), and M and N (GFRV) were initially deployed on 08 May 2010. The sea spider was first retrieved 17 August 2010 and all hardware used to mount the panels was replaced. Pre-Preg panels I and J were replaced with panels U and V because it was discovered that the first set of panels were

not produced to be symmetric about the mid-plane and they were only 12 plies instead of the 16 required for unidirectional composites in ASTM D3518. The panels were next retrieved on 08 November 2010 and all hardware was again replaced and the panels were submerged once again. The panels were next retrieved on 10 February 2011 and at this time panels B, E, M and U were removed from the sea spider and returned to the UW. Figure 5-5 shows the sequence of biofouling observed during this nine-month period.

The progression of biofouling experienced by the various composite systems while attached to the Sea Spider. From top to bottom: 3 months, 6 months and 9 months. The carbon fiber based systems are on the left and the fiberglass systems are on the right.
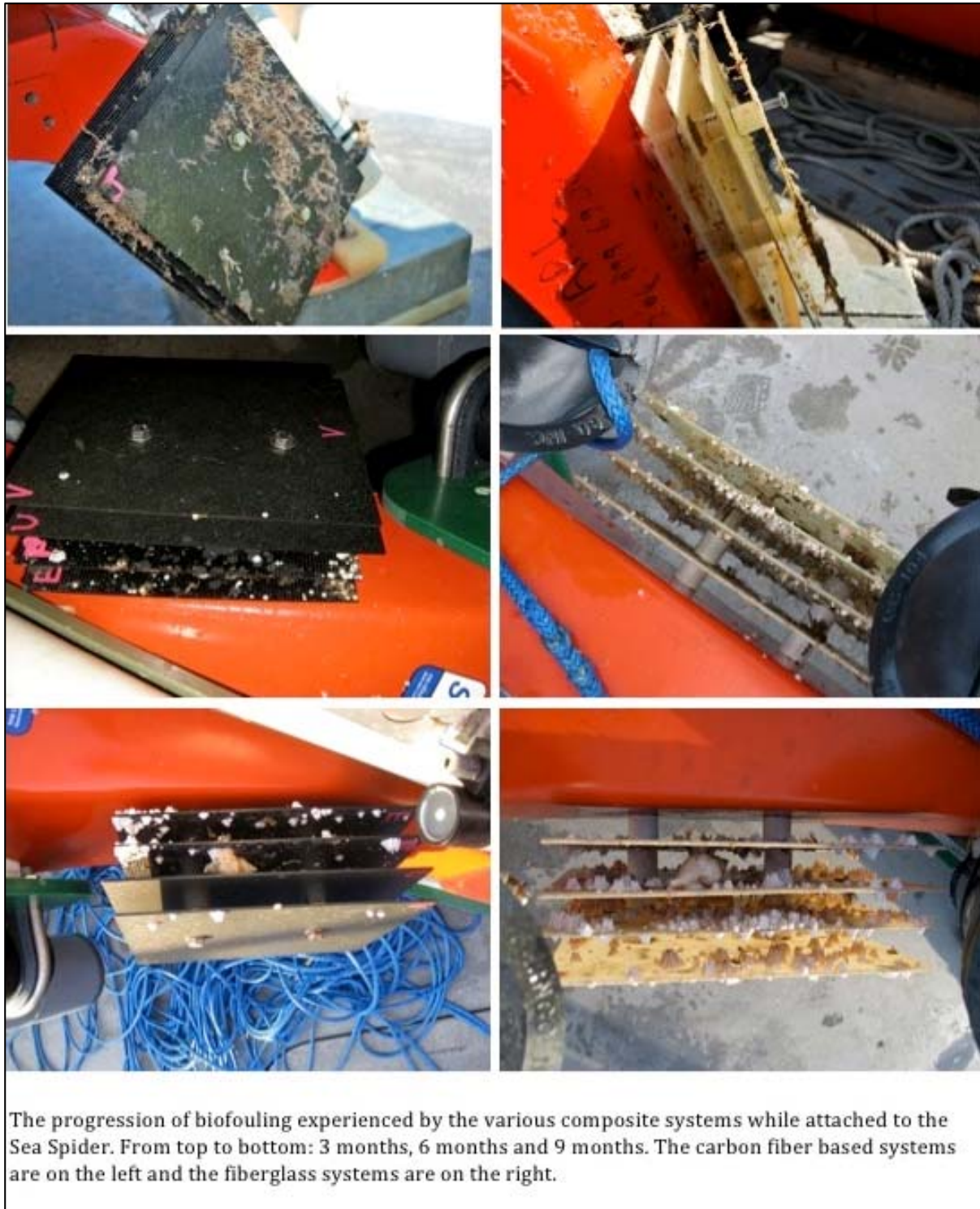
Figure 5-5: Progression of Biofouling Over 9 Months

For the two or three days of each recovery operation that the sea spider was out of the water, the panels were kept in a bucket of salt water drawn from the dockside so that they did not dry out. The four panels that were returned to the UW were also stored in a

closed bucket filled with salt water until they were prepared for testing. All panels were kept submerged until they were cut and strain gages attached. They were also tested within a day of being removed because numerous studies have shown that some of the loss of strength and stiffness observed in composite system exposed to salt water is restored once they dry back out [8,10,12].

During the panels' submersion in Puget Sound from May 2010 to February 2011, the water temperature varied between approximately 8 and 12 ℃. Figure 5-6 shows temperature and salinity recorded by a water quality sampler provided to the project by the Washington Department of Ecology as part of a long-term dissolved oxygen monitoring effort.
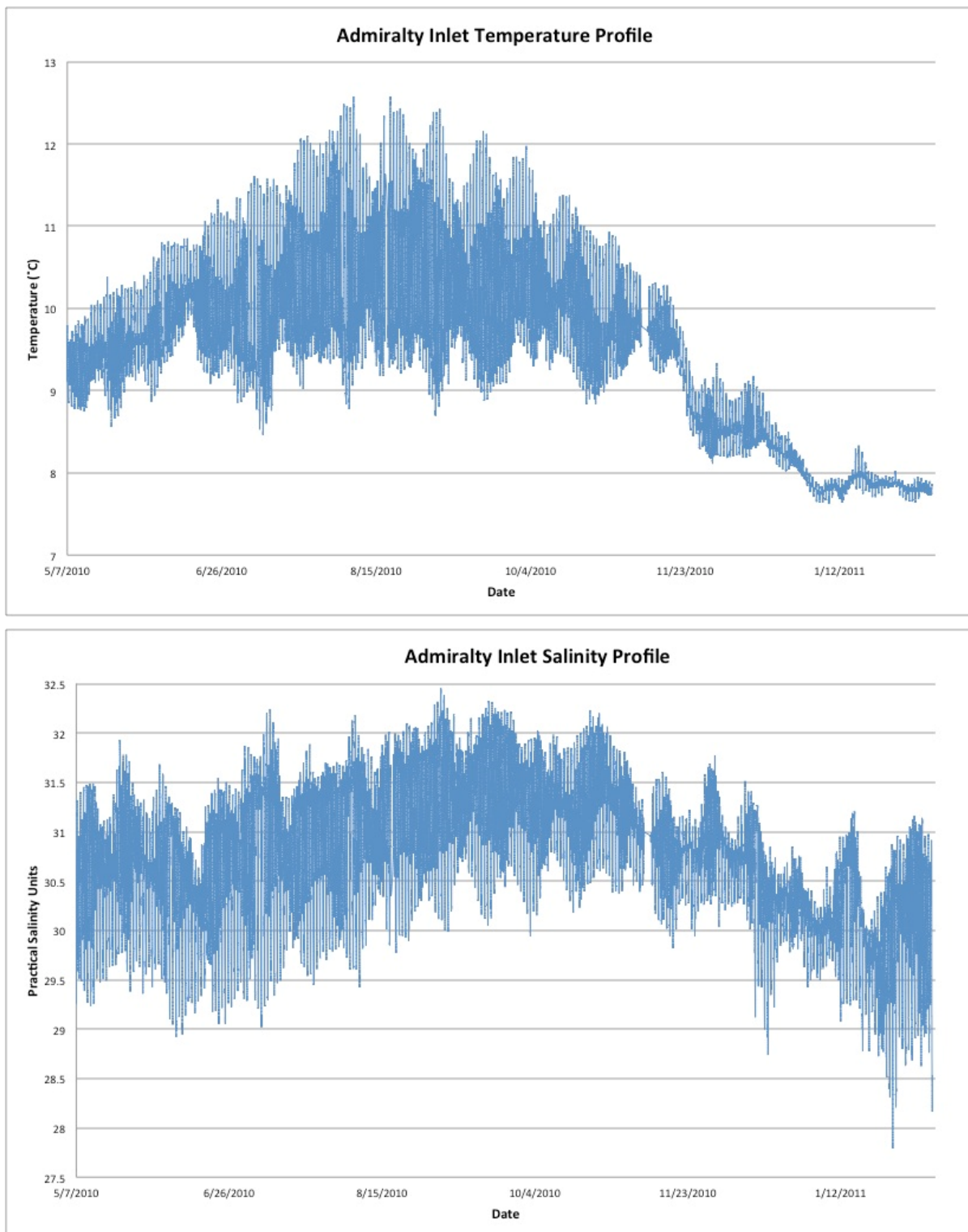
Figure 5-6: Temperature and Salinity At Sea Spider Location

5.1.4 Panel Cleaning

Once the panels were returned to the UW, they needed to be prepared for testing. The panels were covered in a variety of marine growth that was categorized and removed so that specimens could be cut and strain gages attached. The panels needed to be flat on one side to be properly cut using the surface grinder. The growth also needed to be removed in some areas so that the gages could be mounted and the grips used to hold the specimens during testing would not have interference. To satisfy these requirements, all marine growth was removed from one side and almost all was removed from the other side except that in-line with the holes used to mount the panels. The marine growth that remained after cleaning was characterized through microscopy. The panels were weighed before any growth was removed.

The panels were covered in a variety of marine growth including a large number of barnacles and micro algae, but they were easier to clean than expected. The tool that was found to work best was a small wedge shaped stirrer that was designed to stir epoxy. The stirrer was hard enough to scrape off the marine growth, but soft enough that it did not visibly damage the panels. A disposable plastic putty knife was also tried but it was found to not be strong enough to withstand the barnacles. A metal putty knife would have worked well but there was concern that the metal would have damaged the panels. The panels were all scraped in the same direction so that any scratches caused by the broken pieces of barnacle would be in the longitudinal load direction during testing.

The most difficult growth to remove was the barnacles. There were at least two different species of barnacles attached to the panels but both were removed in the same way, by first breaking the shell into pieces and then sanding the remaining deposits off in the areas where the strain gages were to be attached. If the entire growth was scraped off then a large amount of force was required and the risk of damaging the panels was increased. Figure 5-7 shows the deposits left behind by some barnacles once they were scraped off.
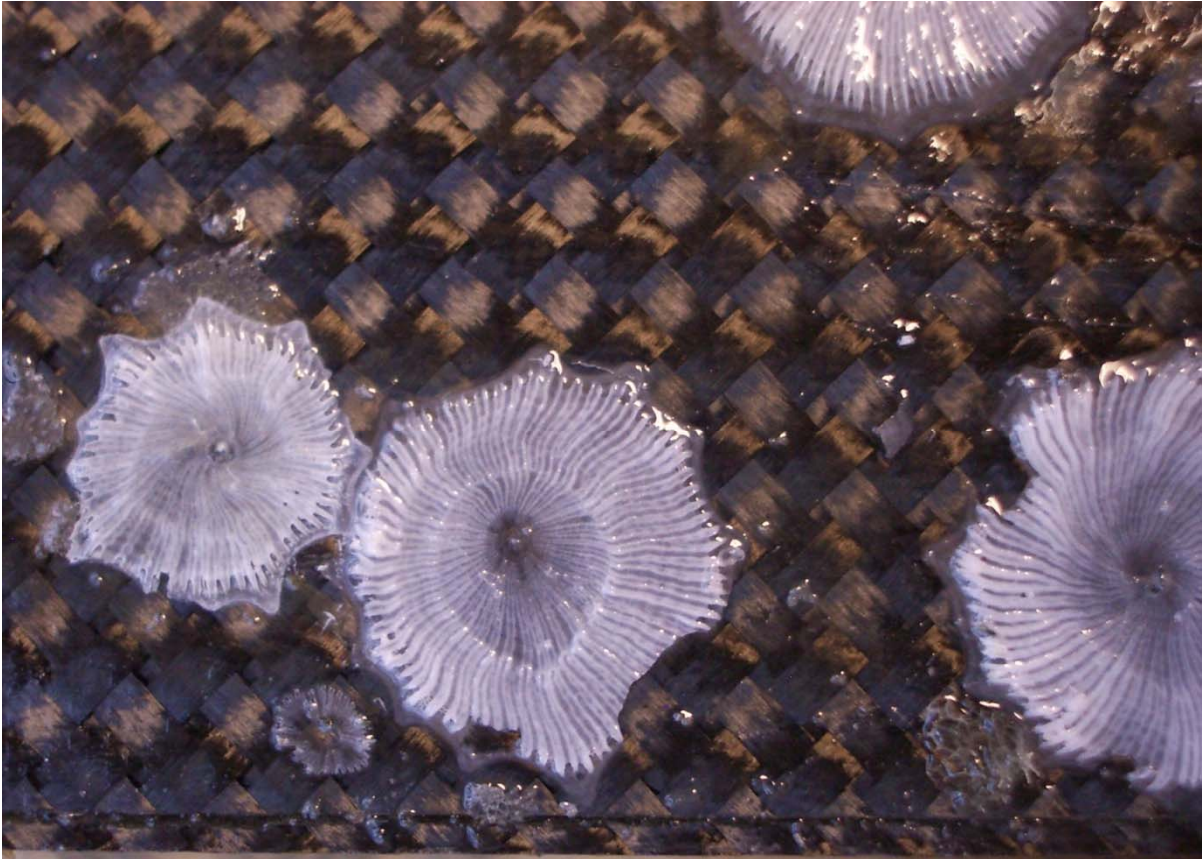
Figure 5-7: Residue Left by Barnacles After Panel E was Cleaned

After the marine growth was removed each panel was weighed and then placed in an oven at 50°C for 30 minutes and weighed again. Initially it was hoped that the weighing of each panel before and after exposure would give an indication of how much water had diffused into the panels during in-situ exposure. However, these weights were difficult to interpret because of the amount of marine deposits still remaining on each panel.

5.1.5   Specimen Construction

Once the panels were cleaned well enough to lay flat in the surface grinder, they were cut into 25 mm strips. To avoid any edge effects, all specimen cuts began at least 10 mm inset from the edge. At least 10 mm of clearance was also maintained around the mounting holes. Five 25 mm-wide (nominal) specimens were machined from each panel. Actual widths ranged from a minimum of 24.70 mm to a maximum of 25.22 mm.

These variations in width were taken into account when calculating stresses experienced during testing.

After the strips were cut, the areas where the strain gages were to be attached were sanded with 400 grit wet/dry sandpaper and any remaining marine growth deposits in the area were removed. The thickness of a specimen was measured at five locations on each specimen and the average was used as the thickness for calculating the stress in that specimen during testing. Care was taken to ensure that the locations chosen did not have obvious marine growth in the area so that false thickness readings were avoided.

One gage was used per specimen and all gages were attached to side B, the smoother side, of the specimens. The gages were attached using Micro-Measurements' M-Bond 200 adhesive and the tape method of bonding the strain gages to the specimens [20]. It would have been more accurate to have placed strain gages on both sides of the specimens so that any twisting during testing was accounted for, but the project budget allowed for only one gage per specimen. Figure 5-8 shows GFRV specimen M1 during testing.
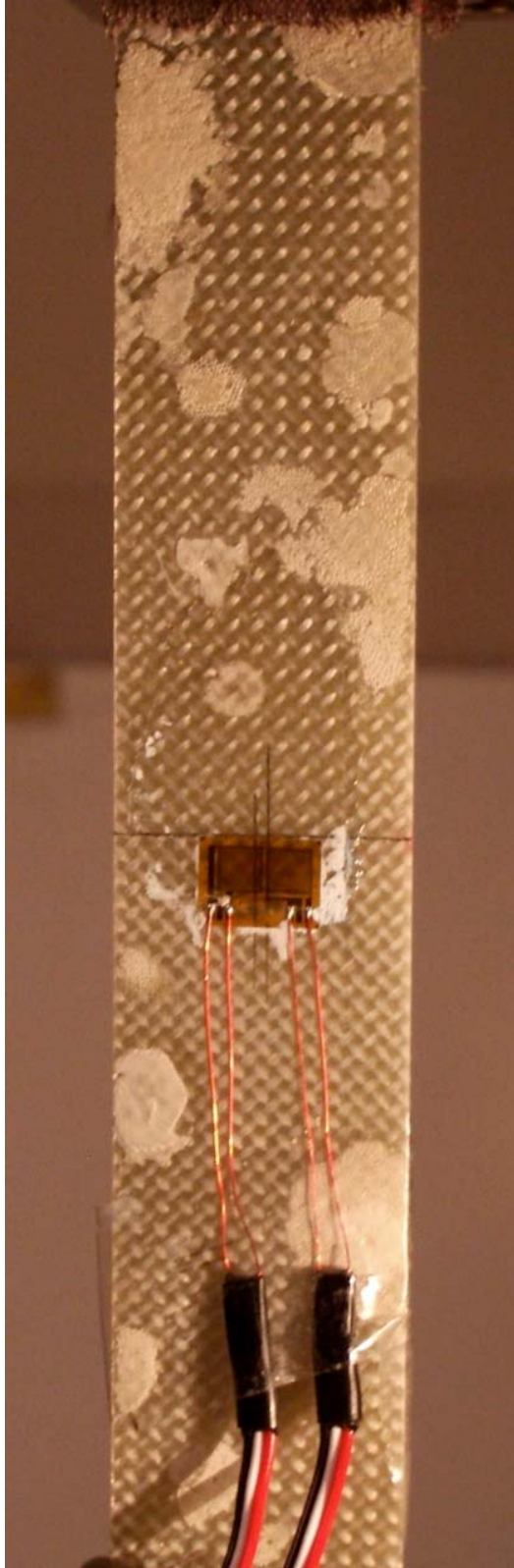
Figure 5-8: GFRV Specimen M1 During Testing

The as-produced panels that were chosen for testing were panels D (GFRE), G (CFRE), T (Pre-Preg) and Y (GFRV). Each of these panels were cut into specimens using the surface grinder. Only four 25 mm specimens were cut from each panel so that future specimens could be cut if needed. Care was taken to ensure that the specimens were cut far enough from the panel edge to avoid any changes in thickness due to ply drop. Specimens were also cut to avoid any obvious manufacturing defects such as indentations. Strain gages were applied in the same manner as described previously for the exposed panels.

5.1.6   Strain Gage Selection

To complete the D3518 test it was necessary to know the strain in the longitudinal and transverse directions during testing. A biaxial tee rosette strain gage was chosen for this reason. The Vishay Micro-Measurements C2A-06-125LT-350 with pre-attached wire leads was chosen because of its relatively low cost, ease of use and ability to measure ±3% strain [21].

The strain gages were wired using a three wire system to minimize the effects of the long lead wires on the resistance measured [20].

5.1.7   Polishing Procedure

Once the specimens required for testing were cut from the panels, the remaining scraps were used to prepare samples that could be examined under a microscope. To be properly examined under a microscope one surface needed to be polished on each sample. One sample was polished for each panel that was tested, for a total of 11 samples. Two of these samples were potted in a two part polyester resin. The two samples that were potted were from panels E (CFRE) and M (GFRV) (Figure 5-9).
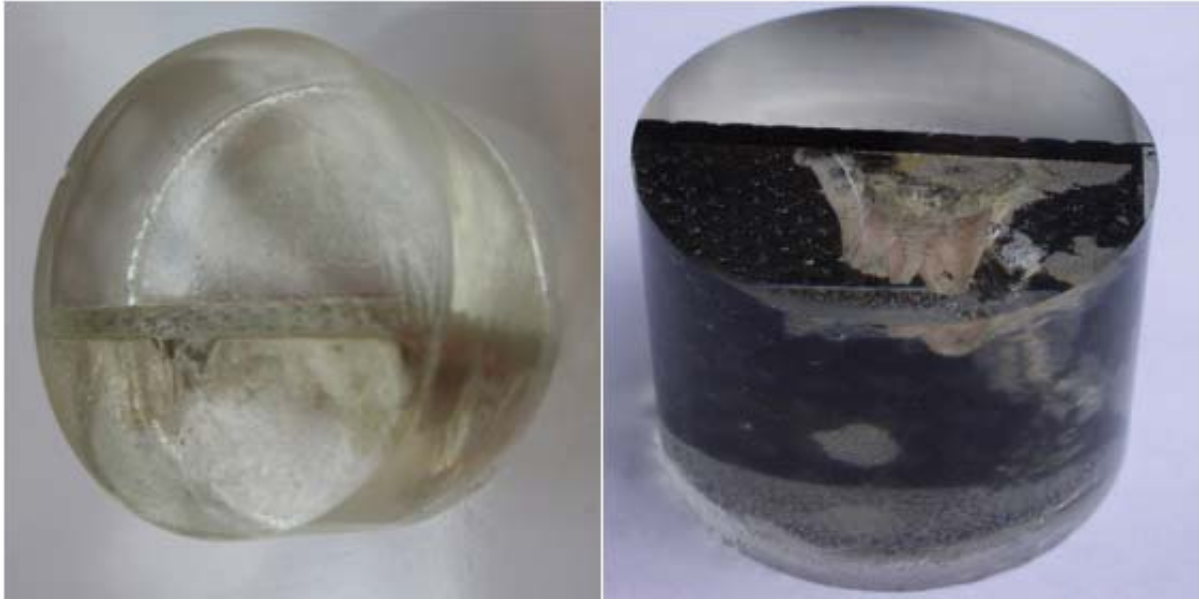
Figure 5-9: Potted Samples, M on the Left E on the Right

These samples were potted because they still had barnacles attached and these barnacles would have broken off if they had been polished without being potted. It was desirable to keep the barnacles attached so that macroscopic and microscopic pictures could be taken that clearly showed how the barnacles interfaced with the materials.

The 11 samples were polished on a polishing wheel. To make the surfaces to be polished have square contact with the polishing wheel they were ground with first 800 grit followed by 1200 grit wet/dry silicon carbide sand paper. Once the surfaces were level they were polished with a one micron alumina slurry until they were sufficiently polished. Each sample was checked visually and under a microscope after every five minutes of polishing. With practice it became apparent when a sample was sufficiently polished so that the individual fibers could clearly be seen. In general this occurred after approximately 20 minutes of polishing.

After the samples were polished, they were dried with a lint free tissue and examined. Examination consisted of taking macroscopic pictures with a camera, such as those in Figure 5-9, and using a microscope and digital camera combination to take pictures at 10x and 200x magnification. Figure 5-10 shows panel T at 200x magnification.
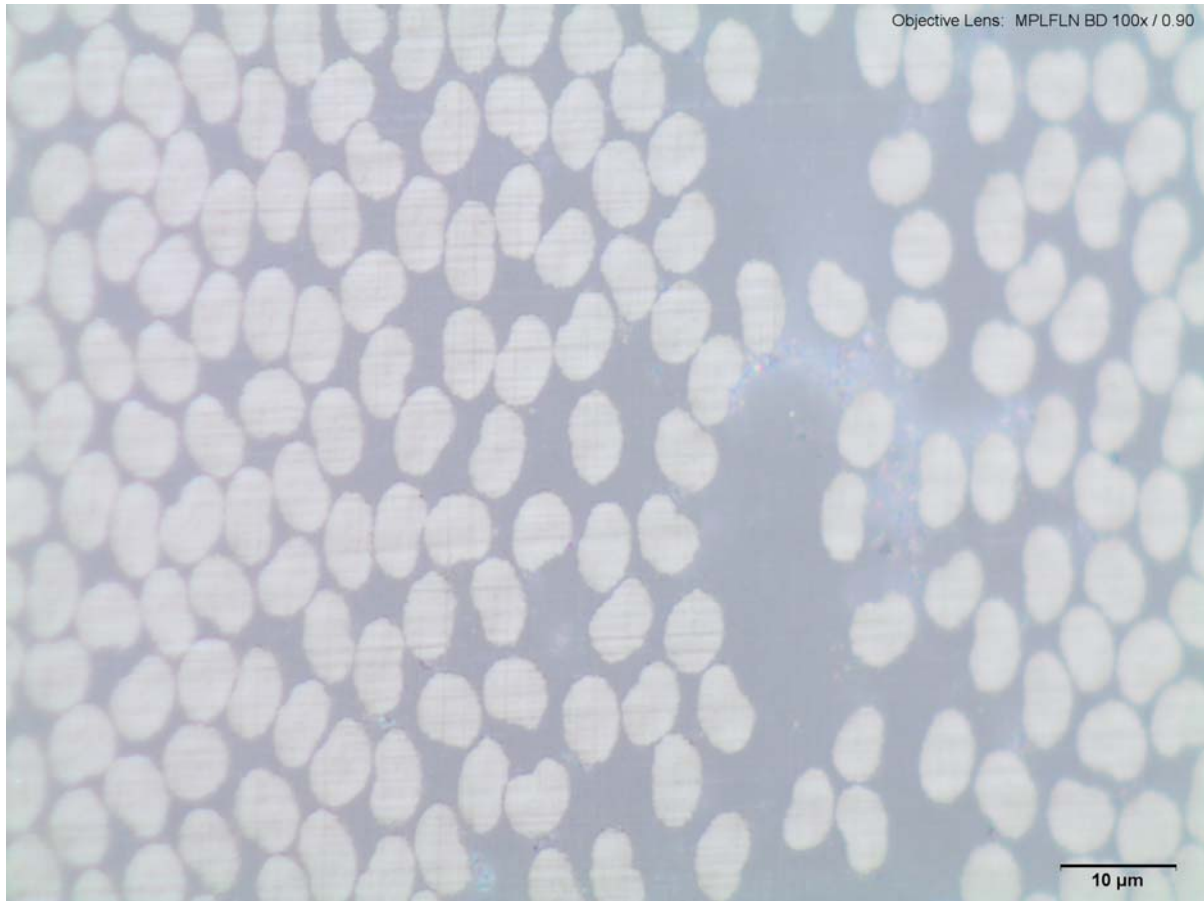
Figure 5-10: A Polished Sample from Panel T at 200x Magnification

The lighter dots are the fibers and the surrounding gray is the matrix. The fibers are white instead of black because a bright field illumination technique was used to illuminate the sample [**22**].

The contrast between the fibers and matrix was very apparent with the carbon fiber reinforced systems, but not as apparent with the fiberglass reinforced systems. This lack of contrast made it difficult to compare the fiberglass samples.

5.1.8 Equipment Used

For the weighing of all panels, a Sartorius electronic scale was used. This instrument has a resolution of 0.01 grams. For the dimensional analysis of all panels and specimens, Mitutoyo Absolute Digimatic electronic calipers were used that had a resolution of 0.01 millimeters. Each panel was dried in a Thermotron oven with a

resolution of one degree Celsius. For the testing of the specimens a 250 kN capacity Instron universal load frame was used. Loading was applied in cross-head displacement mode, controlled by Instron's Bluehill 2 software version 2.0. The Bluehill software also monitored the extension and the load experienced by the crosshead load cell. These signals were also sent to a Vishay System 5000 data acquisition system connected to a Windows XP Pro computer via a 16 bit interface card. The Vishay System 5000 included a model 5100 scanner which used a ¼ Wheatstone bridge to monitor the change in resistance of the strain gages and convert the signal from analog to digital. The computer was running Vishay's Strain Smart software version 4.01 which reported the longitudinal and transverse strain experienced by the strain gages as well as the load and crosshead displacement acquired from the Instron load frame.

There were two types of grips used during testing, Instron's 30 kN 2716-015 wedge grips with MS 516 0-0.25 jaws and the 270 kN W-5072 T wedge grips with W-5061-D-C jaws. The smaller grips were much easier to use and allowed for a lower initial load to be applied to prevent slipping. 200 grit emery cloth was used between the grip and specimen interface to help prevent slipping. The smaller grips also allowed for quicker specimen preparation and were much more likely to keep the specimen vertical during preloading.

The tile saw used was a MK Diamond Products model MK-145. The saw did a good job of making clean cuts, but it was difficult to obtain straight edges.

The surface grinder was a K.O. Lee model S3618HS with serial number 26224YM. The computer control functionality no longer worked so all cuts had to be made by hand. The grinder speed was kept at a constant 1800 RPM and the feed rate was kept constant for all specimens.

The Conductivity, Temperature and Depth (CTD) recorder mounted on the sea spider that captured the salinity and temperature data during the nine month deployment was a Sea-Bird Electronics 16*plus* V2.

The autoclave used to manufacture the Pre-Preg panels was an American Autoclave Company's serial # 761. The autoclave was owned and operated by the UW's Materials Science and Engineering Department. Figure 5-11 shows this autoclave with Pre-Preg panels ready for curing.
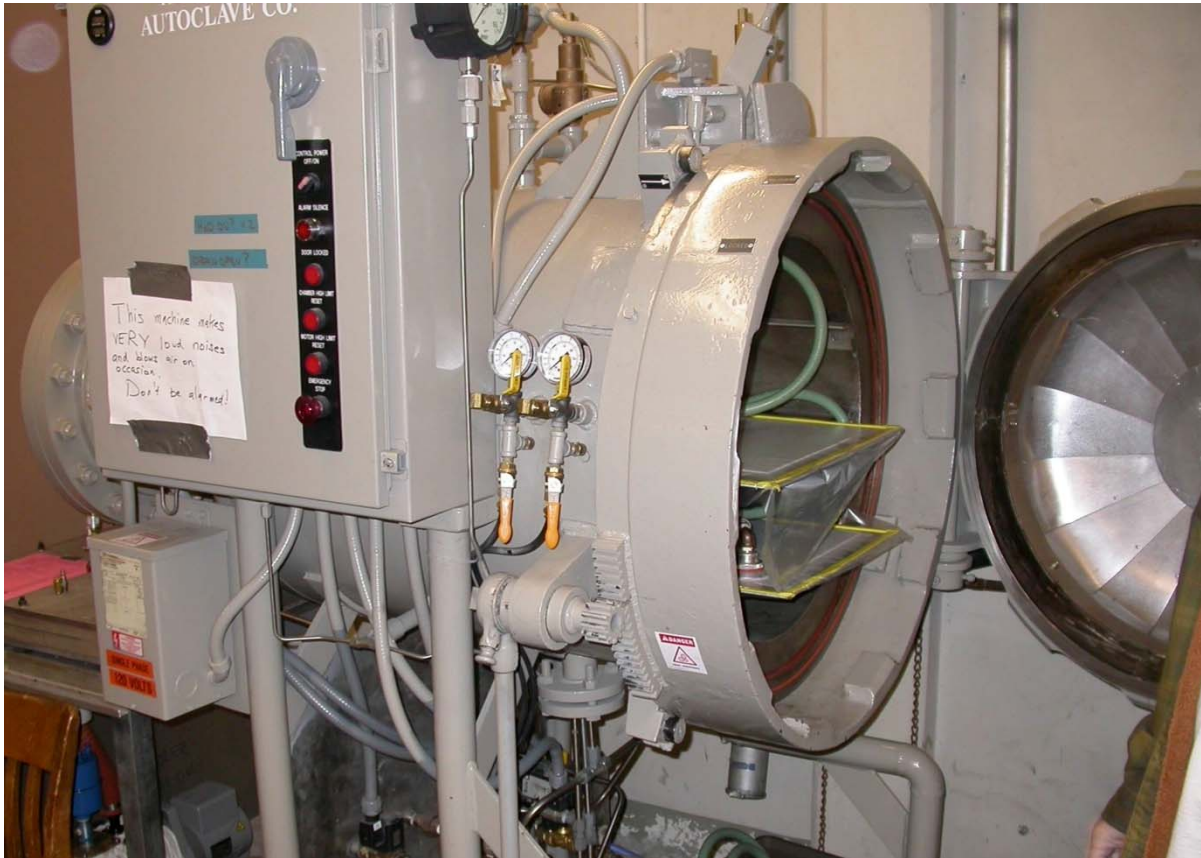
Figure 5-11: Autoclave Used to Cure Pre-Preg Panels

A 200 mm polishing wheel was used to polish the samples. A continuous supply of distilled water was sprayed on the polishing surface to keep it moist. The fastest and best polishing results were achieved using Struers' MD Chem polishing pad (catalog # 405000092) combined with Allied's 1.0 μm alumina slurry suspension (part # 37952).

An Olympus microscope, model number BX51TRF, was used to examine the polished samples. The digital microscopic pictures were captured using Olympus' SC30 camera and Stream Essentials software version 1.5.

6 Method For Accelerated Exposure

6.1 Procedure

6.1.1 Panel Manufacturing

For the accelerated exposure, only the GFRV composite system was tested. Three panels were made for the accelerated exposure test using the same method described in section 5.1.1.These panels were made to be 230 mm by 230 mm so that they could fit in the hot water bath equipment. Panels Q and R were made on 29 June 2010 while Panel X was made 01 February 2011.

6.1.2 Panel Submersion

All panels used were subjected to the same weighing procedures as those described previously in which a panel was wiped with a paper towel and placed in a 50℃ oven for 30 minutes before being weighed. Panel Q was weighed and placed in a 30℃ saltwater bath on 07 January 2011. The panel was suspended in the salt water from a four-beam balance so that its weight could be continually monitored while it was submerged. Figure 6-1 shows how this weight monitoring was conducted for panel Q.
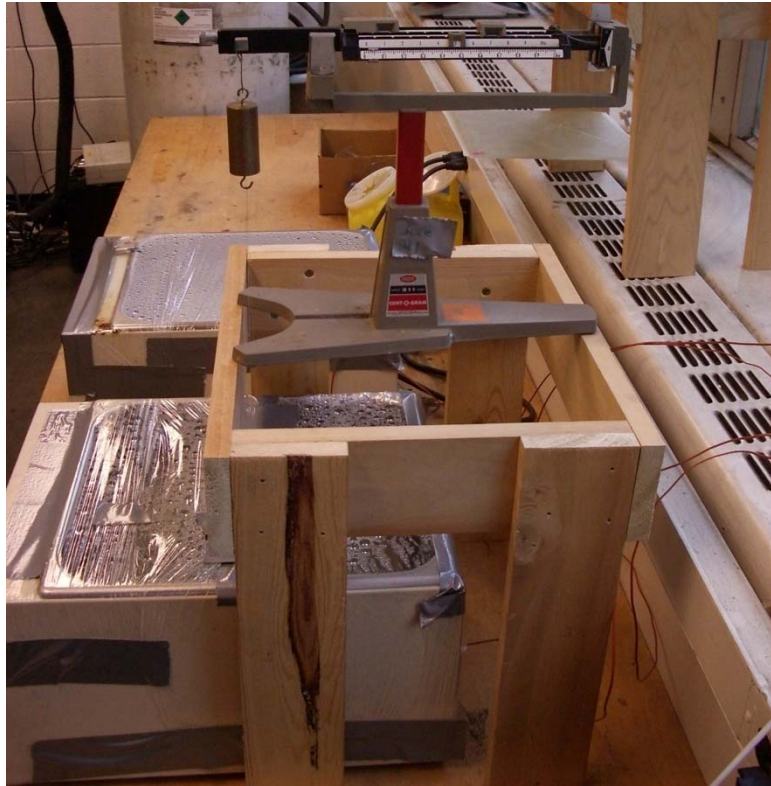
Figure 6-1: Continuous Weighing of Panel Q

The continuous weighing method was used so that the weight change of the panel could be monitored without having to disturb the system every time the weight was recorded. A four-beam balance was used instead of a load cell because a load cell would have had a tendency to creep over the 30 day period in which the weight was monitored. Because the weight gain was expected to be less then one percent of the initial panel weight, this creep would have probably been unacceptable. Panel Q was removed from the water, dried using the same method as before and weighed on 06 February 2011.

Panel R was weighed and placed in a 40°C saltwater bath on 10 January 2011. The weight of panel R was also continuously monitored during the time it was submerged. The scale used to monitor the weight change was similar to the four-beam balance but had two beams plus a dial with a coil spring that replaced the two finer beams. On 19 January 2011 the water bath developed a leak due to the salt water causing corrosion through the stainless steel tub. The pinholes were sealed with silicone RTV and the water was replaced. The panel was removed 09 February 2011, dried and weighed.

Panel X was weighed and placed in a 50°C saltwater bath on 14 February 2011. Its weight was monitored using the same 4-beam scale used for panel Q. It was removed, dried and weighed on 16 March 2011.

The specific gravity of each saltwater bath was measured both before and after the panels were placed in them. Distilled water was added to the baths as needed to replace that which had been lost to evaporation. The salt water was made from distilled water produced at the UW and by the addition of 34.75 grams per liter of Coralife Scientific Grade Marine Salt Mix. According to Coralife, when mixed at this proportion, the salt water's specific gravity should be 1.021-1.023, its pH should be 8.2-8.3, and it should have 390-410 ppm of calcium and 1110-1250 ppm of magnesium. Table 6-1 shows the specific gravity values that were calculated during testing.

Table 6-1: Specific Gravity Values for Accelerated Panels

Panel	Initial Specific Gravity	Final Specific Gravity
Q	1.024 @ 24°C	1.023 @ 27°C
R	1.021 @ 24°C**	1.020 @ 27°C
X	1.021 @ 23°C	1.023 @ 21°C

** This is the specific gravity for the second batch of saltwater made for panel R after the machine had sprung a leak.

Barometric pressure was recorded daily during testing because there was some uncertainty as to how much the fluctuations would affect the weight shown by the scales.

6.1.3 Specimen Construction

Four 25 mm specimens were cut from each panel on the same day that they were removed from the saltwater bath. The surface grinder was used to cut all of these specimens and as in 5.1.5 care was taken to ensure that the specimens were cut far enough from the edge to avoid any edge effects or dropped plies. Strain gages were

attached in the same manner as described in 5.1.5. All specimens were ready for testing within 24 hours of being removed from the saltwater bath.

6.1.4   Equipment Used

The same load frame and strain gage equipment was used as in 5.1.8, as well as the same analysis equipment and oven.

The hot water bath used for panels Q (30℃) and X (50℃) was a VWR Scientific model 1230 with a single controller that was used to set the temperature. The machine's internal thermostat kept the temperature within an acceptable range. The hot water bath used for panel R (40℃) was also a VWR Scientific model 1230 but was a newer model. This machine had two controllers where the user set the high point and the low point and the machine kept the water temperature within that range. This method did not work as well and the machine had a larger temperature fluctuation. This machine also appeared to be made from a lower quality stainless steel as it developed many pinhole leaks during the 30 day test.

Silicone coated k-type thermocouples were used the monitor the water temperature of the baths and the ambient air temperature during the testing. The silicone was removed from the tips of the thermocouples and they were covered in a thin coat of RTV silicone to prevent corrosion. The thermocouples were connected to a Measurement Computing Corporation USB-TC eight channel data acquisition system. According to the manufacture this system has a typical error of ±0.345°C for a K-type thermocouple. The system was connected via a USB to a Windows XP pro PC running Lab View 8.5 that was being used to monitor and record the temperature during the testing.

The four-beam balance used to monitor the weight change of panels Q and X was an Ohaus Cent-O-Gram model 311 with a resolution of 0.01 grams. The scale used to monitor panel R was an Ohaus Dial-O-Gram model 310 with a resolution of 0.01 grams. The pans and pan supports were removed from both scales during testing.

The barometric pressure was determined by using a Princo Instruments Inc. model 453 mercury barometer, which had a resolution of .1 millimeters of mercury.

7   Data Collection and Analysis

7.1   Data Processing

The strain, displacement and load data was collected by the Strain Smart and Bluehill software systems and was reported in .xls and .csv formats respectively. This data was then imported into Microsoft Excel 2011 for Macintosh and was converted to .xlsx format. A spreadsheet was created in which the load, extension and strain data from the Strain Smart and Bluehill software along with the user supplied data of the specimen's width, thickness and distance between the grip faces were entered. The spreadsheet then produced shear stress v. shear strain and tensile stress v. tensile strain curves. The shear curves were based off the strain gage readings while the tensile curves were based off the crosshead displacement of the Instron machine.

The shear moduli of the different specimens were determined from the shear stress/shear strain curve for each specimen. As recommended by ASTM D3518, the moduli were calculated by determining the slope of this curve in the range from 2000 to 6000 micro strain (με) for most of the systems. Because of mistakes made during testing, this range was modified to the 4000 to 8000 με range for the GFRE system[1].

---

[1] The mistake made during testing was that a preload was applied to the specimens before the strain gage data recording was initiated. This was done to ensure that the jaws of the Instron machine did not slip during the initial loading of the specimen. The preload should not have been applied so that the stress-strain curve began at zero. With no preload the jaws may have slipped, but this would not have been seen on the stress-strain curve because it would have occurred in the elastic range of the specimens. Jaw slippage would have affected the tensile strain calculations obtained from the crosshead displacement, but this data was far less important than that associated with the shear modulus calculations. This preload caused a shear strain of more than 2000 με for the GFRE specimens that were subjected to nine months of exposure. This required the modification to the strain range used to determine the shear modulus for the GFRE system.

After the shear moduli were determined, the 0.2% offset method was used to determine the yield shear stress and yield shear strain of each specimen. In this method, a line was created whose slope was determined from the shear modulus calculation above. This line was then moved to the right such that it crosses the x-axis at .002 radians, where this line then crossed the shear stress/shear strain curve was considered to be the yield point. Although it is questionable whether the use of the 0.2% offset method is accurate for composites because composites may not yield in the manner in which isotropic metals do, these values offer another tool to compare the changes between the as-produced and exposed materials.

The maximum shear stress was then calculated for each specimen when possible by following the guidelines in ASTM D3518. The ASTM standard defines the maximum shear stress at the point at which the specimen shows 5% shear strain. The standard uses the 5% shear strain point as the maximum because of the scissoring affect of the fibers which make the fibers no longer 45° to the load. A problem was that for many of the specimens, one or more of the rosette's strain gages failed before this 5% shear strain. According to the manufacture, if the gages are applied correctly, they should be able to withstand ±3% strain, which is approximately 6% shear strain in this application. These results were not always obtained during testing, typical failure modes were debonding of the gage from the material and/or an electrical short in the strain gage. If 5% shear strain was reached and there were no obvious abnormalities present in the data, than the corresponding shear stress was reported.

The strain recorded by the strain gage oriented to monitor the longitudinal strain was used to calculate the tensile moduli of elasticity of the specimens. This test was performed by following the ASTM D3039 Standard Test Method for Tensile Properties of Polymer Matrix Composite Materials. Because this standard is what the specimen preparation and test procedures for the D3518 standard follow, completing the D3518 test essentially completes the D3039 test as well. The tensile modulus of the specimens was calculated by creating a tensile stress vs. tensile strain curve for each specimen and fitting a line to the strains in the 1000 to 3000 $\mu\varepsilon$. The slope of this line is the tensile

modulus of elasticity for the specimen. Again, because of mistakes made during testing, this range was modified to the 2000 to 4000 $\mu\varepsilon$ range for the GFRE system.

The max load, in Newtons, achieved by each specimen was determined from the Instron's transducer and the tensile stress and tensile strain were recorded for this point. Although this was the max load achieved by the specimens, it was inaccurate to state that the stress and strain at this point was the stress and strain at failure because the load typically decreased slightly before the specimen failed. What the profile of the load looked like before failure depended on the composite system being tested.

While the longitudinal stain gage data was used to calculate the tensile modulus of elasticity, the crosshead displacement was used to determine the strain experienced by the specimens at max load. Although the change in crosshead displacement was an inaccurate way to calculate strain, it was necessary to use in this application because the tensile strain experienced at max load varied from 9% to 31% depending on the composite system and this was far above the 3% that these strain gages were designed to measure. The inaccuracies associated with using the crosshead displacement to measure strain included the possibility of the specimen slipping in the jaws, the initial slack in the grip connecting pins and mounting hardware and the difficulty in measuring the initial distance between the grips. While a preload of between 300 and 500 N was applied to most specimens and while no slipping in the jaws was observed for any of the specimens it was still very inaccurate to use the crosshead displacement to determine strain at small strain levels. At higher strains though these initial inaccuracies had less influence on the measured strain (i.e., higher signal to noise), so the use of the crosshead displacement to measure the tensile strains at max load is an acceptable indicator of the actual strain experienced by the specimen. The use of the crosshead displacement to measure these high strains was also probably more accurate than using extensometers because most clip gage style extensometers have a gage length somewhere between 15 and 50 mm, but the initial distance between the jaws was in the range of 120 to 150 mm for all specimens. Since these were straight-sided specimens, it was virtually impossible to know where in this 120 to 150 mm range the

specimens were going to fail. If extensometers had been used, the strains measured could have potentially been far lower than those actually experienced by the specimens.

During testing, the noises emitted by the specimens and the type of failure experienced by each specimen were noted. After each specimen was tested the percent of change between the initial width and the final width, commonly known as necking, was measured as accurately as possible. It was difficult to determine the percentage of necking experienced by some of the specimens, particularly those that failed in a gradual and controlled manner as apposed to those which failed explosively, therefore there is larger a larger coefficient of variation in this data than in most of the other data.

7.2   Statistical Processing

Statistical analysis was completed for each panel and consisted of determining the mean, the sample standard deviation and the coefficient of variation for each calculation completed on each panel. Except where noted, the sample size for these calculations was n=4 instead of the n=5 or more which was recommended by the ASTM standard. Because of mistakes made during testing or anomalies in some of the strain gage data collected, statistics for some panels only have a sample size of n=3. The sample standard deviation was calculated as

$$s = \frac{\sqrt{\sum_{i=1}^{n}(x_i - \bar{x})^2}}{(n-1)} \qquad \text{\textbf{Equation 7-1}}$$

where s was the sample standard deviation, n was the number of specimens tested for that panel, x was the value of the parameter being examined and $\bar{x}$ was the mean calculated for this parameter for these same specimens. The coefficient of variation (CV) is presented in percentage and calculated by

$$CV = 100 * \frac{s}{\bar{x}} \qquad \text{\textbf{Equation 7-2}}$$

where s was the sample standard deviation and $\bar{x}$ iwas the mean as calculated previously.

A more in-depth statistical analysis was completed on the shear modulus calculation to determine if differences were statistically significant. A 95% confidence, two sided, paired T-test was conducted in which the hypothesis tested was whether there was a difference in the means of the shear modulus calculated between as-produced and exposed panels. The null hypothesis test

$$H_0: \mu_D = \Delta_0 = 0 \qquad\qquad \text{Equation 7–3}$$

was used, where H_0 was the null hypothesis, μ_D was the mean of the shear modulus differences between the samples and Δ_0 was the tested value, which in this case was zero.

The test statistic used for the paired T-test uses the t-distribution because of the small sample size of four specimens for each panel. The degrees of freedom for the t-distribution was given by

$$\nu = n_1 + n_2 - 2 \qquad\qquad \text{Equation 7–4}$$

where ν was the degrees of freedom, n_1 was the sample size of the as-produced panel and n_2 was the sample size of the exposed panel.

The test statistic was

$$T_0 = \frac{\overline{D} - \Delta_0}{\frac{S_D}{\sqrt{n}}} \qquad\qquad \text{Equation 7–5}$$

where T_0 was the test statistic, $\overline{D}$ is the sample average of the n differences $D_1, D_2, \dots, D_n$ and S_D is the sample standard deviation of these differences. Minitab software's Minitab 16 was used to complete this hypothesis testing.

7.3   Analysis and Reporting of Data

Table 7-1 shows all the calculations completed for all the specimens.

Table 7-1: Data Calculations for all Specimens

	Specimen	% necking	Shear Modulus Slope (GPa)	Yield Shear Stress (MPa)	Yield Shear Strain (%)	Shear Stress at 5% Shear Strain	Tensile Modulus Slope (GPa)	Max Load (N)	Max Load Shear Stress (MPa)	Max Load Tensile Stress (MPa)	Max Load Tensile Strain (%)
GRFE	D1	15.58%	2.51	37.85	1.71%	50.91	9.33	8224.11	76.83	153.65	14.47%
	D2	14.43%	2.45	35.49	1.65%	48.37	9.22	8306.23	74.07	148.15	14.36%
	D3	13.89%	2.51				9.09	8395.69	78.13	156.26	14.51%
	D4	8.42%	2.40	34.45	1.63%	47.26	8.72	8393.14	75.85	151.71	14.23%
	B1	25.18%	0.84	8.37	1.20%	15.68	3.31	4154.73	37.38	74.76	29.86%
	B2	24.81%	0.81	8.20	1.21%	15.30	3.17	4159.63	37.11	74.23	29.60%
	B3	25.80%	0.77	9.20	1.40%		2.92	4199.62	37.17	74.34	30.94%
	B4	24.54%	0.92	7.81	1.05%		3.51	4159.63	38.32	76.63	30.04%
CFRE	G1	32.96%	3.36	32.36	1.16%		12.50	7543.57	77.09	154.18	11.65%
	G2	37.94%	3.20	32.01	1.20%		11.67	7614.44	76.11	152.23	12.63%
	G3	39.78%	3.38	32.57	1.16%		12.60	7589.67	75.49	150.98	12.06%
	G4	37.01%	3.22					7483.66	72.80	145.59	9.95%
	E1	31.99%	2.40	25.56	1.27%	41.91	9.22	7075.59	64.20	128.40	15.02%
	E2	34.87%	2.45	25.18	1.23%		9.11	7081.51	64.02	128.04	15.01%
	E4	30.75%	2.47	25.75	1.24%		9.00	7327.24	64.66	129.32	14.63%
	E5	26.27%	2.42	25.26	1.25%	42.71	8.91	7636.44	66.17	132.33	16.47%
Pre Preg	T1	11.82%	4.12	42.46	1.23%		15.62	11187.06	99.64	199.28	18.42%
	T2	11.78%	4.15	41.62	1.20%	59.41	15.86	11391.62	100.74	201.47	18.98%
	T3	11.94%	4.00	42.87	1.27%	59.64	15.69	11318.69	101.10	202.19	18.80%
	T4	12.19%	4.16	47.29	1.34%		15.72	11581.68	103.88	207.76	18.80%
	U1	12.14%	3.77	39.27	1.24%	54.56	14.29	11294.49	101.23	202.45	20.88%
	U2	12.81%	3.88	38.69	1.20%		14.50	11373.82	101.57	203.15	20.85%
	U3	11.54%	3.83	39.59	1.24%	55.50	14.34	11502.71	102.08	204.17	21.40%
	U4	13.71%	3.83	39.31	1.23%	55.10	14.52	11537.33	101.90	203.80	21.27%
GFRV	Y1	27.08%	2.29	21.36	1.14%		8.42	4485.34	39.41	78.82	13.39%
	Y2	33.16%	2.19	20.79	1.15%	30.69	7.89	4483.85	37.66	75.32	15.05%
	Y3	33.95%	2.20	20.42	1.13%	30.15	9.26	4192.17	36.24	72.48	10.30%
	Y4	33.99%	2.22	21.60	1.17%	31.11	8.20	4137.86	37.21	74.43	9.35%
	M1	13.68%	1.88	17.48	1.13%	25.68	6.92	3413.05	33.69	67.38	12.14%
	M2	18.02%	1.96	18.61	1.15%	27.75	7.07	3308.58	32.38	64.76	10.18%
	M3	16.30%	1.91	17.69	1.13%	25.98	6.93	3235.27	31.29	62.58	10.26%
	M4	8.50%	2.00	18.37	1.12%		7.50	3310.50	32.88	65.76	10.51%

Specimen	% necking	Shear Modulus Slope (GPa)	Yield Shear Stress (MPa)	Yield Shear Strain (%)	Shear Stress at 5% Shear Strain	Tensile Modulus Slope (GPa)	Max Load (N)	Max Load Shear Stress (MPa)	Max Load Tensile Stress (MPa)	Max Load Tensile Strain (%)
Q1	11.52%	1.27	15.40	1.41%		5.26	4495.95	40.73	81.45	13.95%
Q2	11.88%	1.27				5.11	4353.45	39.89	79.79	13.37%
Q3	15.05%	1.56	13.42	1.06%	26.34	6.41	4312.08	39.11	78.22	14.05%
Q4	11.78%	1.42	13.68	1.17%		5.94	4295.48	39.08	78.15	14.17%
R1	8.01%	1.50	19.00	1.47%	35.73	6.61	5146.81	46.41	92.82	12.01%
R2	7.58%	1.50	17.48	1.37%		5.97	5329.88	48.44	96.87	11.84%
R3	6.56%	1.42	18.25	1.49%		5.87	5288.57	49.01	98.02	11.72%
R4	8.09%	1.58	16.37	1.24%		6.27	5294.76	46.01	92.01	11.37%
X1	8.46%	1.58	16.56	1.25%	27.22	5.95	3959.50	34.17	68.34	9.52%
X2	7.65%	1.49	17.59	1.38%		6.02	3827.28	34.33	68.67	9.42%
X3	10.50%	1.47	16.37	1.32%	25.79	5.87	3716.62	32.45	64.89	9.14%
X4	6.05%	1.40	15.96	1.34%	24.41	5.64	3825.57	33.37	66.74	10.12%

The cells that are highlighted indicate that accurate data could not be determined for these values. For example there is no yield shear stress or strain available for specimen D3 because the strain gage data has an obvious anomaly associated with it before the yield point was reached. It is possible to determine the slope of the shear modulus for this specimen though because the anomaly occurred after the 2000 to 6000 με range used in this calculation. This anomaly can be seen in the shear strain range of .01 to .015 radians in Figure 7-1.
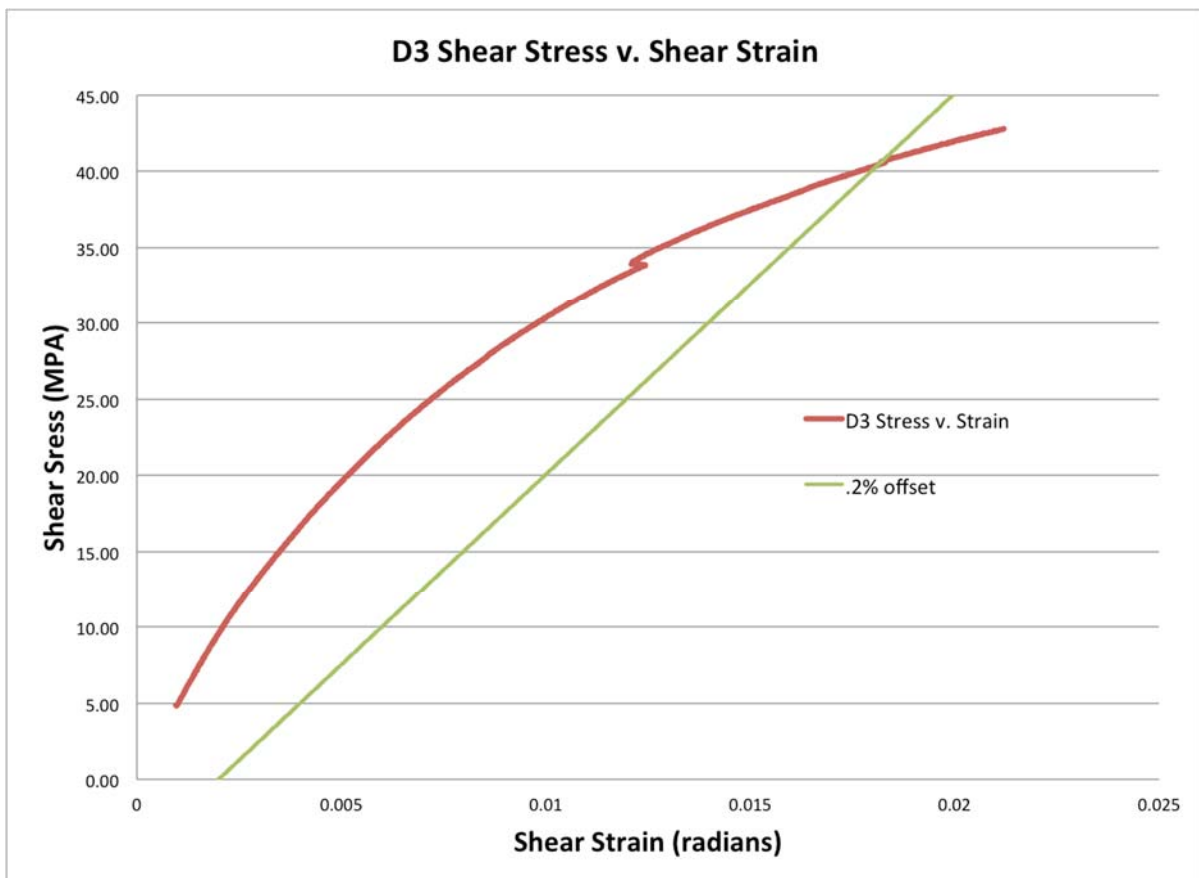
Figure 7-1: GFRE Specimen D3's Shear Stress v. Shear Strain Curve Showing Strain Gage Failure

Also in Figure 7-1 it can be seen that one or more of the strain gages failed at about 2.2% shear strain (.022 radians) because there is no more stress/strain curve after this point. This is an example of a gage failing before the 5% strain point required to calculate the maximum shear stress/shear strain as required by ASTM D3518.

7.3.1 Data Associated With Both In Situ and Accelerated Specimens

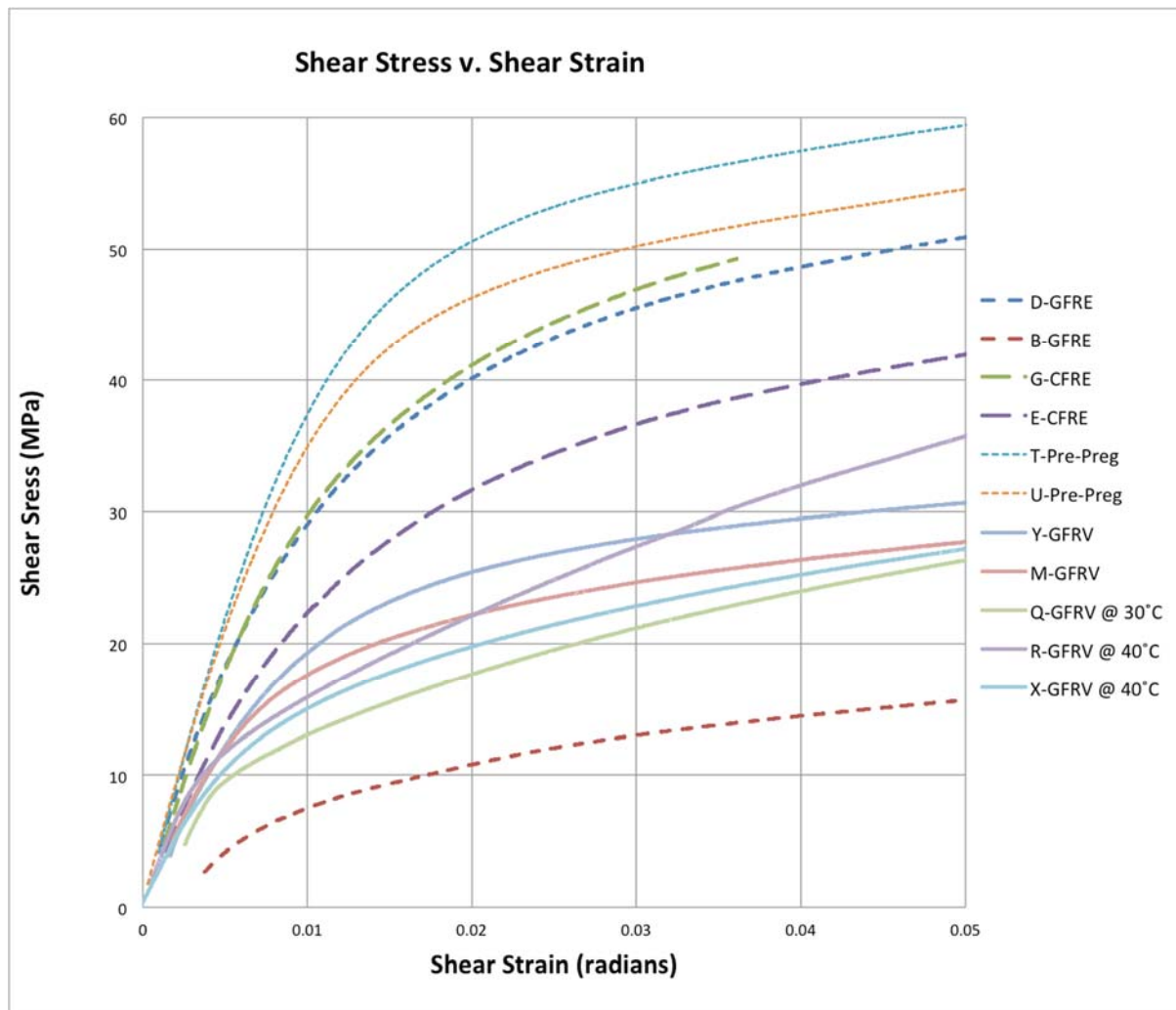Figure 7-2 shows the typical shear stress v. shear strain curve obtained from each material system.

Figure 7-2: Typical Shear Stress v. Shear Strain Curves for All Panels

It can be seen in this figure that panel G is the only material system and exposure combination that does not have at least one specimen reach 5% strain before strain gage failure occurs. The large range of shear moduli calculated for each panel and exposure combination can clearly be determined in this figure as well, with the as-produced Pre-Preg panel ,T, achieving the highest shear modulus and the exposed GFRE panel ,B, achieving the lowest.

In Figure 7-2 the strains do not start at zero for most of the specimens because a preload was applied before the recording of the data started. During the last days of testing, this preload was lowered or removed, so some of the specimens do have initial strains that started at or near zero.

Figure 7-3 shows the typical tensile stress v. tensile strain curve for each material system. These curves are obtained from a typical specimen in the named panel and not the mean of all the specimens in a given panel. The strain data used to produce these curves is taken from the crosshead displacement.
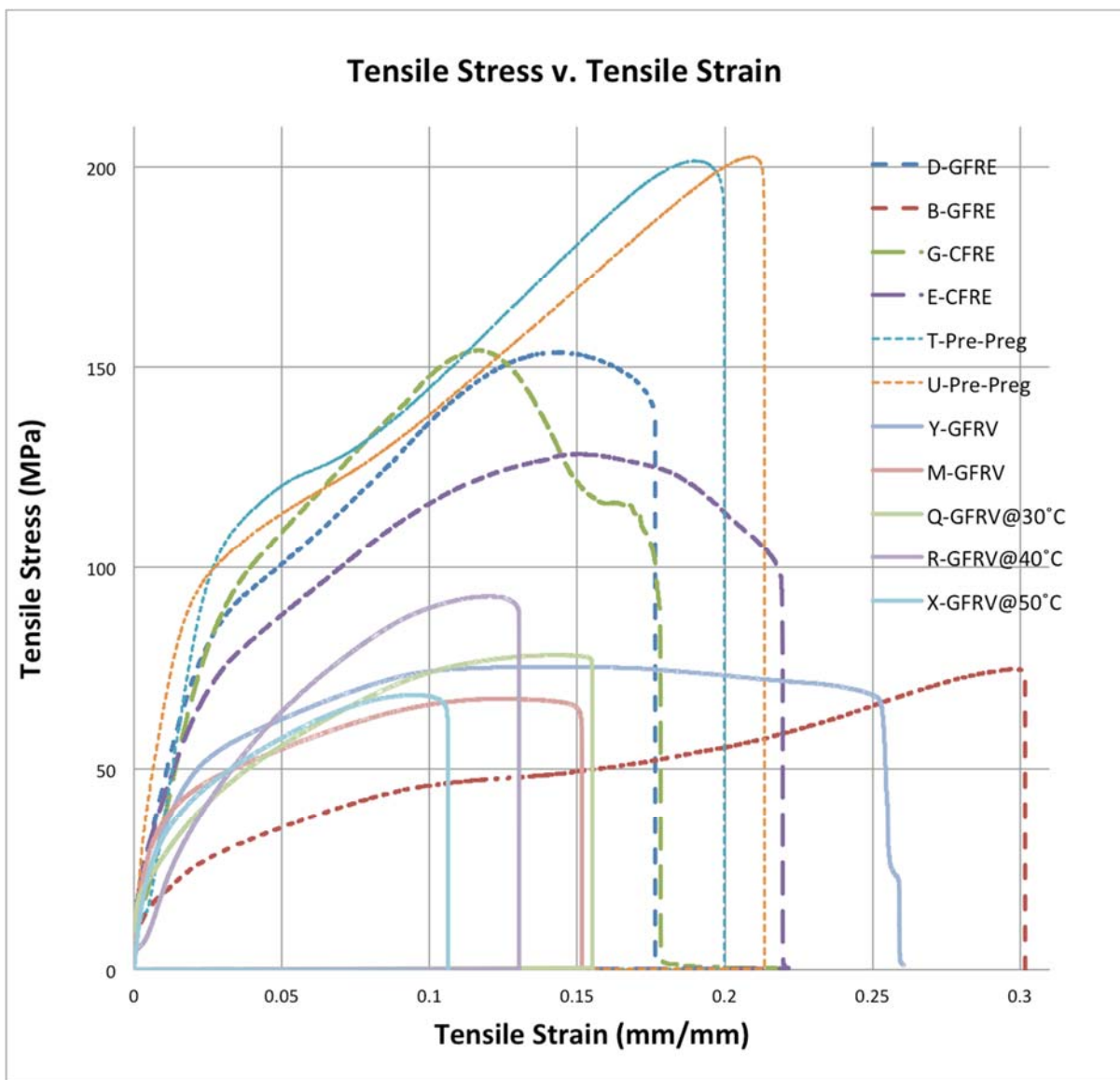
Figure 7-3: Typical Tensile Stress v. Tensile Strain Curves for All Panels

In this figure it can be seen that the Pre-Preg panels, T and U, obtain the highest tensile stress by far. The as-produced GFRE and CFRE panels, D and G, obtain very similar stress and strain values but after nine months exposure the GFRE panel, B, loses a large amount of tensile stress, and gains a large amount of tensile strain. While the exposed CFRE panel, E, dose lose some stress and gain some strain, it is not too much different than the as-produced panel. One big difference between panels G and E though is in the manner in which they fail, panel G fails more gradually and has a short leveling of the stress values right before failure while panel E shows some gradual failure but does not have any leveling off before failing completely.

The values in Figure 7-3 do not start at 0,0 because of the preload that was applied to the specimens before testing to prevent the jaws from slipping, as discussed in 7.1. The crosshead position is zeroed after the preload is applied, which is why all the specimens start at zero strain but have some amount of positive stress at this zero strain.

Table 7-2 presents the results of the statistical calculations completed on each of the panels. The mean values from this table are presented graphically in Figure 7-4 to Figure 7-10.

Table 7-2: All Statistics Calculated for All Panels

Material System		% necking	Shear Modulus Slope (GPa)	Yield Shear Stress (MPa)	Yield Shear Strain (%)	Shear Stress at 5% Shear Strain	Tensile Modulus Slope (GPa)	Max Load (N)	Max Load Tensile Stress (MPa)	Max Load Tensile Strain (%)
GFRE (D and B)	Mean	13.08%	2.47	35.93	1.67%	48.85	9.09	8329.79	152.44	14.39%
	Standev	3.19%	0.05	1.74	0.04%	1.87	0.27	81.81	3.42	0.13%
	Coef of Variation	24.37%	2.05%	4.85%	2.55%	3.83%	2.92%	0.98%	2.24%	0.87%
	Mean	25.08%	0.84	8.39	1.21%	15.49	3.23	4168.40	74.99	30.11%
	Standev	0.55%	0.07	0.58	0.14%	0.27	0.25	20.94	1.12	0.58%
	Coef of Variation	2.18%	7.90%	6.95%	11.93%	1.74%	7.69%	0.50%	1.49%	1.93%
CFRE (G and E)	Mean	36.93%	3.29	32.31	1.18%	Unknown	12.25	7557.83	150.75	11.57%
	Standev	2.88%	0.09	0.29	0.02%	Unknown	0.51	57.51	3.68	1.15%
	Coef of Variation	7.81%	2.81%	0.89%	1.81%	Unknown	4.18%	0.76%	2.44%	9.95%
	Mean	30.97%	2.44	25.44	1.25%	42.31	9.06	7280.19	129.52	15.28%
	Standev	3.58%	0.03	0.26	0.02%	0.56	0.13	264.86	1.95	0.81%
	Coef of Variation	11.55%	1.26%	1.04%	1.25%	1.33%	1.47%	3.64%	1.50%	5.30%
Pre Preg (T and U)	Mean	11.93%	4.11	43.56	1.26%	59.53	15.72	11369.76	202.68	18.75%
	Standev	0.18%	0.08	2.54	0.06%	0.16	0.10	164.70	3.61	0.24%
	Coef of Variation	1.53%	1.84%	5.83%	4.73%	0.27%	0.64%	1.45%	1.78%	1.26%
	Mean	12.55%	3.83	39.22	1.23%	55.05	14.41	11427.09	203.39	21.10%
	Standev	0.93%	0.05	0.38	0.02%	0.47	0.11	112.98	0.76	0.28%
	Coef of Variation	7.42%	1.23%	0.96%	1.66%	0.85%	0.79%	0.99%	0.37%	1.31%
GFRV (Y,M,Q,R and X)	Mean	32.05%	2.22	21.04	1.15%	30.65	8.44	4324.81	75.26	12.02%
	Standev	3.33%	0.04	0.54	0.02%	0.48	0.59	185.84	2.65	2.65%
	Coef of Variation	10.39%	1.96%	2.55%	1.80%	1.56%	6.95%	4.30%	3.53%	22.07%
	Mean	14.12%	1.94	18.04	1.13%	26.47	7.10	3316.85	65.12	10.78%
	Standev	4.15%	0.05	0.54	0.01%	1.12	0.27	73.07	2.01	0.92%
	Coef of Variation	29.39%	2.76%	2.98%	1.15%	4.24%	3.84%	2.20%	3.08%	8.56%
	Mean	12.56%	1.38	14.17	1.21%	26.34	5.68	4364.24	79.40	13.89%
	Standev	1.67%	0.14	1.08	0.18%	N/A	0.61	91.13	1.56	0.35%
	Coef of Variation	13.29%	10.13%	7.61%	14.93%	N/A	10.69%	2.09%	1.96%	2.55%
	Mean	7.56%	1.50	17.78	1.39%	35.73	6.18	5265.01	94.93	11.74%
	Standev	0.70%	0.06	1.12	0.11%	N/A	0.33	80.87	2.96	0.27%
	Coef of Variation	9.28%	4.31%	6.32%	8.20%	N/A	5.40%	1.54%	3.12%	2.34%
	Mean	8.17%	1.49	16.62	1.32%	25.81	5.87	3832.24	67.16	9.55%
	Standev	1.85%	0.07	0.69	0.06%	1.41	0.16	99.38	1.73	0.41%
	Coef of Variation	22.70%	4.97%	4.17%	4.17%	5.44%	2.76%	2.59%	2.58%	4.34%

Figure 7-4 shows the mean shear modulus calculated for all panels. The sample standard deviation is so small for these values that they could not be meaningfully displayed on the figure, these values are presented later in the study.
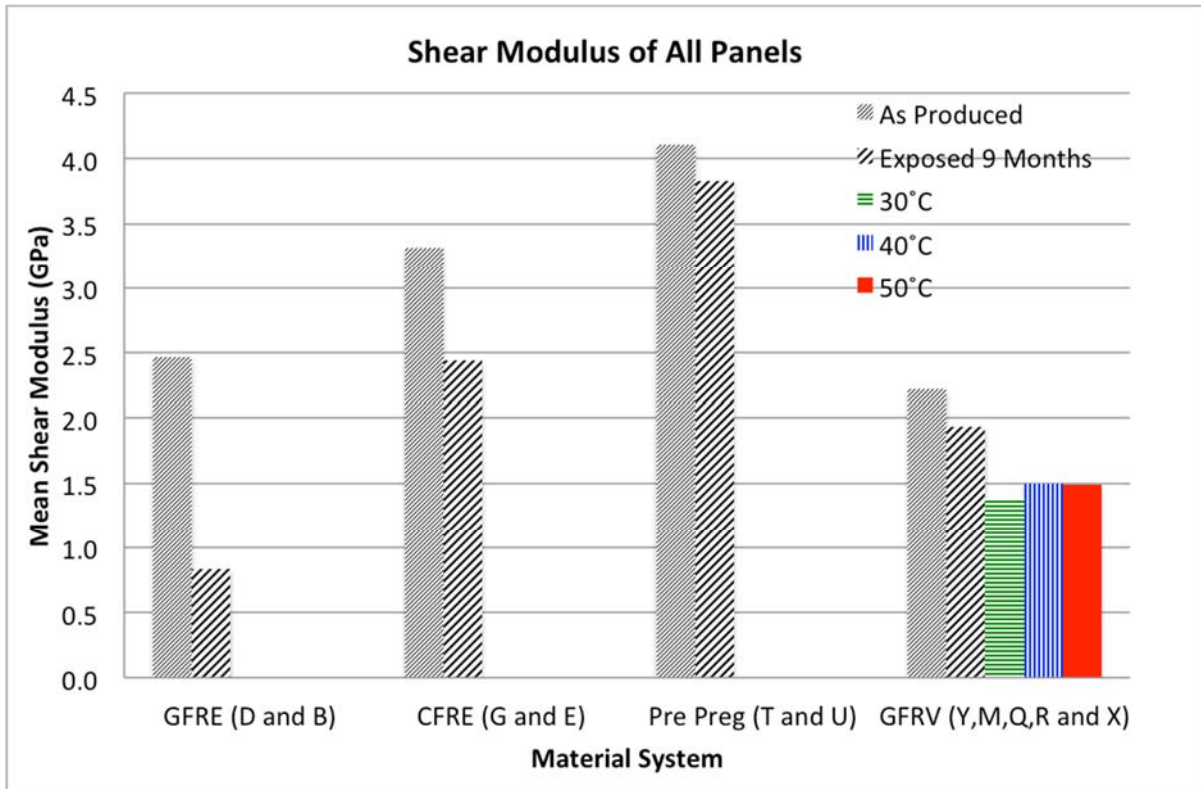

Figure 7-4: The Mean Shear Modulus for All Panels

It can be seen in Figure 7-4 that, for all materials systems, the shear modulus is reduced following exposure to the marine environment. The GFRE system experiences the largest reduction, while the Pre-Preg has the smallest.

Figure 7-5 shows the shear stress at yield calculated by the 0.2% offset method.
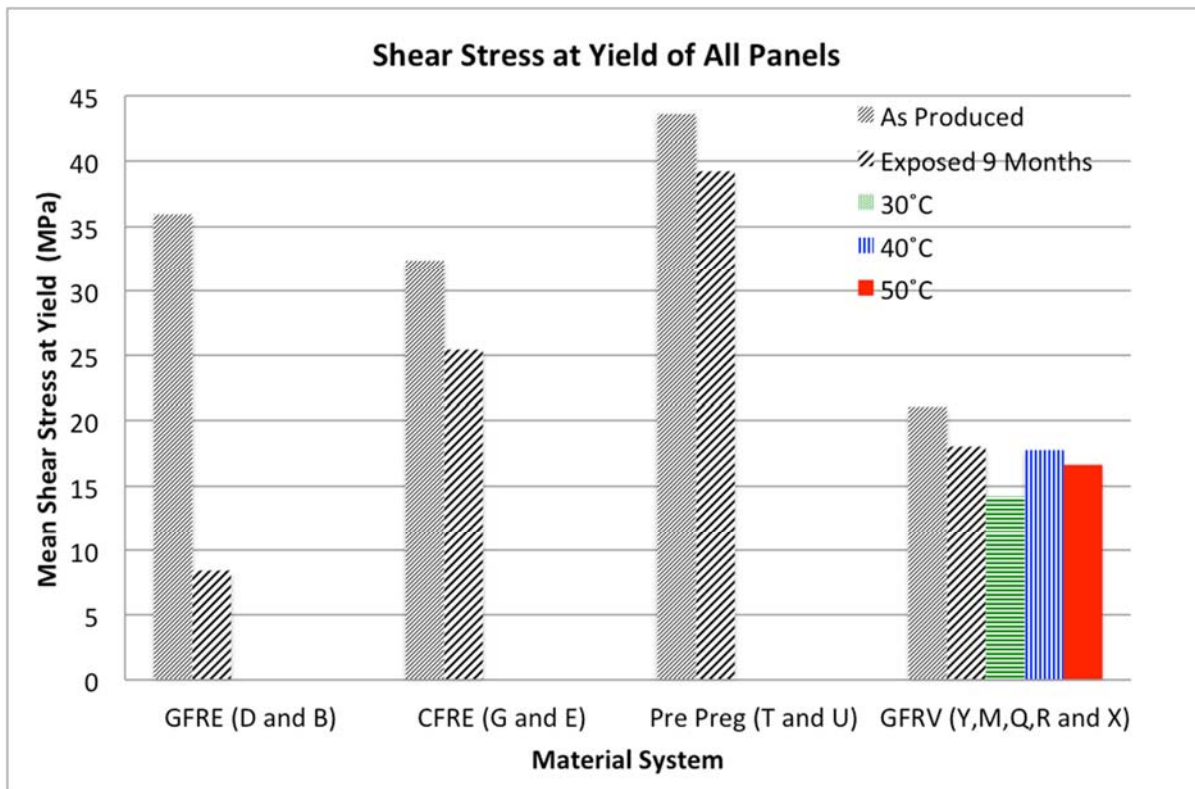
Figure 7-5: The Mean Shear Stress at Yield Determined From the 0.2% Offset Method

In Figure 7-5 the shear stress at yield decreased for all panels, with the GFRE system having the most severe change again. The mean calculation is based on a sample size of four for all panels except for D, G and Q which all use a sample size of three.

Figure 7-6 shows the shear strain at yield calculated by the 0.2% offset method.
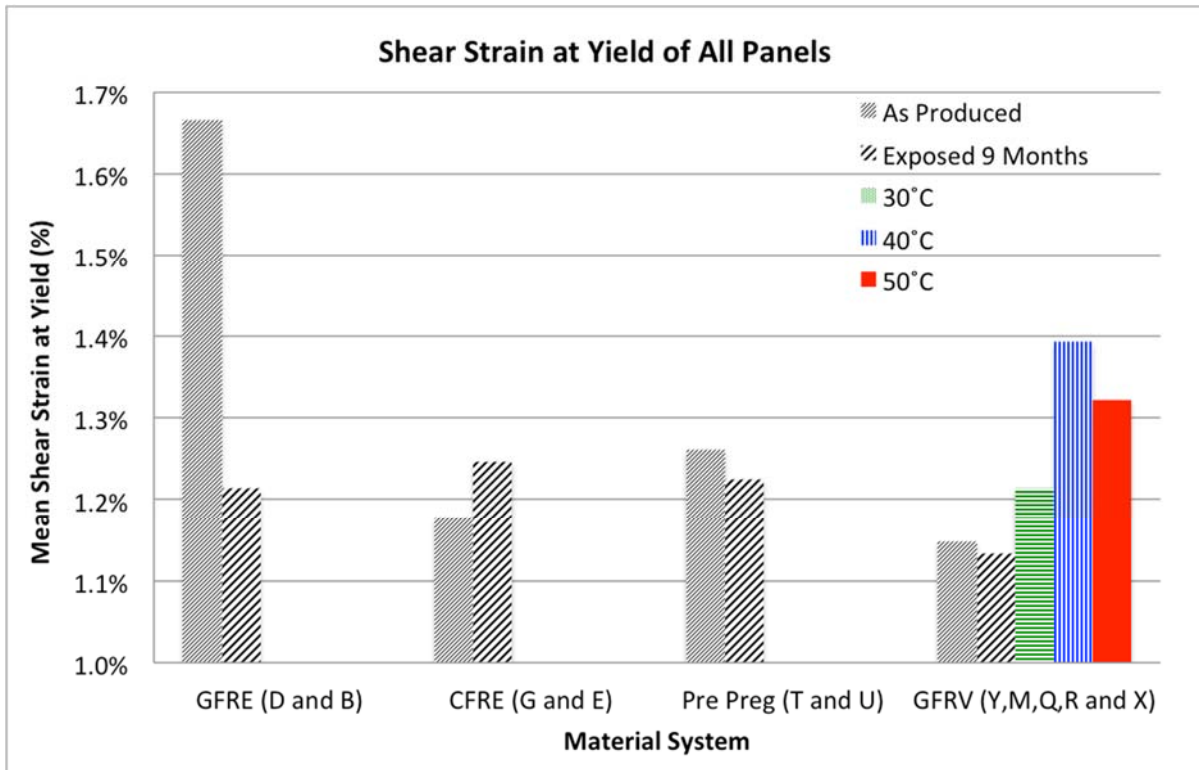
Figure 7-6: The Mean Shear Strain at Yield Determined From the .2% Offset Method

In Figure 7-6 it is very apparent that the GFRE system had the greatest change in the shear strain at yield but in this case not all the systems had a decrease in the percentage of strain. The CFRE panel that has been exposed for nine months has an increase in strain, as did all the GFRV panels that are exposed to the warm saltwater baths in the lab.

Figure 7-7 is the maximum shear stress calculation as required by the ASTM D3518. As described in 7.1, the strain gages on many specimens failed before the 5% shear strain point was reached.
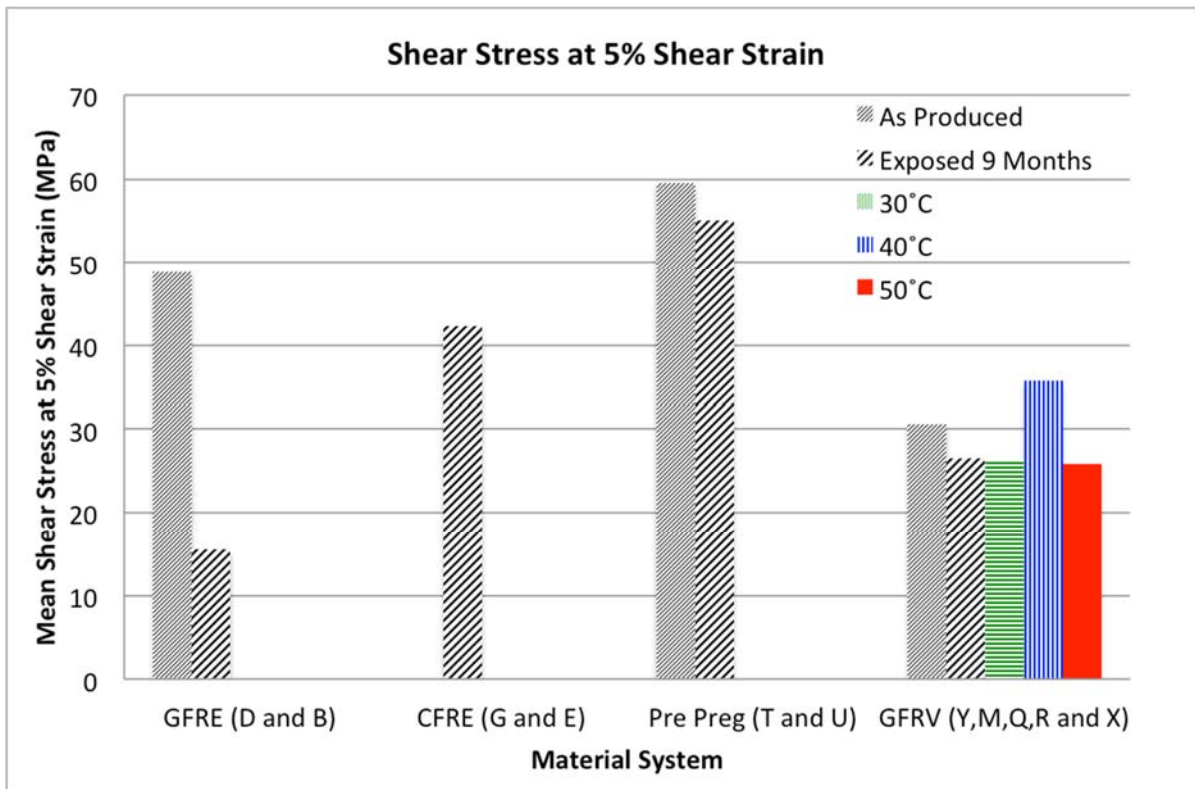
Figure 7-7: Shear Stress at 5% Shear Strain for All Panels

The conclusions that can be draw from examining Figure 7-7 are not as robust as those that can be drawn from the other data presented because of how few of the strain gages reached the 5% shear strain point. For example the mean values for panels Q and R are based off of a sample size of one, while panel G has no data at all.

Figure 7-8 shows the mean tensile modulus calculated for all panels.
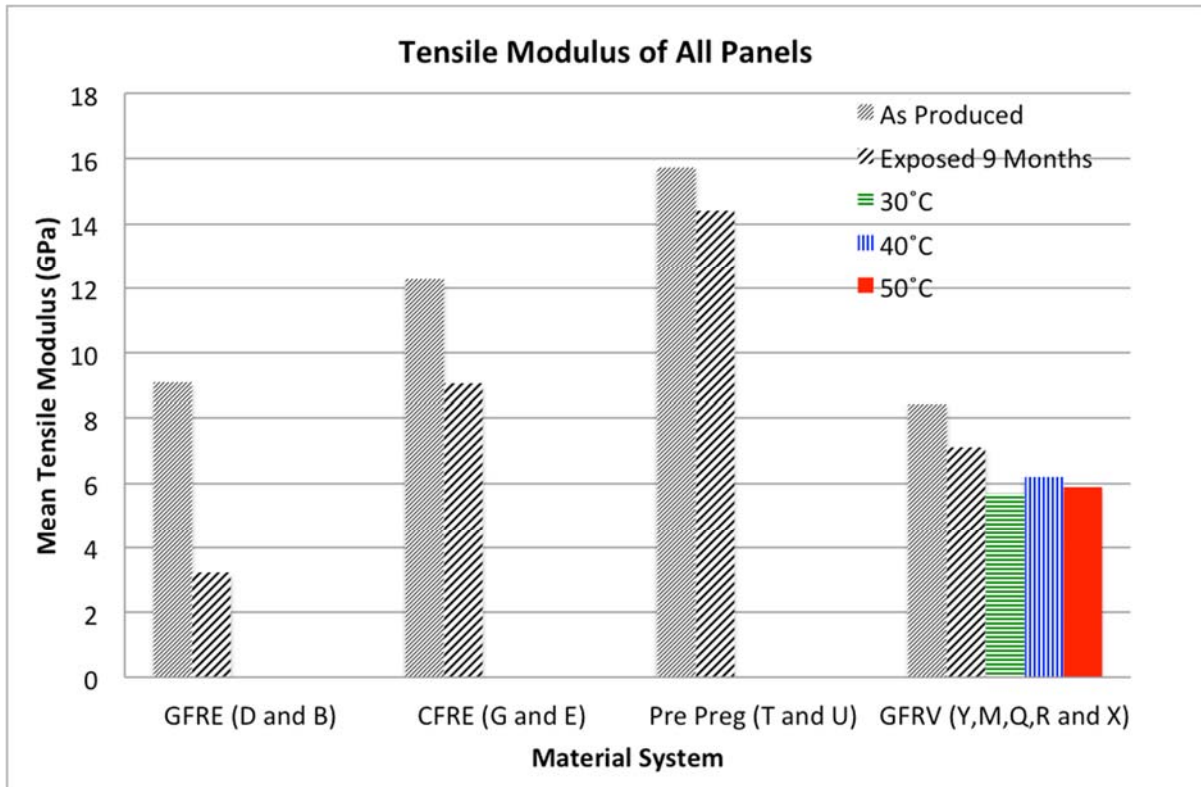
Figure 7-8: Tensile Modulus of All Panels Obtained from Crosshead Displacement

It can be seen in Figure 7-8 that all of the exposed systems lose some amount of tensile modulus. Similar to the shear modulus results, the GFRE system has the largest change in tensile modulus and the Pre-Preg system has the smallest change.

Figure 7-9 shows the maximum load that is achieved by all panels. Because this figure does not take into account the differences in cross-sectional area between panels, it is not as accurate or useful a gage of differences between panels as the stress and strain figures.
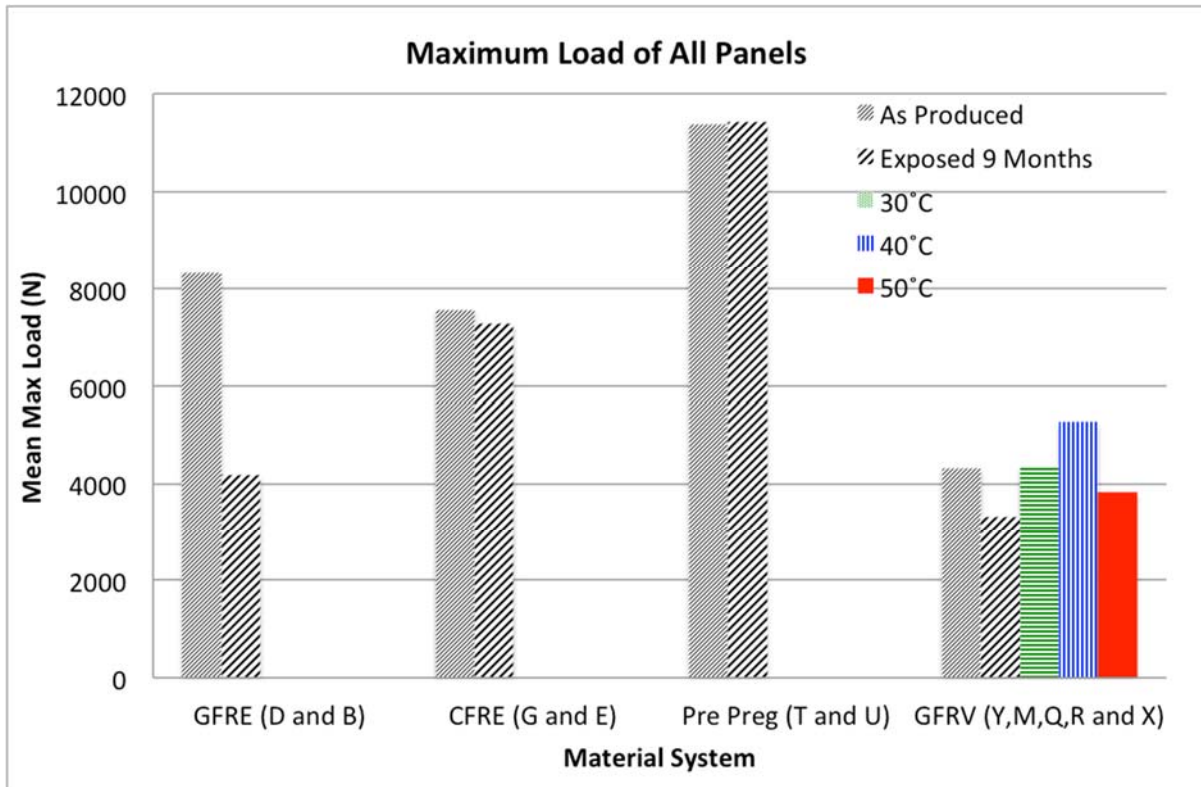
Figure 7-9: Maximum Load Achieved by All Panels

Figure 7-10 Shows the tensile stress and tensile strain achieved by each panel at the maximum load shown in Figure 7-9.
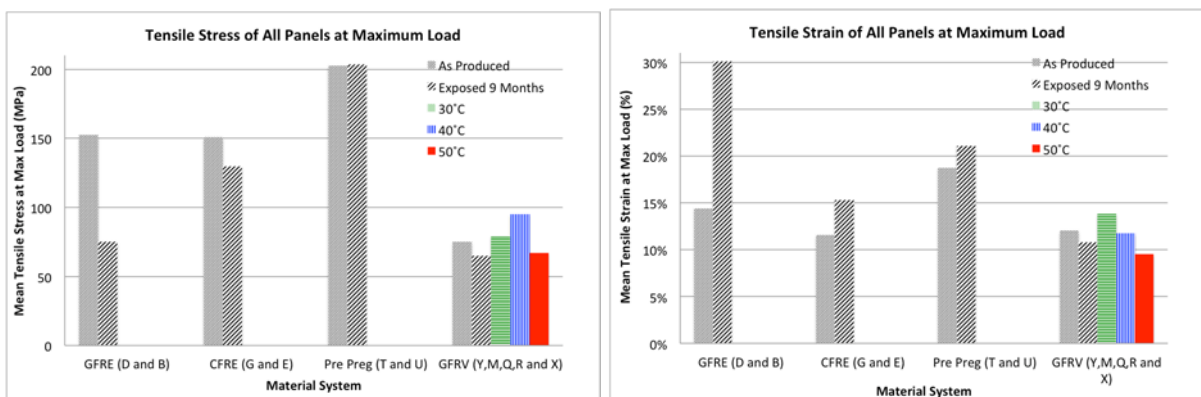
Figure 7-10: Tensile Stress and Strain Achieved by All Panels

The tensile stress figure looks very similar to the max load figure because the cross-sectional area of all the specimens was very close. The tensile strain figure shows how almost all of the panels allowed for more strain after exposure, with the exception of some of the panels made from the GFRV system. All the data involving maximum load

calculations uses a sample size of four because there are no inconsistencies noticed in any of the load or crosshead displacement data. This is partially important because all the data comes from Instron's Bluehill software, so there was no interfacing needed between the Bluehill and Strain Smart software.

Figure 7-11 shows the mean necking measured for each of the systems.
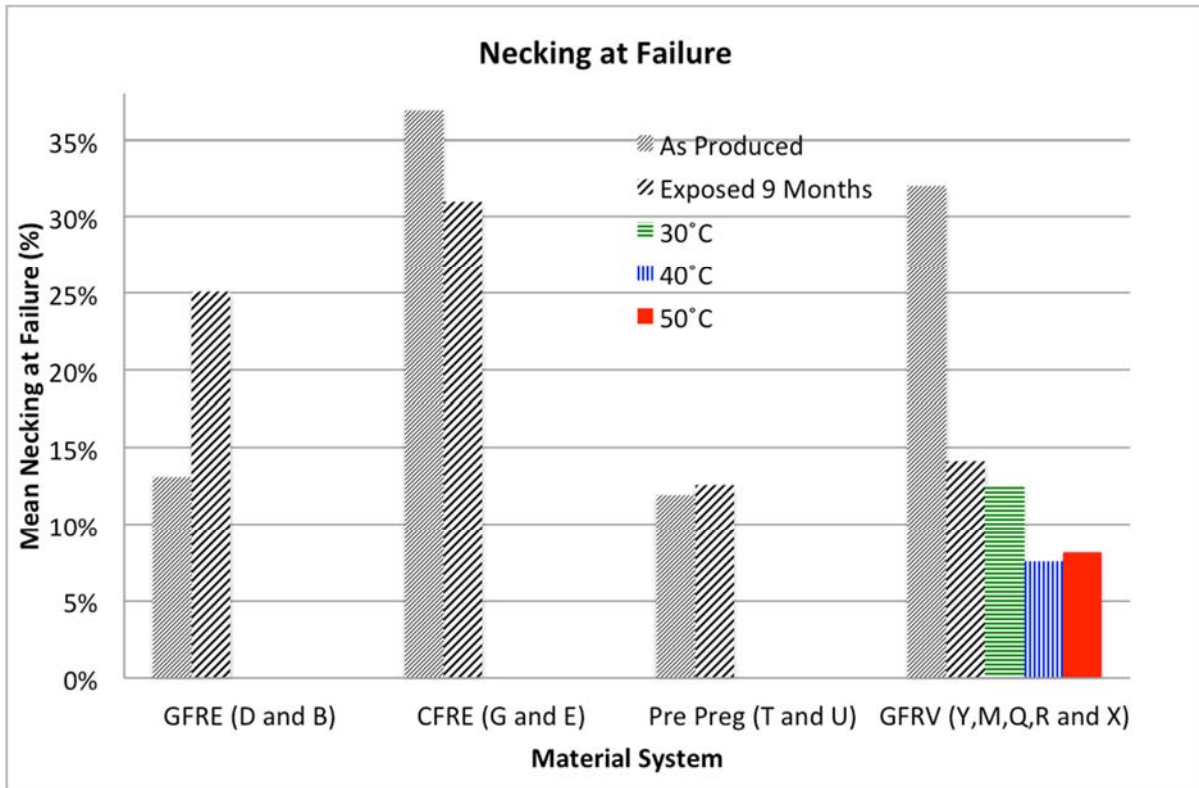
Figure 7-11: Percentage of Necking at Failure for All Panels

The determination of the percentage of necking is difficult because it is completed after the specimens have already fractured into two pieces. This means that judgment has to be used to best determine the narrowest point of a specific specimen before it fractured. This is part of reason why the coefficient of variation is higher for the calculation of these means than for any other mean calculation.

Figure 7-12 shows all of the specimens after testing.

Figure 7-12: All Specimens After Testing

It can be seen in Figure 7-12 that all of the specimens of a particular panel failed in roughly the same manner and none of the specimens failed in the grips. The color change experienced by the specimens can also be seen in the fiberglass reinforced systems. The GFRE system changed from slightly transparent to opaque white, while the GFRV system changed from a greenish tinged transparent to opaque white.

Figure 7-13 shows a close up of the fracture types experienced by each material system. The order was rearranged from Figure 7-12 so that each system type can more easily be compared.

All ten panel specimen fracture types. First row: D,B (GFRE) and G. Second row: E (CFRE),T and U (Pre-Preg). Third row Y, M and Q. Forth row: X (GFRV)

Figure 7-13: Example Fracture Types Experienced by Each Panel

During testing, the noises produced by each specimen were noted. In general those specimens that failed explosively gave very little indication that failure was imminent. Panels D, B, M, Q and X fit this category. Panels G, E and Y emitted small snapping and clicking sounds for the 30 to 120 seconds leading up to final failure. Panels T and U emitted snapping sounds associated with rapid fiber failure about 10 seconds before explosively fracturing. The fracture of panels T and U was also associated with the throwing of fibers in the range of 10 to 15 mm in length, while the other panels did not throw fibers large enough to be seen. Figure 7-14 shows a T panel specimen seconds before final explosive failure.

Figure 7-14: Pre-Preg Specimen T1, Seconds Before Final Fracture

Evidence of fiber fracturing and ply delamination can be seen in Figure 7-14.

7.3.2 In Situ Specific Data

Weight changes for the panels that were exposed in the Puget Sound for 9 months can be see in Table 7-3.

Table 7-3: Summary of Weight Gain of 9 Month Exposure Panels

Panel	Initial weight (grams)	Weight with biofouling ±.05 (grams)	Weight after biofouling removed (grams)**	Weight after drying (grams)	Difference between initial and final (grams)	Percent change
B	154.08	194.15	164.91	164.34	10.26	6.24%
E	128.11	154.7	133.64	132.23	4.12	3.12%
U	157.64	160.45	158.44	158.39	0.75	0.47%
M	150.96	219.98	159.95	157.11	6.15	3.91%

** Although most biofouling was removed, some was left on one side of each panel so that macroscopic and microscopic examination could be more accurately completed

Because of the addition of biofouling and the inability to remove all of the biofouling without damaging the panels, the differences between the initial and final weights are not meaningful. It is also suspected that some weight loss occurred due to wallowing of the mounting holes over repeated exposure to strong tidal currents.

Figure 7-15 shows one mounting hole each from panel M and panel B.
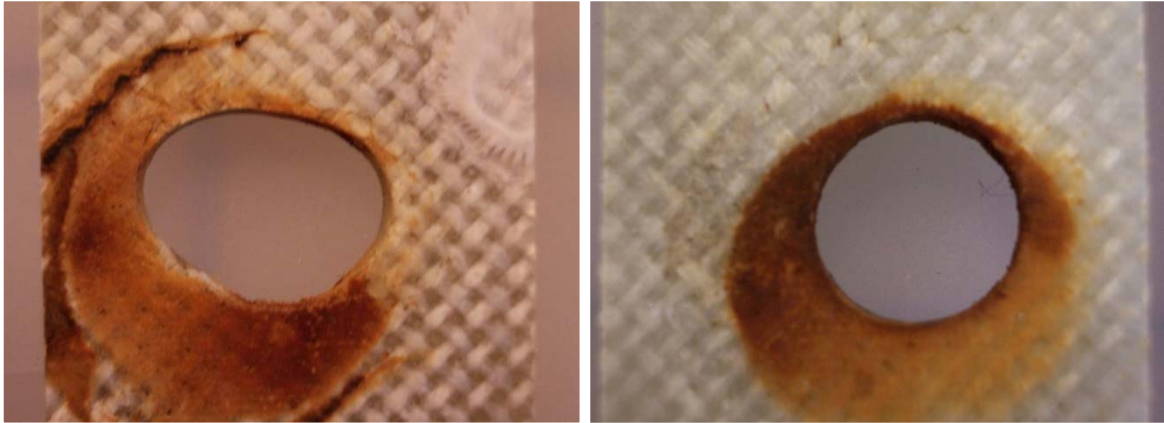
Figure 7-15: Mounting Holes After Exposure Panel M on the Left, B on the Right

Figure 7-15 indicates that some panels experience more wallowing than others during exposure. GFRV panel M experienced the worst wallowing, while GFRE panel B is representative of the rest of the panels.

Figure 7-16 shows the differences in biofouling observed for the different material systems.
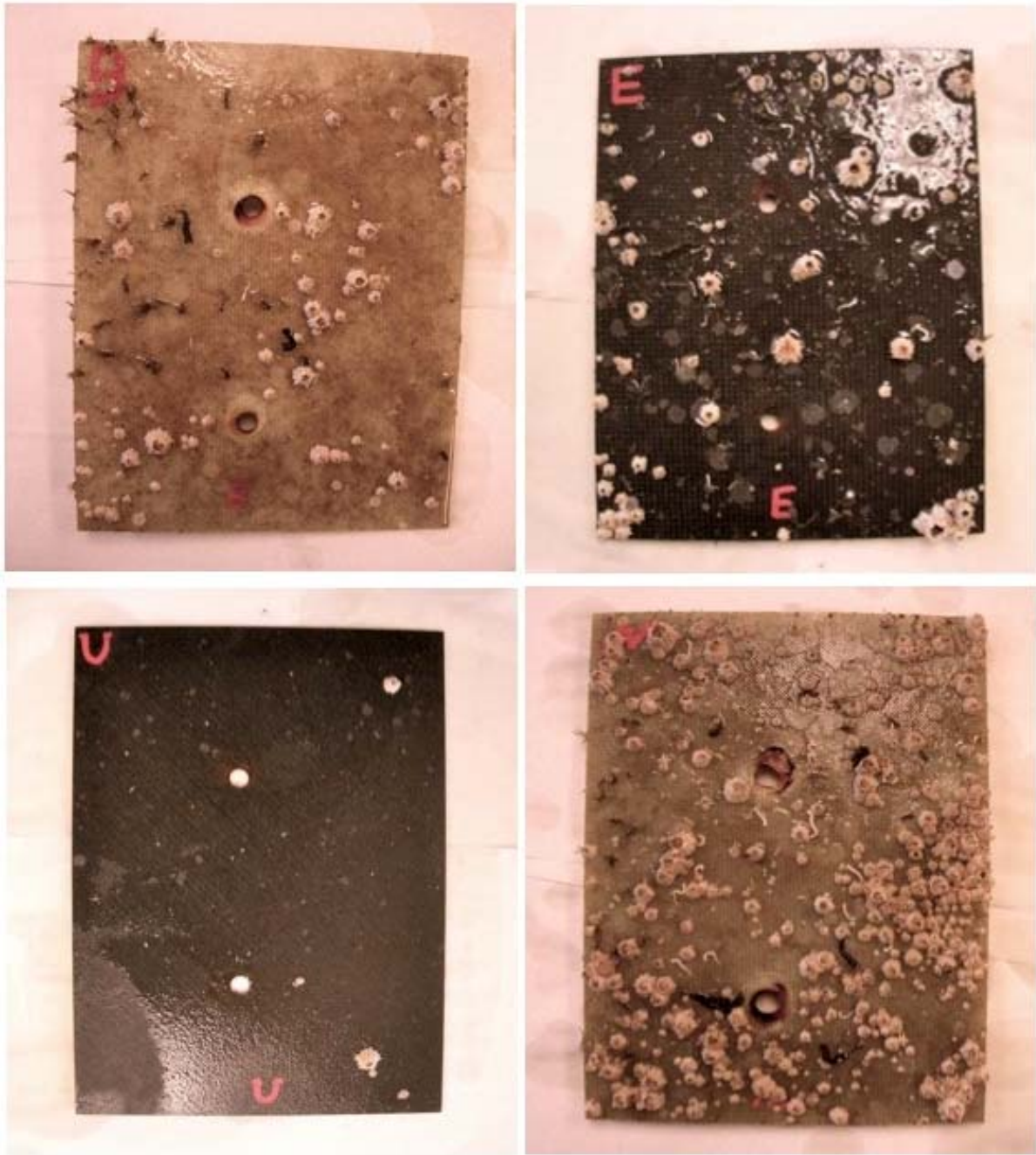
Figure 7-16: Biofouling Accumulation On Side A of Panels B,E,U and M

All the images in Figure 7-16 are of side A because this is the rougher side, and in general there was more biofouling on this side.

There was concern that the biofouling residue left on the panels after cleaning would affect the stress and strain values obtained from testing. During testing the residue was observed to begin to flake off around 2% shear strain and be completely gone by about

4% shear strain. After the residue fell off, the area where the residue was appeared no different than the areas where it wasn't. Figure 7-17 shows some biofouling residue on CFRE specimen E1 specimen during testing, and how the residue detached with strain.
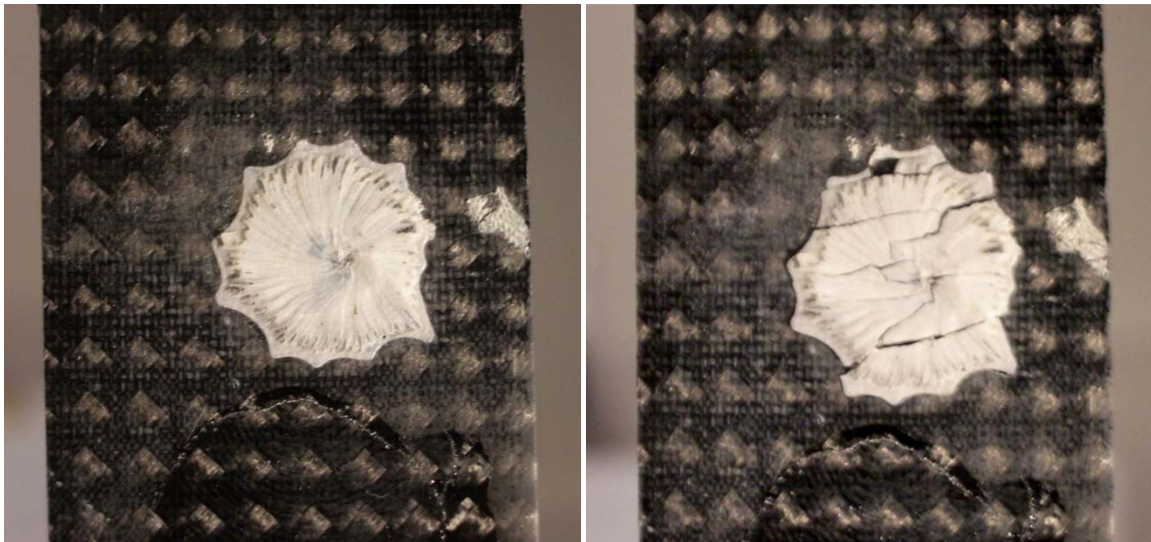
Figure 7-17: Biofouling Residue on CFRE Specimen E1: 0% Strain on the Left, 2% Shear Strain on the Right

7.3.3   Accelerated Exposure Specific Data

Figure 7-18 shows the temperature profile of the saltwater baths that the GFRV panels which were subjected to accelerated exposure in the lab were placed in.
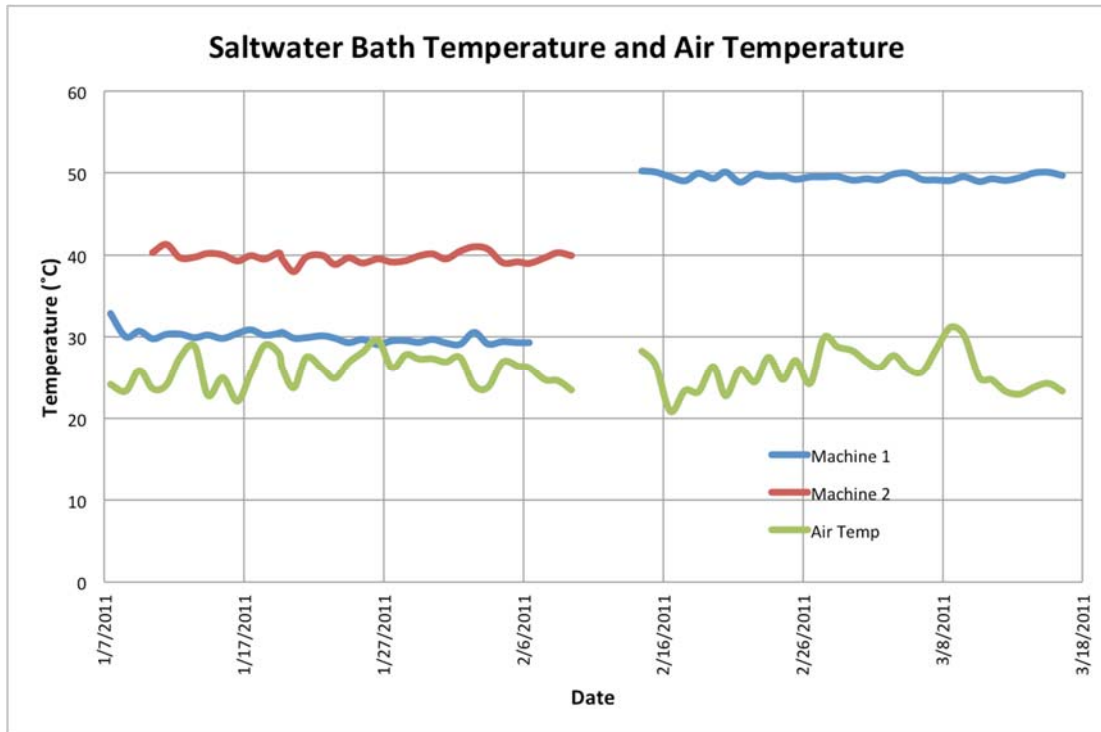
Figure 7-18: Saltwater Bath and Air Temperatures of GFRV Panels Q, R and X During Exposure

It can be seen in Figure 7-18 that the water bath temperatures vary very little over the 30 day exposure time, even though the air temperature vary approximately a 10 degree range. Panels Q and X were exposed in machine 1, and panel R was exposed in machine 2.

All of the panels experience weight gain during exposure. Table 7-4 summarizes the weight gain calculated by weighing the panel before exposure and then again after exposure.

Table 7-4: Summary of Weight Gain of Accelerated Exposure Panels

Panel	Exposure Temperature (°C)	Initial Weight (grams)	Final Weight (grams)	Weight Difference (grams)	Percent Change	Initial Specific Gravity	Final Specific Gravity
Q	30	191.90	192.77	0.87	0.45%	1.024 @ 24°C	1.023 @ 27°C
R	40	193.29	194.23	0.94	0.48%	1.021 @ 24°C**	1.020 @ 27°C
X	50	188.67	190.01	1.34	0.71%	1.021 @ 23°C	1.023 @ 21°C

** This is the specific gravity for the second batch of saltwater made for panel R after the machine had sprung a leak.

Table 7-5 shows the differences in initial and final weights of the panels by using the weights obtained from the balances.

Table 7-5: Summary of Balance Weight Change of Accelerated Exposure GFRV Panels

Panel	Exposure Temperature (°C)	Initial Weight Shown on Balance (grams)	Final Weight Shown on Balance (grams)	Weight Difference (grams)	Percent Change
Q	30	75.04	76.13	1.09	1.43%
R	40	136.74	137.92**	1.18	0.86%
X	50	69.52	73.38	3.86	5.26%

** This panel had large weight changes after machine #2 sprung a leak.

The possible reasons for the differences in weight gains between those reported in Table 7-4 and those reported in Table 7-5 are discussed in section 8.2.

Figure 7-19 shows the weight gain and barometric pressure recorded during the accelerated exposure of GFRV panels Q, R and X.
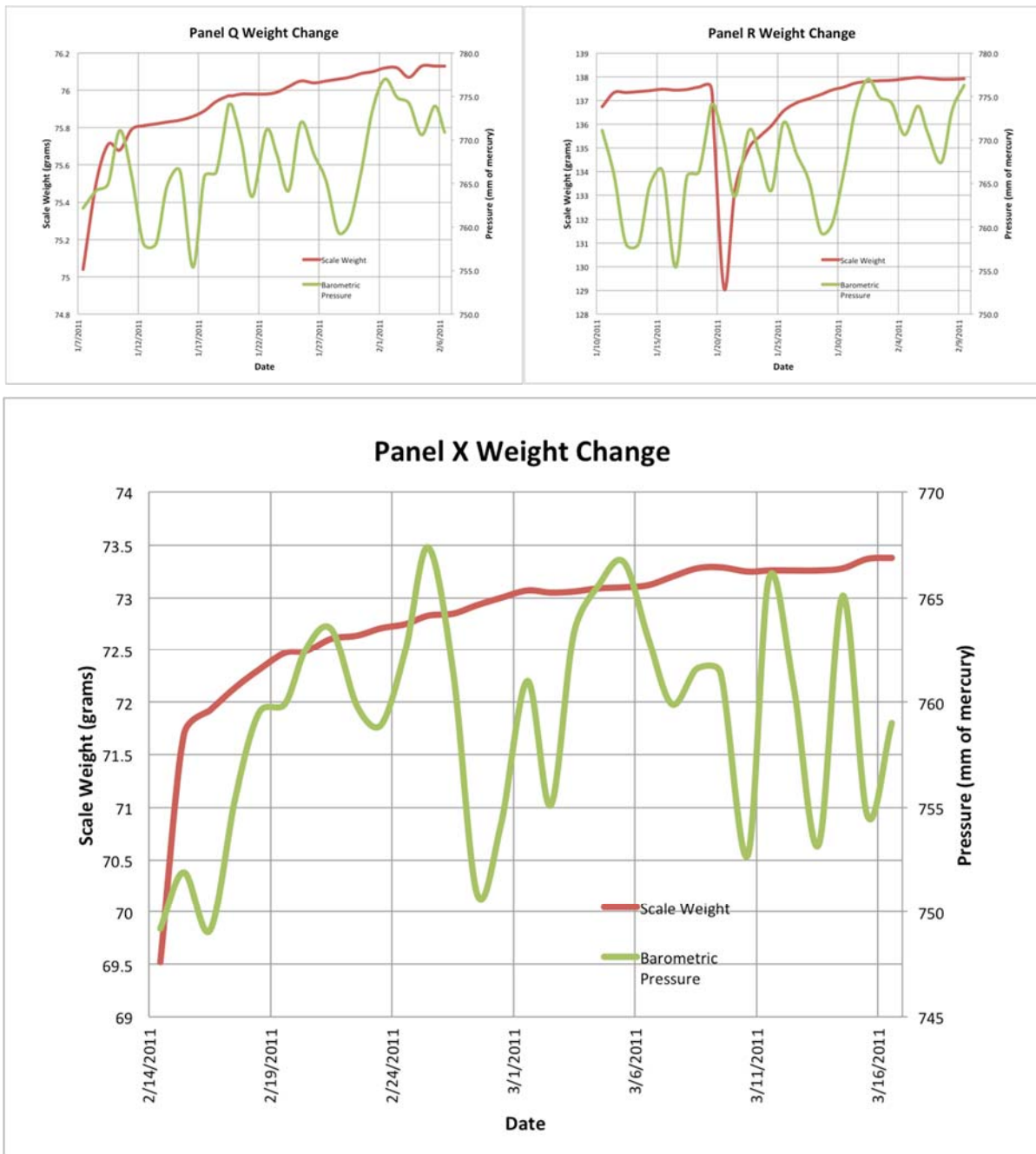
Figure 7-19: The Weight Gain and Barometric Pressure Recorded During Accelerated Exposure for GFRV Panels Q (30°C Exposure), R (40°C), and X (50°C)

Figure 7-20 shows the weight change of panels Q and X plotted with the percent mass change v. the square root of time as was done in much of the literature that was reviewed.
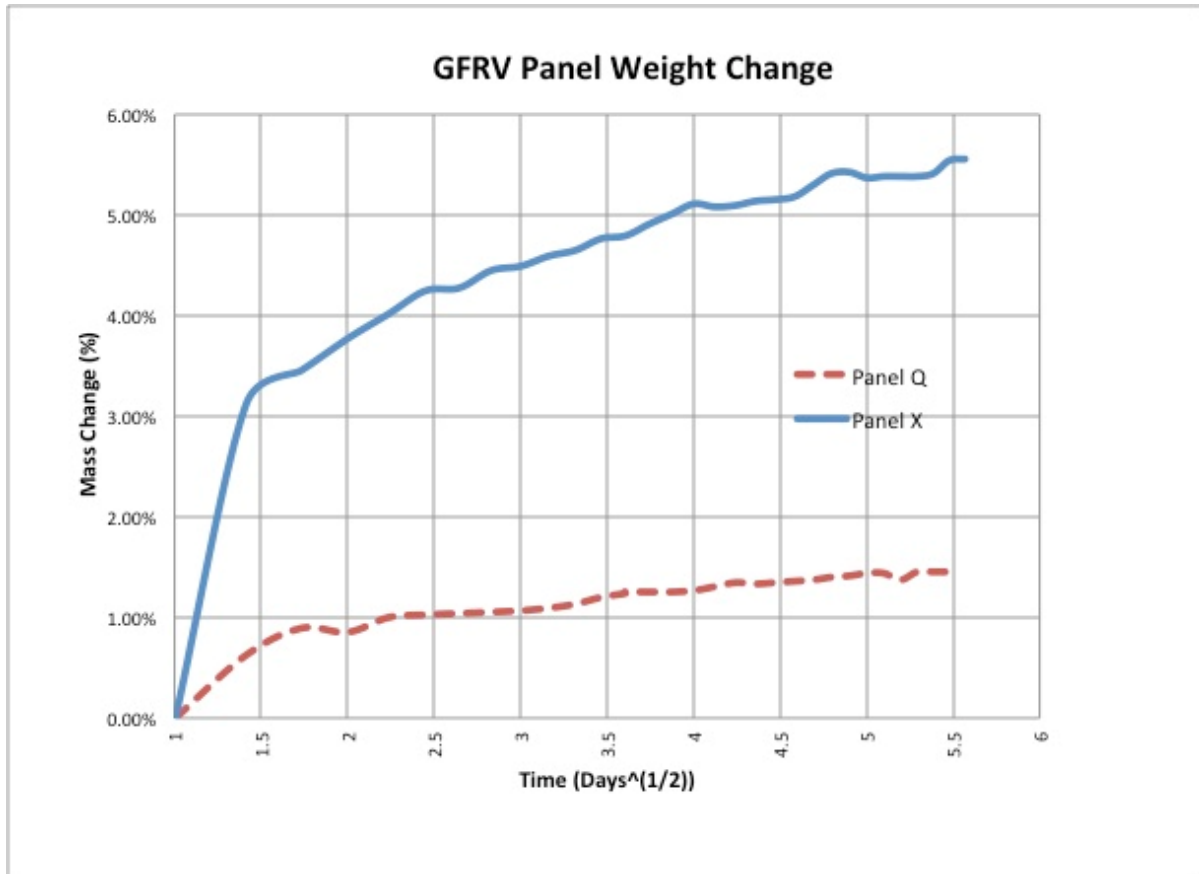
Figure 7-20: Accelerated Weight Gain of GFRV Panels Q (30°C Exposure) and X (50°C Exposure)

Panel X's water required replenishment during the test due to evaporation. 500 mL of distilled water was added four times; on February 9th and 26th and March 6th and 14th. The total volume of water at both the beginning and end of the exposure time period was approximately nine liters. The addition of water did not have a noticeable affect on the weight indicated by the balance.

The large drop in weight experienced by panel R beginning on the 19th of February coincides with when machine #2 developed a leak and, to effect repairs, the saltwater had to be emptied and replaced with newly made saltwater. This event and the large associated weight change rendered the data collected for panel R unusable.

In Figure 7-21 it can be seen that there was a change in color due to the panels being subjected to accelerated exposure.
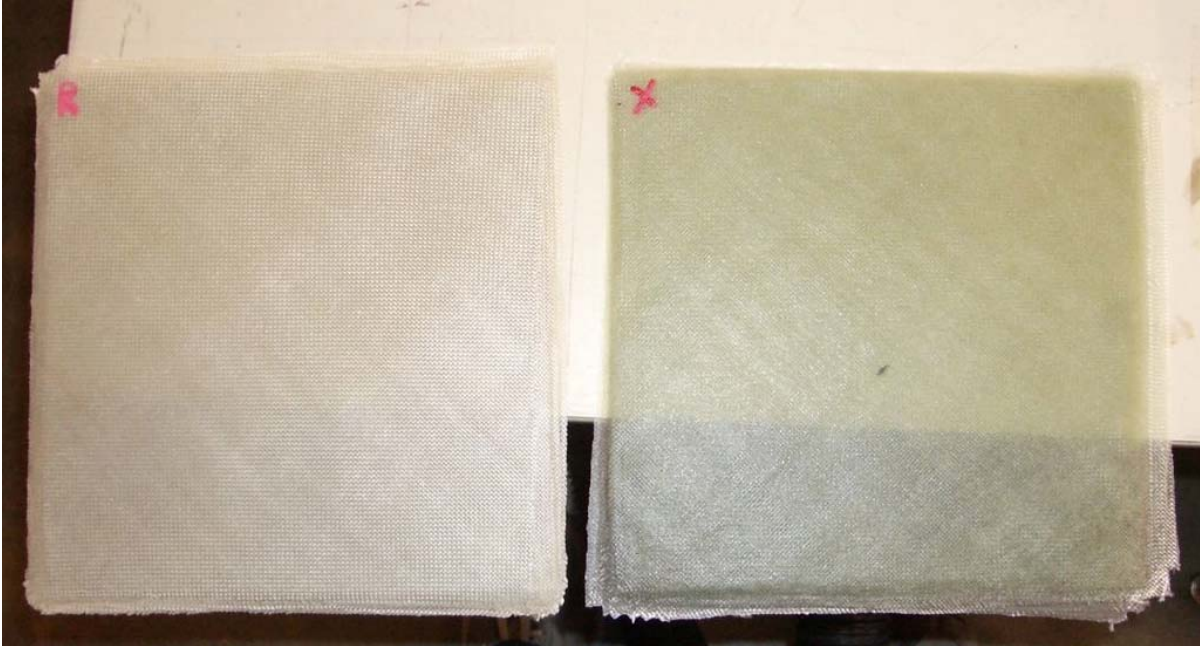
Figure 7-21: Color Difference After and Before Exposure of GFRV Panels

The panel on the right is panel R after it had been removed from the saltwater bath and before it had been dried in the oven. The panel on the left is panel X a few days before it was placed in the saltwater bath. Panel R is less transparent and has less of a green tinge to it than panel X does.

7.3.4   Statistical Significance of Shear Modulus Calculations

Figure 7-22 shows the shear modulus calculations of the as-produced panels and those that were exposed nine months.
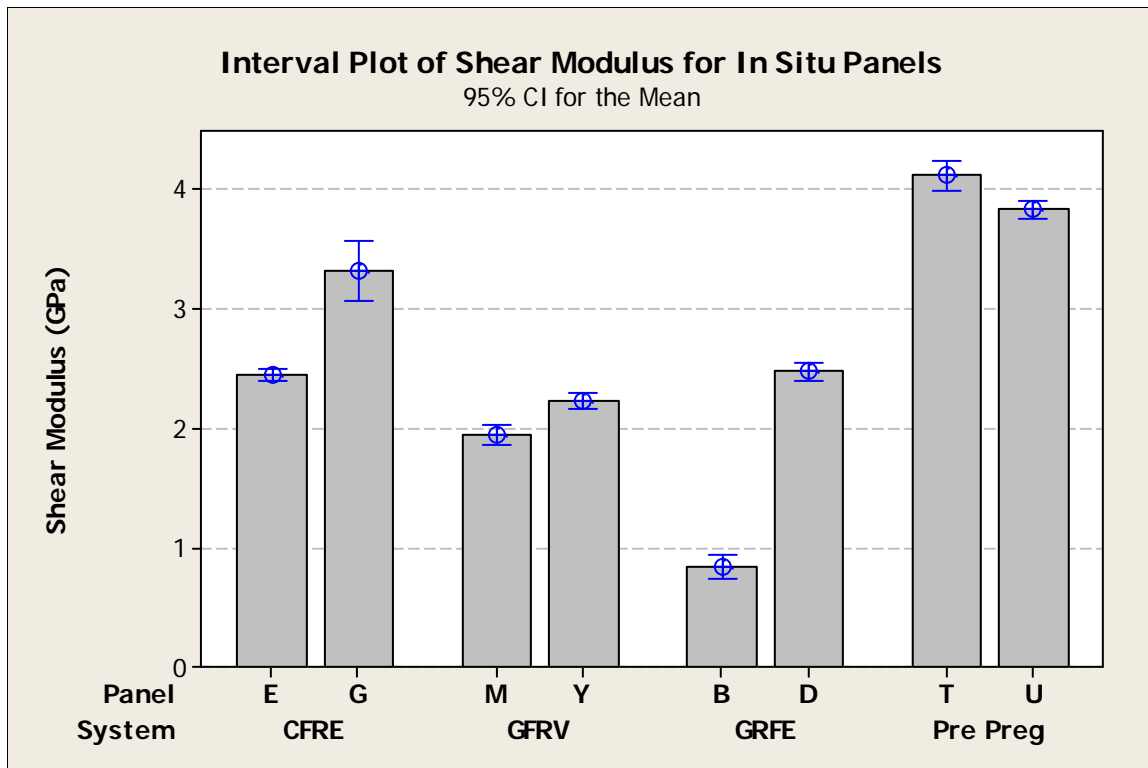
Figure 7-22: Mean Shear Modulus with 95% Confidence Intervals

In Figure 7-22 the blue range bars indicate the confidence interval in which it can be predicted that, if nothing changes, 95% of the shear modulus calculations conducted in the future will be within. It can be seen that the mean shear modulus for the GFRE panels and CFRE panels obviously have a large and meaningful difference but that the statistical significance of the GFRV and Pre-Preg panels is in question. To determine if there is a statistical significance for these systems, a paired T-test is completed.

For GFRV and Pre-Preg panels there are six degrees of freedom, therefore, the absolute value of the T-value must be 2.447 or greater to reject the hypothesis that the means are the same. For the GFRV panels Y (as-produced) and M (exposed nine months) there is a T-value of 6.59 so the null hypothesis is rejected. There is a statistical significance between the mean shear modulus values. The significance of the difference in the means can be seen in Figure 7-23.
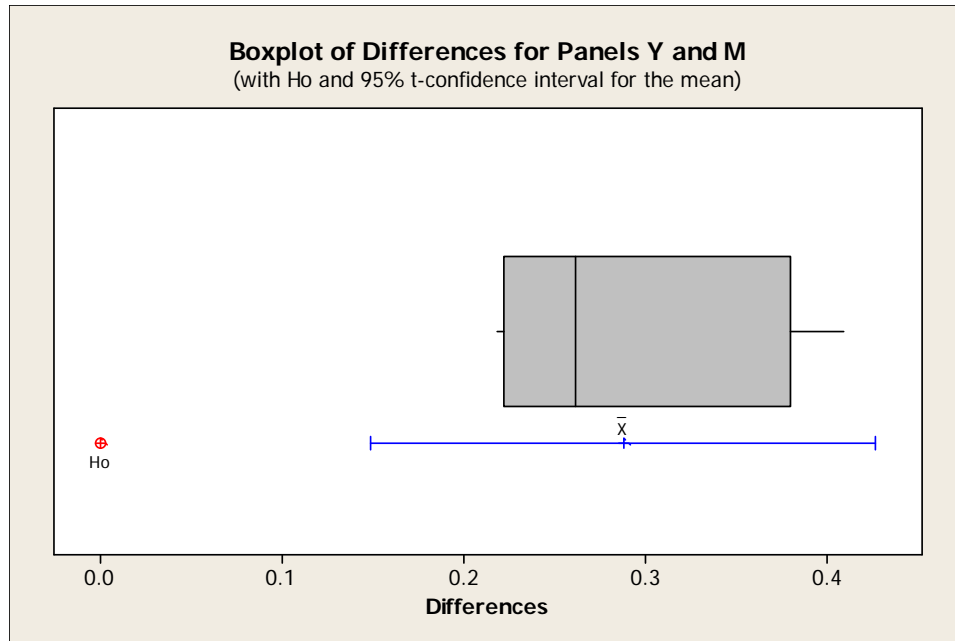
Figure 7-23: Boxplot of Paired T-Test for GFRV Panels Y (As-produced) and M (9 Month Exposure)

For the Pre-Preg panels T and U, the paired T-test returns a T-value of 6.74, which is again well above the required value of 2.447. This indicates that the difference in the shear modulus means is statistically significant, this can be seen in Figure 7-24.
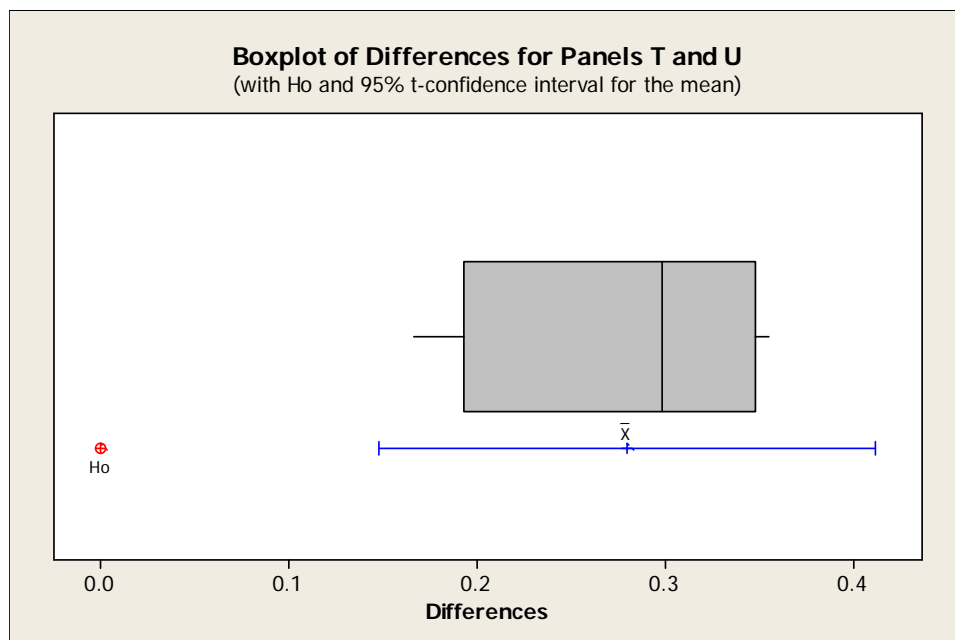

Figure 7-24: Boxplot of Paired T-Test for Pre-Preg Panels T (As-produced) and U (6 Month Exposure)

Figure 7-25 shows the shear modulus of all of the GFRV panels.
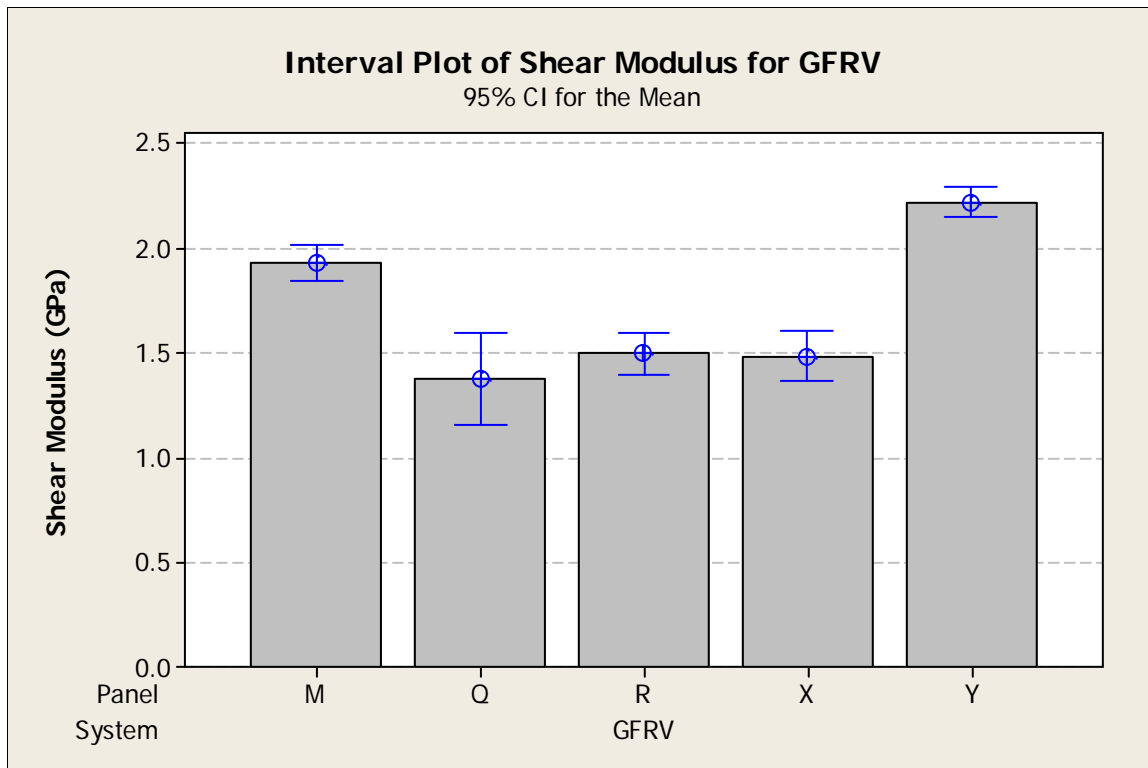
Figure 7-25: Mean Shear Modulus of GFRV Panels with 95% Confidence Intervals

It can be seen in Figure 7-25 that the mean shear modulus of the different GFRV panels is close. It has already been show previously that the M and Y panels did have a statistical significance. It appears from Figure 7-25 that Panels Q (30°C), R (40°C), and X (50°C), may not have a statistically significant difference in their shear modulus means.

A paired T-test is conducted between panels Q and R. A T-value of -1.36 (an absolute value of 1.36) is calculated, which is well below the 2.447 value needed to reject the null hypothesis. This indicates that there is no statistical significance between the shear modulus means, this can be seen in Figure 7-26.
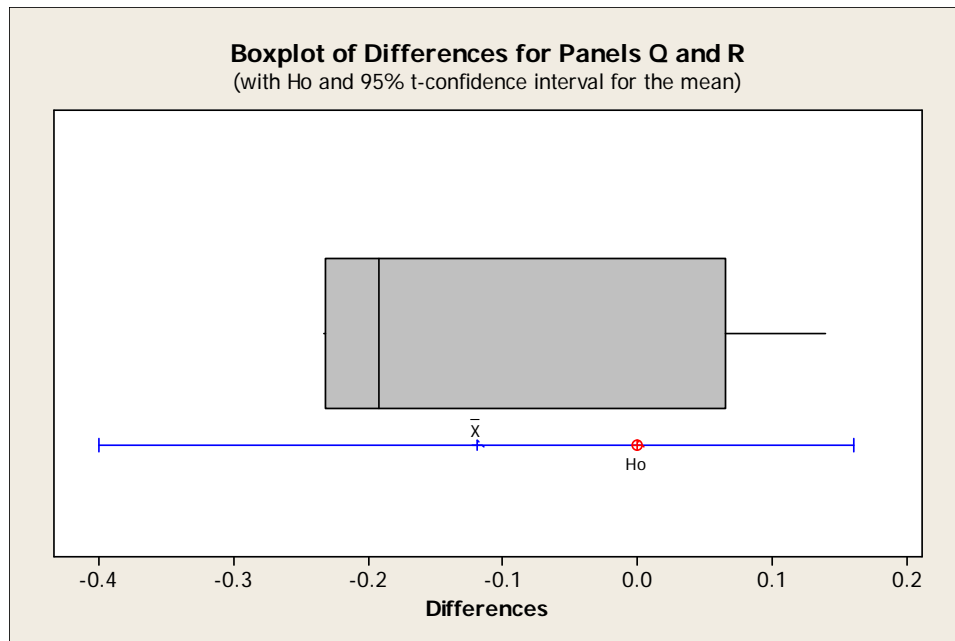
Figure 7-26: Boxplot of Paired T-Test for GFRV Panels Q (Accelerated at 30°C) and R (Accelerated at 40°C)

A paired T-test is also completed to compare panels Q and X and the T-Value returned is -1.13. This indicates that there is no statistical significance between shear modulus means of panels Q and X. Figure 7-27 shows the results of this test.
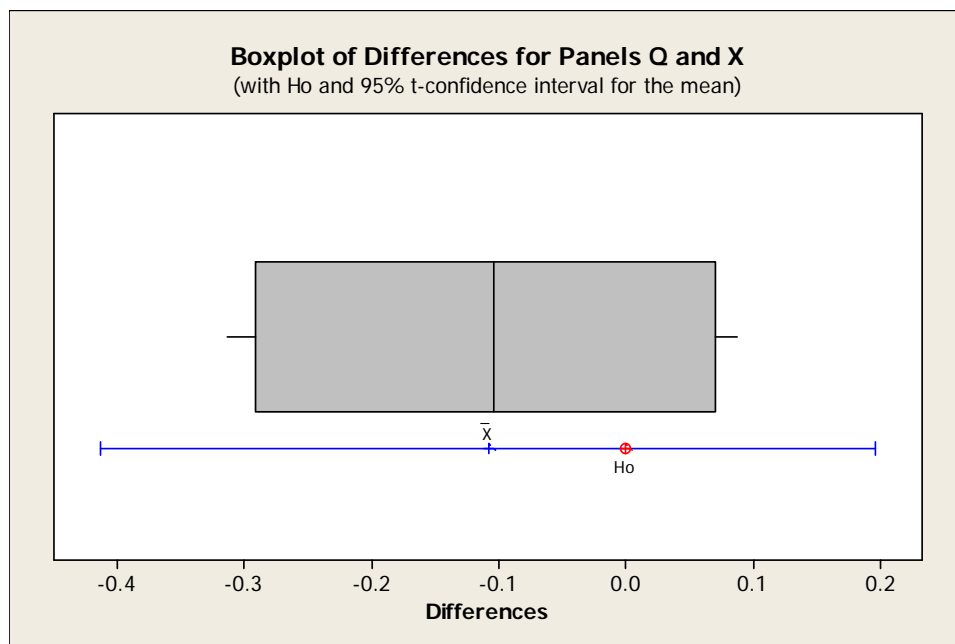

Figure 7-27: Boxplot of Paired T-Test for GFRV Panels Q (Accelerated at 30°C) and X (Accelerated at 50°C)

The paired T-test is also completed between panels R and X to guarantee that there is no statistical significance among the three panels subjected to accelerated exposure. The T-value calculated was 0.20, which is well below the threshold of 2.447 required to reject the hypothesis. The results of this test can be seen in Figure 7-28.
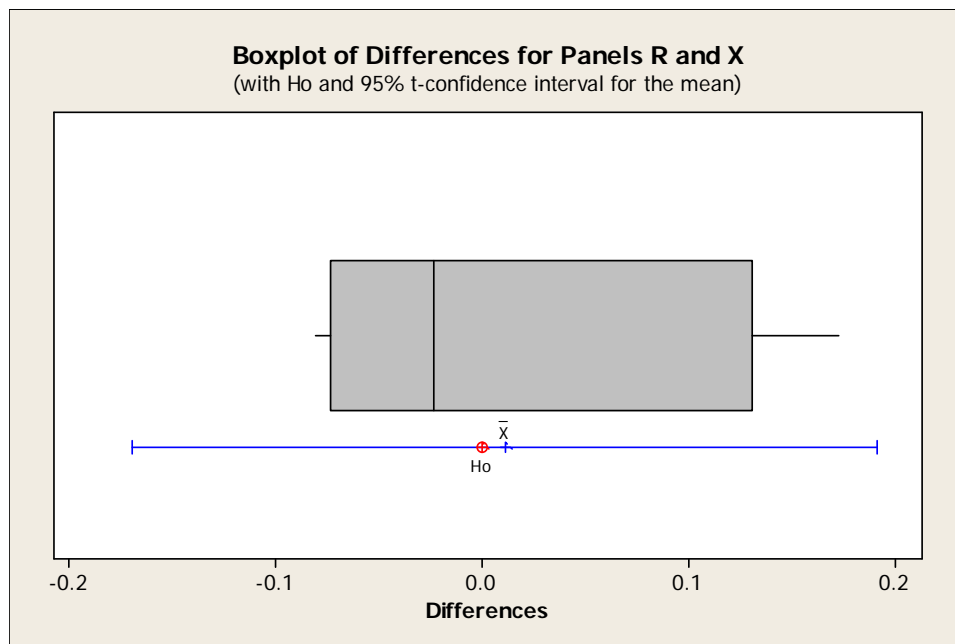

Figure 7-28: Boxplot of Paired T-Test for GFRV Panels R (Accelerated at 40°C) and X (Accelerated at 30°C)

The paired T-test was also conducted between panel M and the panel subjected to accelerated exposure that had the closest mean shear modulus/95% confidence interval combination, which is panel Q. The results of this test can be seen in Figure 7-29.
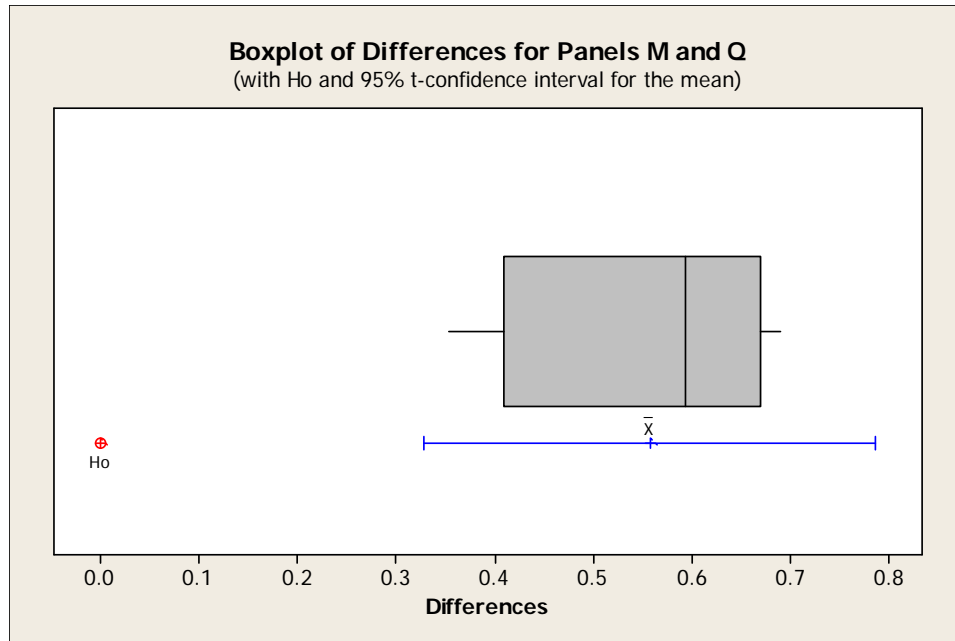
Figure 7-29: Boxplot of Paired T-Test for GFRV Panels M (Exposed 9 Months) and Q (Accelerated at 30°C)

The resulting T-value between panels M and Q was 7.75, which is well above the threshold required to reject the hypothesis. This means that there is a statistically significant difference between the mean shear moduli of panel M and the panels subjected to accelerated exposure. It is inferred from this result that the accelerated testing does a poor job of accurately predicting the exposure experienced by the in situ panel over a nine month period.

Table 7-6 shows the results of the statistical significance testing for all of the panel comparisons.

Table 7-6: Paired T-test Results

System	Panels Compared	Differences in the Means (GPa)	T-Value	Statistically Significant?
GFRE	D to B	1.63	29.31	yes
CFRE	G to E	0.87	14.10	yes
Pre-Preg	T to U	0.28	6.74	yes
GFRV	Y to M	0.29	6.59	yes
	Y to Q	0.84	10.53	yes
	M to Q	0.56	7.75	yes
	Q to R	-0.12	-1.36	no
	Q to X	-0.11	-1.13	no
	R to X	0.01	0.20	no

7.3.5 Microscopy Results

Figure 7-30 gives an example of the microscopy analysis completed for each panel. The results for all 11 panels can be seen in Appendix A:.
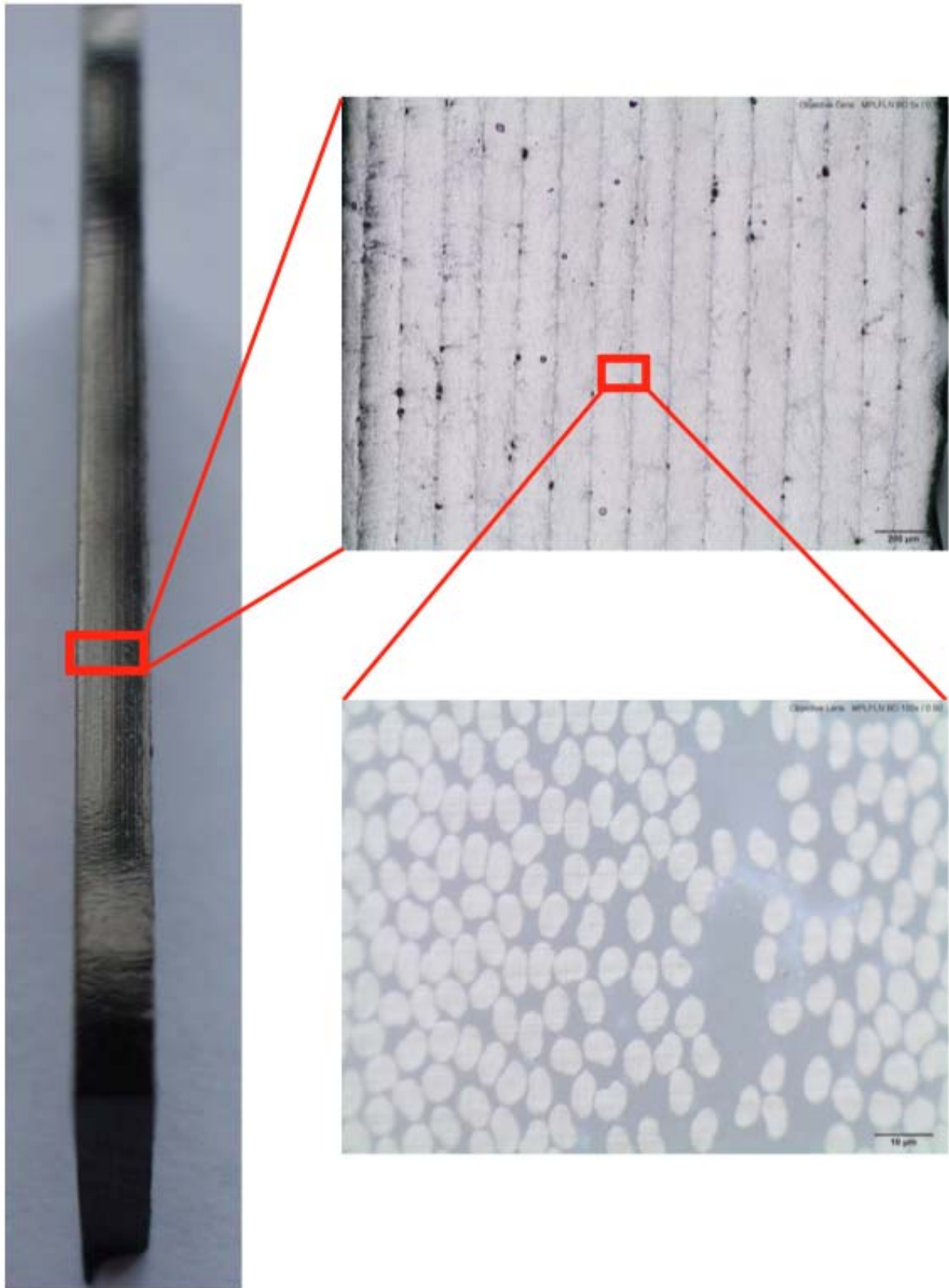
Figure 7-30: Pre-Peg Panel T (As-Produced) Microscopy

The microscopy pictures provide little information as to the cause for the losses in strength properties between the exposed and as-produced panels. When comparing Figure A-3 to Figure A-4 it appears that the carbon fibers in panel E have experienced some color change around the core of the fiber. This color change may be the result of the development of small voids around the core. It can also be seen in Appendix A: that it is difficult to glean any information from the microscopic pictures of the fiberglass reinforced systems because of the lack of contrast between the fibers and the matrix. It can be seen in Figure 7-31 that with dark field microscopy it was easier to see the glass fibers, but there was little visual information about changes in the matrix.
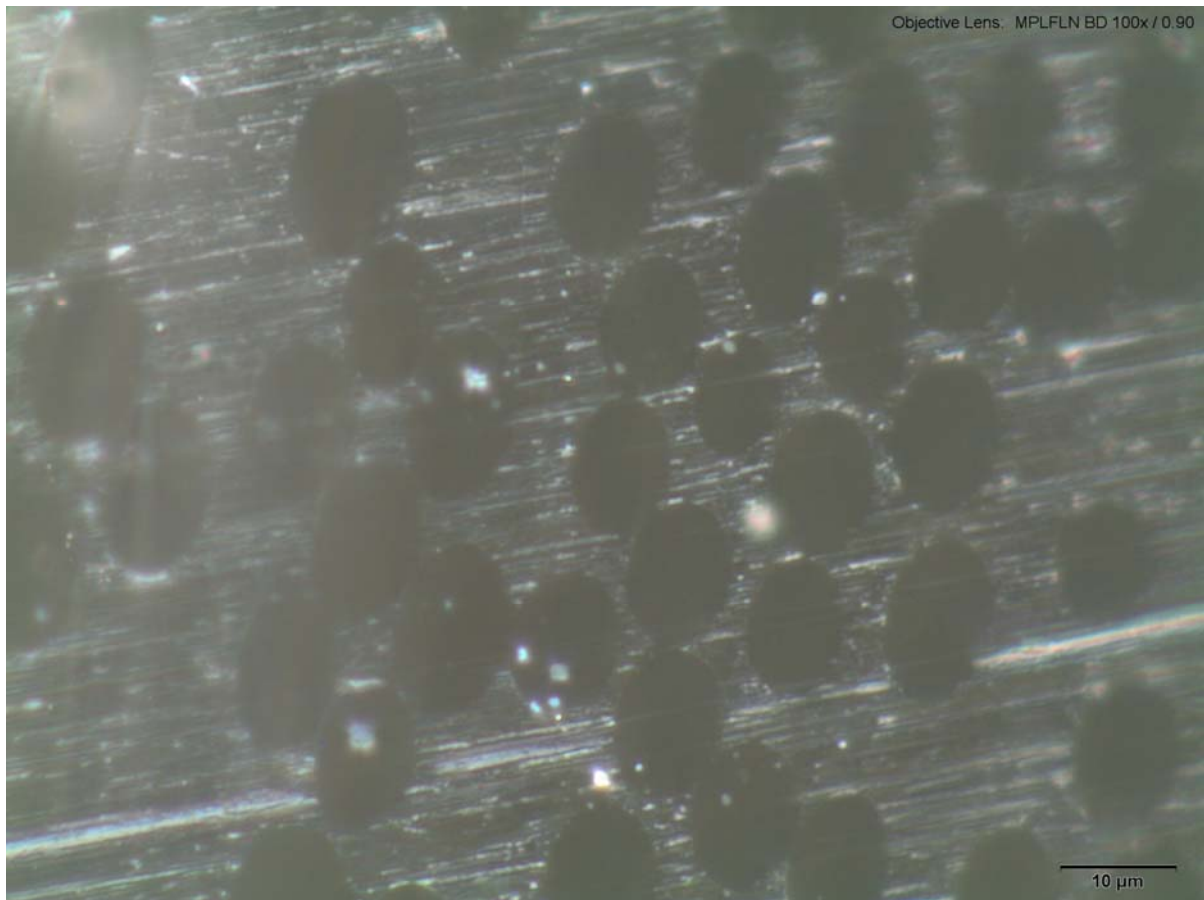

Figure 7-31: GFRV Panel Q (Accelerated at 30°C) with Dark Field Microscopy

8 Results and Conclusions

8.1 Results

The GFRE system's loss of 66% of its shear modulus is the worst shear modulus result calculated and the Pre-Preg system's loss of 7% is the best. The results of the three most important properties compared are summarized in Table 8-1.

Table 8-1: Summary of Results

Panel	Shear Modulus Loss (GPa)	Standard Deviation (GPa)	CV	Percent Loss	Max Shear Stress Change (MPa)	Standard Deviation (MPa)	CV	Percent Change	Tensile Modulus Loss (GPa)	Standard Deviation (GPa)	CV	Percent Loss
GFRE	1.63	0.08	5%	66%	33.36	1.89	6%	68%	5.86	0.36	6%	64%
CFRE	0.88	0.10	12%	26%					3.19	0.53	17%	26%
Pre-Preg	0.28	0.09	32%	7%	4.47	0.50	11%	8%	1.31	0.15	12%	8%
GFRV	0.29	0.07	24%	13%	4.18	1.22	29%	14%	1.34	0.65	48%	16%
GFRV @ 30	0.84	0.15	17%	38%	4.31			14%	2.76	0.84	31%	33%
GFRV @ 40	0.73	0.08	11%	33%	-5.08			-17%	2.26	0.68	30%	27%
GFRV @ 50	0.74	0.09	12%	33%	4.84	1.48	31%	16%	2.57	0.61	24%	30%

It can be seen that the standard deviation for all of the changes in shear modulus is mostly consistent throughout the different material systems and exposure conditions. This indicates that the shear modulus test is repeatable and its performance is independent of the materials and exposures. This consistent standard deviation increased the author's confidence in the results and in the decision to use the ASTM D3508 standard.

Besides the three important properties that were presented in Table 8-1 all of the panels subjected to in situ exposure have a loss of performance in all of the properties that are monitored, with three exceptions. The first exception is that the CFRE system has an improvement of the shear strain at yield. The second exception is that the Pre-Peg system shows an increase in the tensile stress at maximum load, and the third exception is that the GFRV system shows a decrease in the tensile strain at maximum load.

In general, the GFRV panels subjected to accelerated exposure do not perform in the same manner as the GFRV placed in situ. The shear modulus and tensile modulus of all

three panels decrease more than the in situ panel. The shear stress at yield decreases, but the shear strain at yield increased, particularly for panel X (accelerated at 40℃) and panel R (accelerated at 50℃). The tensile strain and stress at maximum load increases for some panels and decreases for others, with no apparent correlation between an increase in stress and a decrease in strain or vise versa. A paired t-test conducted on the panels that were exposed in the lab shows that there is no statistical significance between the mean shear moduli calculated for these panels.

8.2   Conclusions

From the results, it is the author's recommendation that device developers focus their efforts on the use of both Pre-Preg and Vinylester composite systems.

8.2.1   Changes in Shear Modulus and Other Properties

The Pre-Preg system performs far better than any of the other systems, and the GFRV system performs the second best. The Pre-Preg represents the higher cost system whereas the GFRV represents the lower cost system. This indicates that the GFRV system may be a perfectly acceptable system to use in tidal energy devices, although the lower strength to weight ratio of the GFRV system will negate some of the cost advantages of this system because more of it will be needed. The reader should also be reminded that the Pre-Preg was only exposed for six months, whereas the other three systems were exposed for nine months.

From the review of the literature it was expected that the GFRV system would absorb less moisture than the other systems, but that the GFRE and CFRE systems would be affected less by the absorption of moisture. These are not quite the results that are observed in the study. Although the actual amount of moisture absorbed by the different systems can not be calculated because of biofouling, the shear moduli of the CFRE and GFRV systems are only moderately affected by exposure and the shear modulus of the GFRE system are severely affected. One possible explanation for this may be that the epoxy system used in the GFRE system does not bond as well with the sizing on the glass fibers, whereas the vinylester matrix in the GFRV system is possibly

unaffected by the sizing or designed to be used with that type of sizing. Another possible reason for this result may be the manufacturing differences between GFRE panels B (exposed 9 months) and D (as-produced). It appears in Figure 8-1 that panel B may have larger voids in it than panel D does. This may mean that a large part of the strength differences observed in the GFRE system may be due more to manufacturing differences than to exposure.
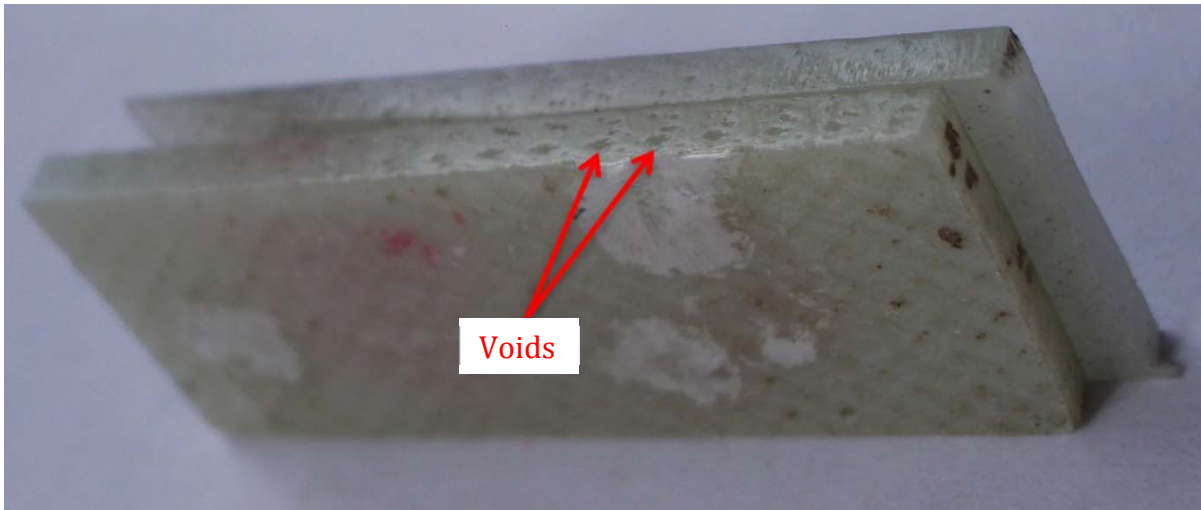

Figure 8-1: Polished Edge of GFRE Panels. B in the Foreground (Exposed 9 Months), D in the Background (As-Produced)

For the in situ results, the percent changes in all the properties are fairly consistent across all the properties that were examined. The GFRE system loses about 65% of all its properties, the CFRE loses about 26%, the Pre-Preg loses about 8% and the GFRV loses about 14%. This indicates that the shear modulus test is a good predictor of the overall effects of exposure on a material system. This may also indicate that the tensile modulus test can be conducted by easier and less expensive means, such as with an extensionometer, and give a good approximation of the probable amount of loss in shear modulus a material system might experience. If this is true, this could provide tidal energy device developers with a very quick and low cost testing procedure that could be performed without the use of strain gages.

Because there are no statistical differences in the shear modulus means of the GFRV panels subjected to accelerated exposure, any variation observed may be common

cause variation. If there is any assignable cause variation, some possible sources may be increased crosslinking of the polymer bonds and the increased leaching of chemical compounds from the panels due to higher temperatures. If increased crosslinking did occur, these gains may have been reduced at higher temperatures because of leaching. This could explain why panel R (40℃) experiences an increase of shear strain at yield, an increase of shear stress at 5% shear strain and an increase of tensile stress and tensile strain at maximum load, but panel X (50℃) shows a decrease in all of these properties. Although panel X's decreases may also be attributed to the fact that it was placed in a saltwater bath two weeks after manufacture, whereas panels Q (30℃) and R were produced six months before being placed in a saltwater bath. If panel X was at a lower percentage of cure, it may have lost chemical compounds at a higher rate.

One possible explanation for the lack of statistically significant differences between the shear moduli of the GFRV panels subjected to accelerated exposure could be that the maximum amount of loss is reached before the 30 days of exposure are completed. Other studies [**12**,**13**] have experienced a leveling of the changes in properties due to exposure. To test this theory the accelerated testing procedure will need to be changed.

8.2.2   Necking

Necking is not consistent across the material systems. Some systems experience more necking after exposure and others experienced less. Necking also does not correlate well with the maximum tensile strain experienced by the system. For example the GFRE system shows much more necking due to exposure and almost double the tensile strain at maximum load, while the CFRE system shows a decrease in necking and an increase in maximum tensile strain.

The necking and fracture type observed in GFRV panel Y (as-produced) is very similar to that which is observed in CFRE panels G (as-produced) and E (nine month exposure) even though panel Y uses different matrix and fiber materials. Since panel Y fails in this manner it is expected that GFRE panel D (as-produced) would fail in this manner as well because panel D uses the same fibers as Y and the same matrix as G and E, but this

is not the case. One possible reason that Panel Y fails in the way it does is because it is tested six days after it is manufactured, whereas the other panels are tested nine or ten months after they are manufactured. Panel Y may not be as fully cured as the other panels before testing. If panel Y was allowed more time to cure, it may show less necking and have a failure mode similar to the other glass fiber reinforced panels.

8.2.3 Weight Gain

The differences in weight gain between the two methods of weighing the accelerated exposure panels can possibly be explained by the voids and defects on the surface of the panels and the entrained air in the saltwater baths. It can be seen in Figure 7-19 that the panels gain between a half and one and a half grams in the first two days of exposure. This initial weight gain may be caused by the saltwater requiring a day or two to displace the trapped air in the voids on the surface of the panels. Once the panels are removed from the bath, they are placed in the oven to dry for 30 minutes at 50℃ so that weight measurement procedures are consistent and repeatable. This brief drying period may be enough to evaporate the water trapped in the surface voids and therefore the weights measured by the scale were lower than those measured by the balances. The balances may have measured absorbed and diffused moisture, whereas the scale just measures the diffused moisture. It is also noticed that for the first few days of testing, small air bubbles attach to the panels and that a light tap on the machine is required to knock the bubbles loose. After the first few days these bubbles do not reappear. These air bubbles may also contributed to the rapid weight gain shown on the balances in the first few days of exposure. It is recommended that future researchers using this continuous weight monitoring technique allow the water to settle a few days before exposing the panels so that entrained air has a chance to escape. Also, the method of continuously measuring the weight of the submerged panels does not appear to be affected by the barometric pressure.

It is possible that the large initial weight gain of the accelerated panels is not only due to water absorption but also because of the nature of diffusivity as characterized by Fick's law. Many other studies [8,9,10,12] have shown a large initial weight gain but many of

these studies didn't show a leveling of the weight gain until after 100 days of exposure or more. It is difficult to compare weight gain results with other studies because no other studies were found which used continuous weight monitoring techniques. Typically in other studies, the specimens were removed from the fluid, wiped dry by hand and weighed.

8.2.4 Microscopy

From the macroscopic and microscopic examination it appears that the growth of biofouling on the panels actually has no effect on the visual properties of the materials.
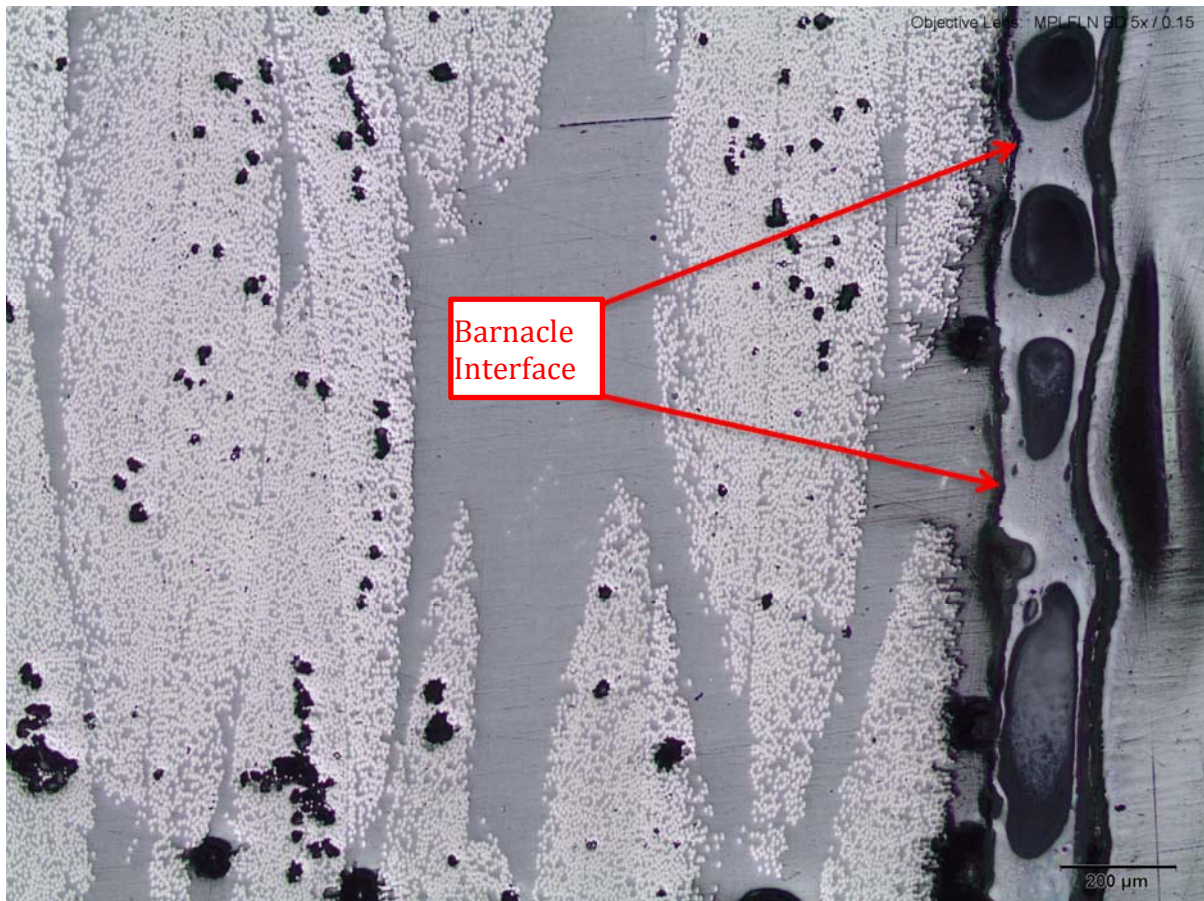
Figure 8-2: CFRE Panel E (Exposed 9 Months) with Barnacle Structure at 10x Zoom

Figure 8-2 shows the panel E sample with a barnacle still attached. It can be seen that the barnacle appeared to grow on the surface of the panel and not penetrate into the matrix at all.

It was thought that the color change experienced in the GFRV panels (Figure 7-21) might be attributable to microcracking due to the thermal contraction and expansion of the panels. The microscopy analysis does not show any evidence of microcracking at the 10μm scale, therefore it is assumed that the color change is due to water diffusion and possibly changes in the chemical structure of the vinylester matrix.

8.3   Future Work

Future work that could be completed would be to remove the remaining four panels from the sea spider and test them in the same manner that was done previously. This additional data would help verify the conclusions presented here and may also provide the ability to draw different conclusions. When doing this work, the smaller jaws should be used for the load frame and no preload should be applied.

A change in the accelerated testing procedures to test for a change in shear modulus due to time instead of temperature could be created. The testing procedures for this would need to be substantially different than the procedures used for this study, especially if continuous weight monitoring was desired. The goal of this type of exposure would be to understand how the systems perform over time. For example it would be useful to know how 1, 5, 10, 15, 20 and 25 days of exposure at 30℃ affect the GFRV system. If there is a leveling of the change in shear modulus over time, than it might be possible to understand what 9 and 18 months of in situ exposure are equal to in the laboratory.

Other future work would be to further examine the mechanisms that caused such a dramatic change in the shear modulus and other properties of the GFRE system. A better understanding of these mechanisms might help guarantee that tidal energy device developers choose the right fibers, that have been treated with the right post processing, such as sizing, for the matrix that they want to use.

An area that needs further examination before any conclusions can be drawn is whether the tensile modulus obtained from the load cell and extensionometer displacement of a tensile test of a ±45˚ laminate is actually a good approximation of the

percentage of shear modulus loss. If it can be shown that this test is a good approximation, device developers could more quickly and cheaply test various materials. If these tests were completed, they would not provide specific material property information but they would provide general guidance about how the specific matrix and fiber system will perform.

9 Bibliography

[1] U.S. Government, MARINE AND HYDROKINETIC ENERGY TECHNOLOGY: FINDING THE PATH TO COMMERCIALIZATION, Dec. 3, 2009, Available via the World Wide Web: http://www.science.house.gov.

[2] National Oceanic and Atmospheric Administration. (2010, November) NOAA Tides and Currents. [Online]. http://tidesandcurrents.noaa.gov/tide_predictions.shtml

[3] M.J. Khan, G Bhuyan, Iqbal M.T., and Quaicoe J.E., "Hydrokinetic energy conversion systems and assessment of horizontal and vertical axis turbines for river and tidal applications: A technology status review," *Applied Energy*, vol. 86, pp. 1823-1835, 2009.

[4] B Polagye, B Van Cleve, A Copping, and K. Kirkendall, "Environmental effects of tidal energy development," 2008.

[5] Y.L. Young, J.W. Baker, and M.R. Motley, "Reliability-based design and optimization of adaptive marine structures," *Composite Structures*, vol. 92, pp. 244-253, 2010.

[6] Ching-Chieh Lin, Ya-Jung Lee Lee, and Chu-Sung Hung, "Optimization and experiment of composite marine propellers," *Composite Structures*, vol. 89, pp. 206-215, 2009.

[7] Marine Current Turbines. (2011) Marine Turbines. [Online]. http://www.marineturbines.com/21/technology/

[8] George S. Springer, *Environmental Effects on Composite Materials*. Westport, CT, USA: Technomic, 1981-1988, vol. I.

[9] A Kootsookos and A.P. Mouritz, "Seawater durability of glass- and carbon-polymer composites," *Composites Science and Technology*, vol. 64, pp. 1503-1511, 2004.

[10] P Davies, F Mazéas, and P Casari, "Sea Water Aging of Glass Reinforced Composites: Shear Behaviour and Damage Modelling," *Journal of Composite Materials*, vol. 35, no. 15, pp. 1343-1372, 2001.

[11] Paul H. Miller, "Effects of Moisture Absorption and Test Method on the Properties of E-glass/Polyester Hull Laminates," *Journal of Composite Materials*, vol. 36, no. 09, pp. 1065-1078, 2002.

[12] H.N. Narasimha Murthy, M. Sreejith, M. Krishna, S.C. Sharma, and T.S. Sheshadri, "Seawater Durability of Epoxy/Vinyl Ester Reinforced with Glass/Carbon Composites," *Journal of Reinforced Plastics and Composites*, vol. 29, no. 10, pp. 1491-1499, 2010.

[13] Daniel J. Hoffman and William J. Bielawski, "ENVIRONMENTAL EXPOSURE EFFECTS ON COMPOSITE MATERIALS FOR COMMERCIAL AIRCRAFT," Commercial Airplane Group, Boeing, Hampton, NASA Contractor Report 187478 1991.

[14] S.K. Rege and S.C. Lakkad, "Technical Note: Effect of Salt Water on Mechanical Properties of Fibre Reinforced Plastics," *Fibre Science and Technology*, vol. 19, pp. 317-324, 1983.

[15] P.H. Petit, "A Simplified Method of Determining the In-plane Shear Stress/Strain Response of Unidirectional Composites," in *STP 460 Composite Materials: Testing and design*, York, 1969, pp. 83-93.

[16] ASTM International, D3518 In-Plane Shear Response of Polymer Matrix Composite Materials by Tensile Test of a ±45° Laminate, 2007.

[17] A.C. Loos, G.S. Springer, B.A. Sanders, and R.W. Tung, "Moisture Absorption of Polyester-E Glass Composites," *Journal of Composite Materials*, vol. 14, pp. 142-154, 1980.

[18] G.S Springer, B.A. Sanders, and R.W. Tung, "Environmental Effects on Glass Fiber Reinforced Polyester and Vinylester Composites," *Journal of Composite Materials*, vol. 14, pp. 213-232, 1980.

[19] Richard D. Granate, "DURABILITY OF COMPOSITE MATERIALS AND STRUCTURES," Department of Ocean and Mechanical Engineering, Florida Atlantic University, Dania Beach, 2009.

[20] Arun Shukla and James W. Dally, *Experimental Solid Mechanics.* Knoxville, TN, USA: College House Enterprises, 2010.

[21] Vishay Precision Group, 125LT General Purpose Strain Gages - Tee Rosette, January 29, 2010.

[22] A.R. Clarke and Eberhardt C.N., *Microscopy techniques for materials science*, 1st ed. Boca Raton, FL, USA: CRC Press LLC, 2002.

[23] Douglas C. Montgomery and George C. Runger, *Applied Statistics and Probability for Engineers*, 4th ed. Hoboken, NJ, USA: John Wiley & Sons, 2007.
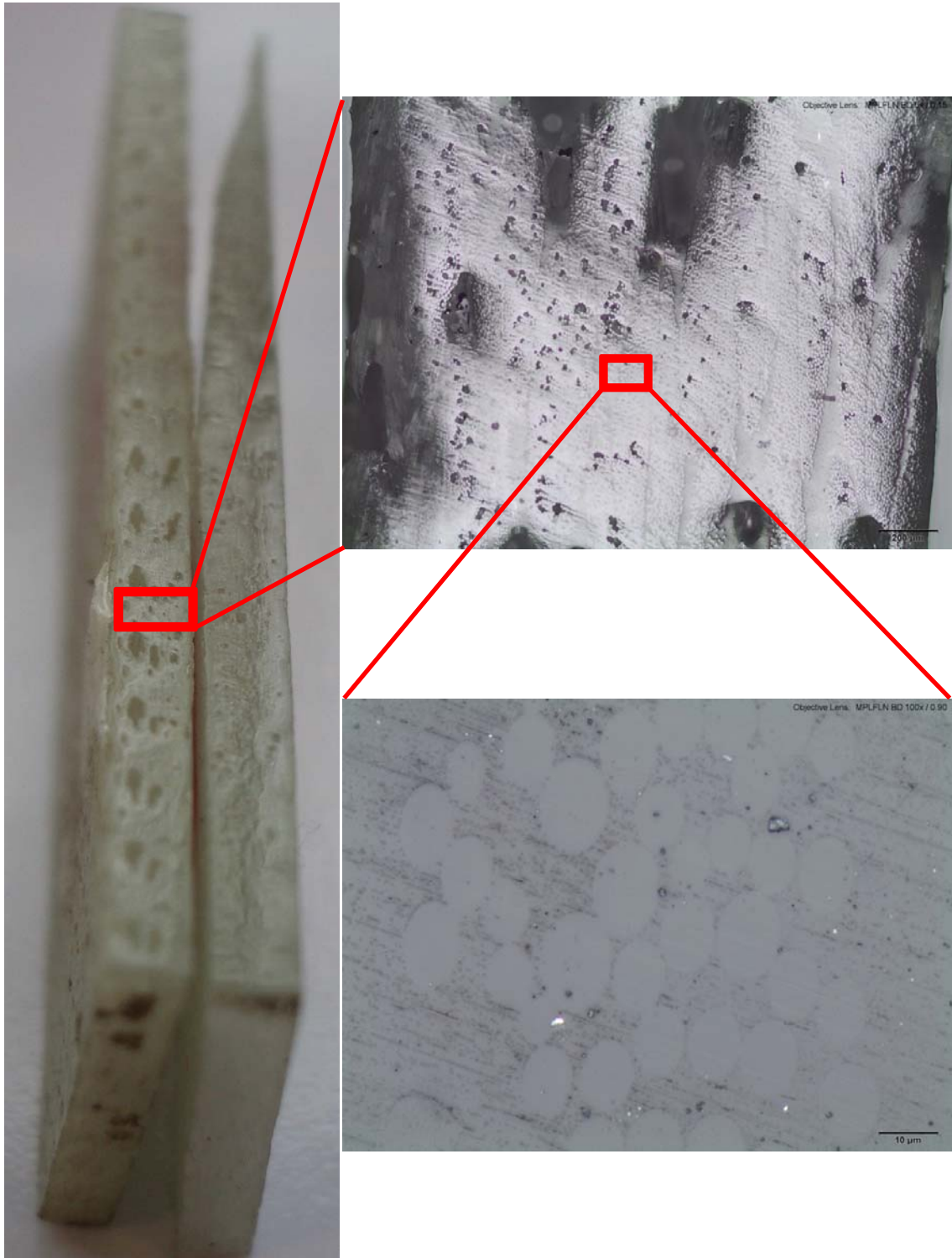
Appendix A: Macro Photography and Microscopy Results
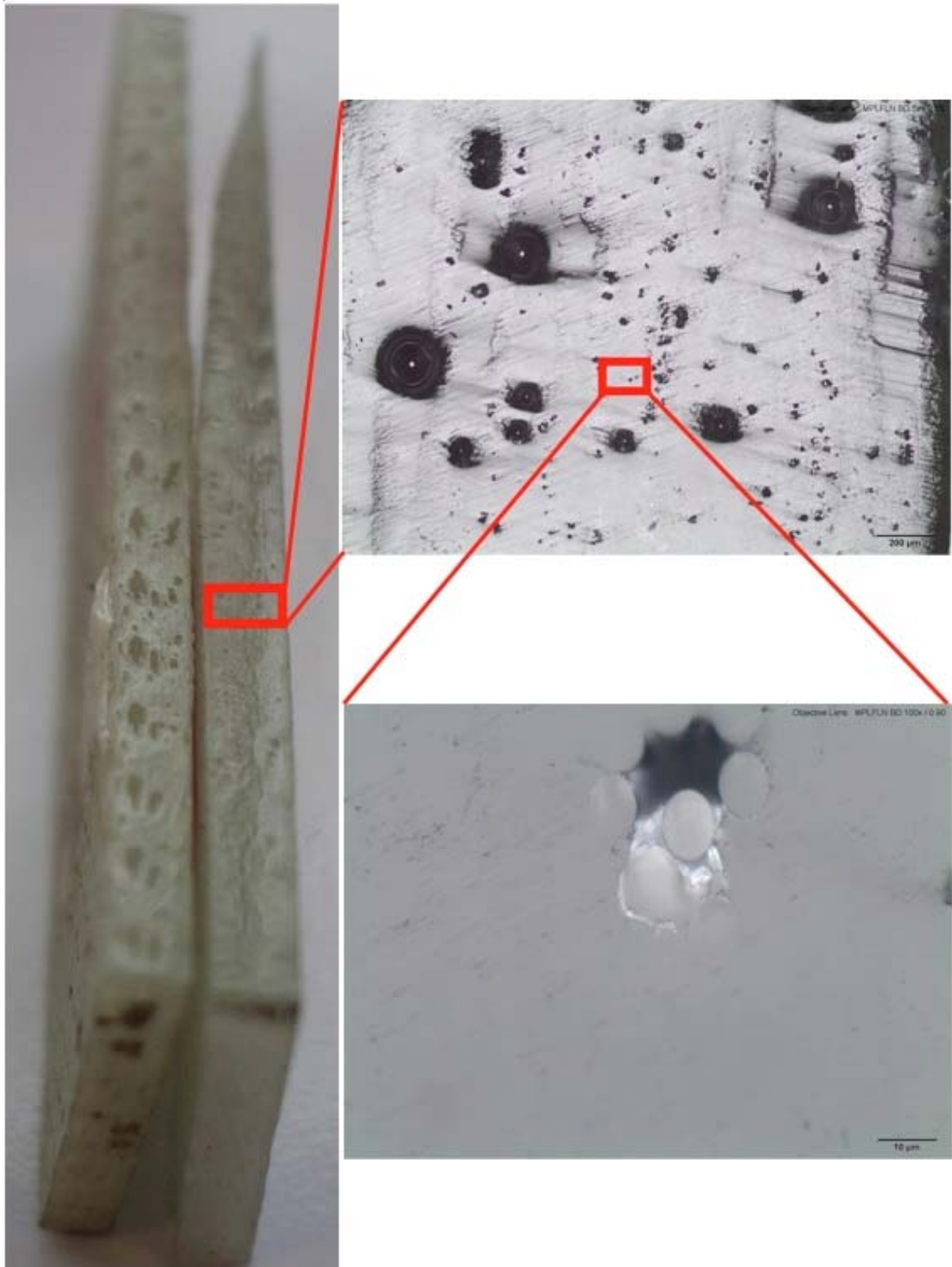

Figure A-1: GFRE Panel B (Exposed 9 Months) Microscopy
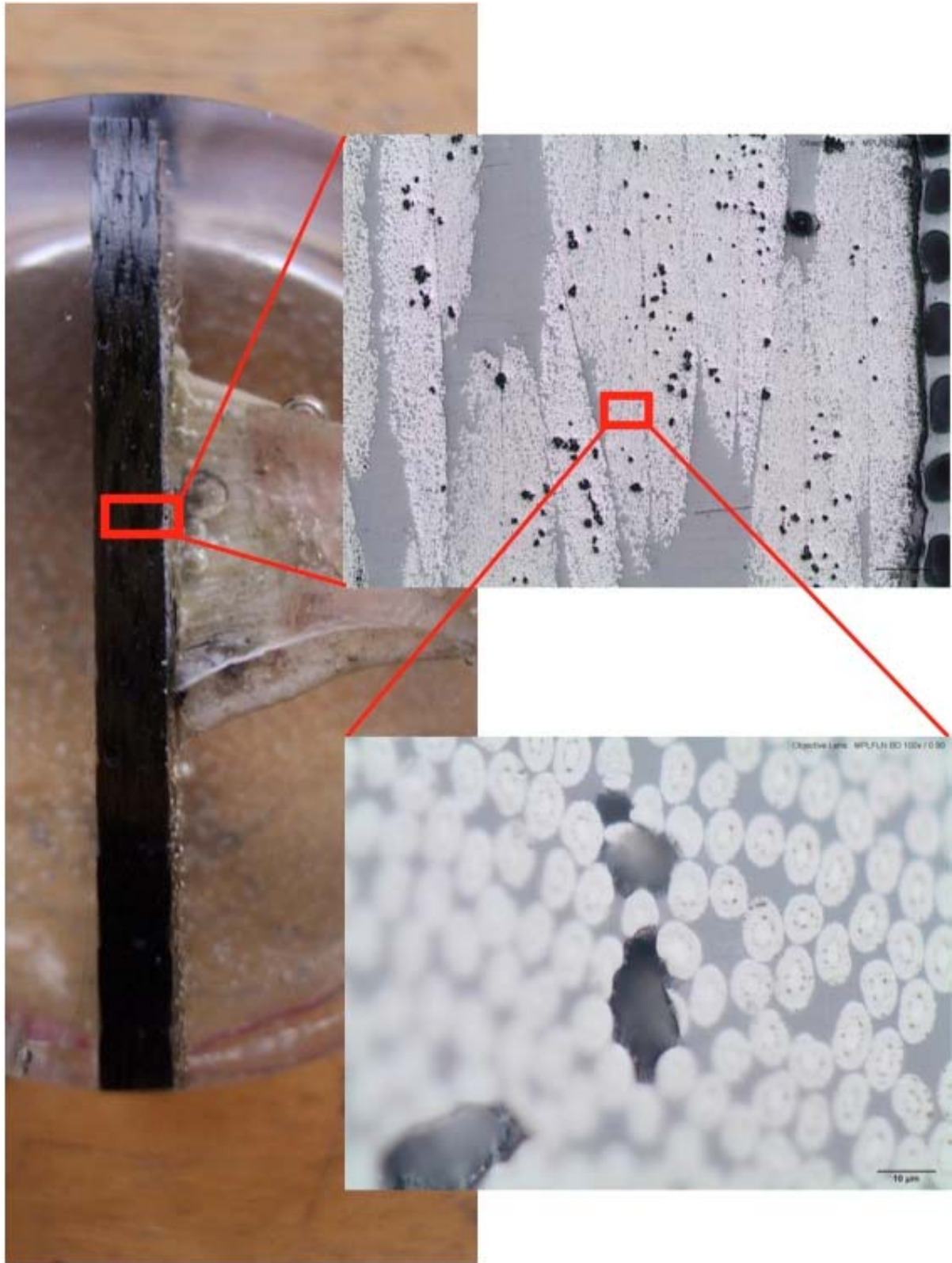
Figure A-2: GFRE Panel D (As-Produced) Microscopy

Figure A-3: CFRE Panel E (Exposed 9 Months) Microscopy
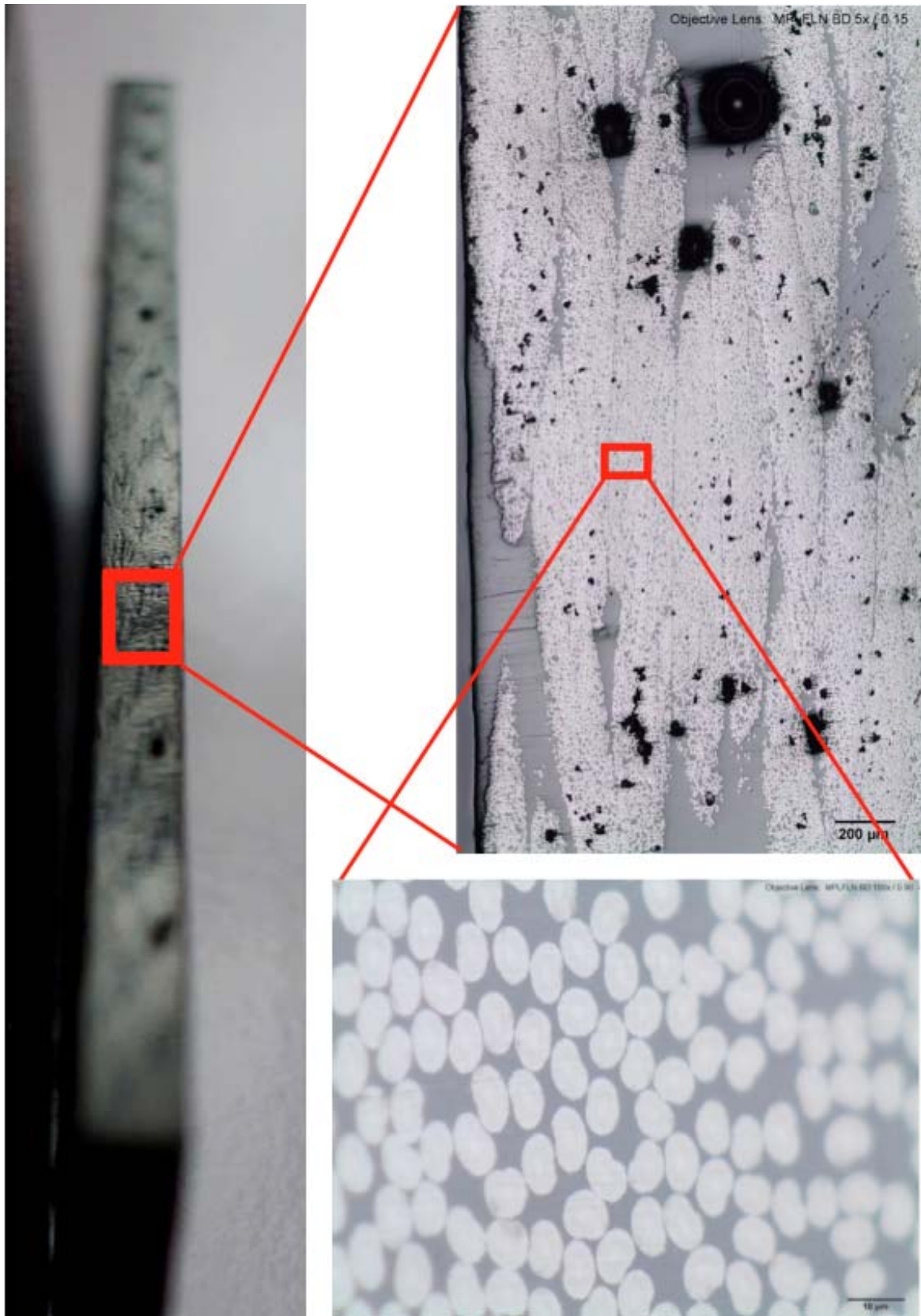
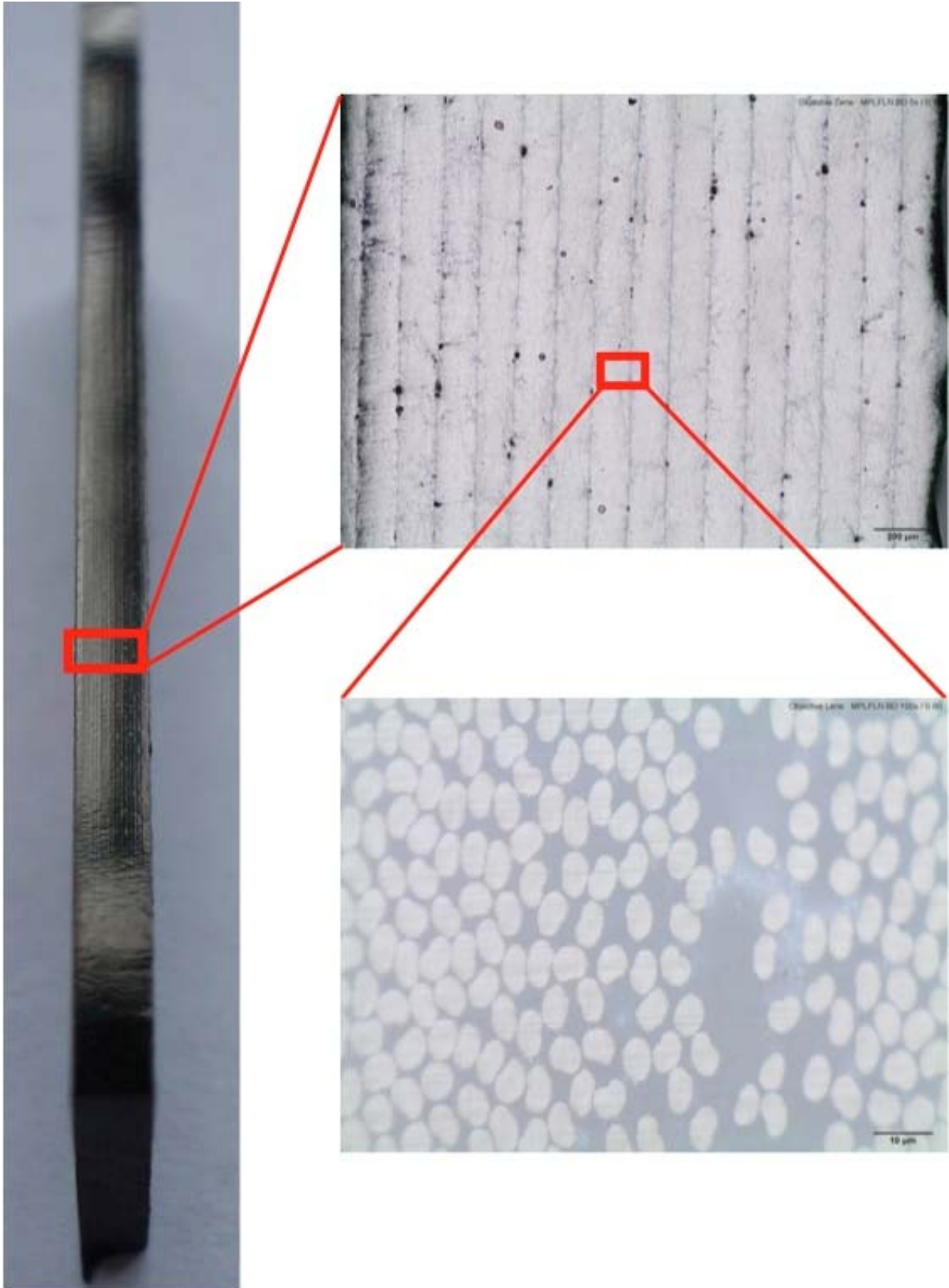**Figure A-4: CFRE Panel G (As-Produced) Microscopy**

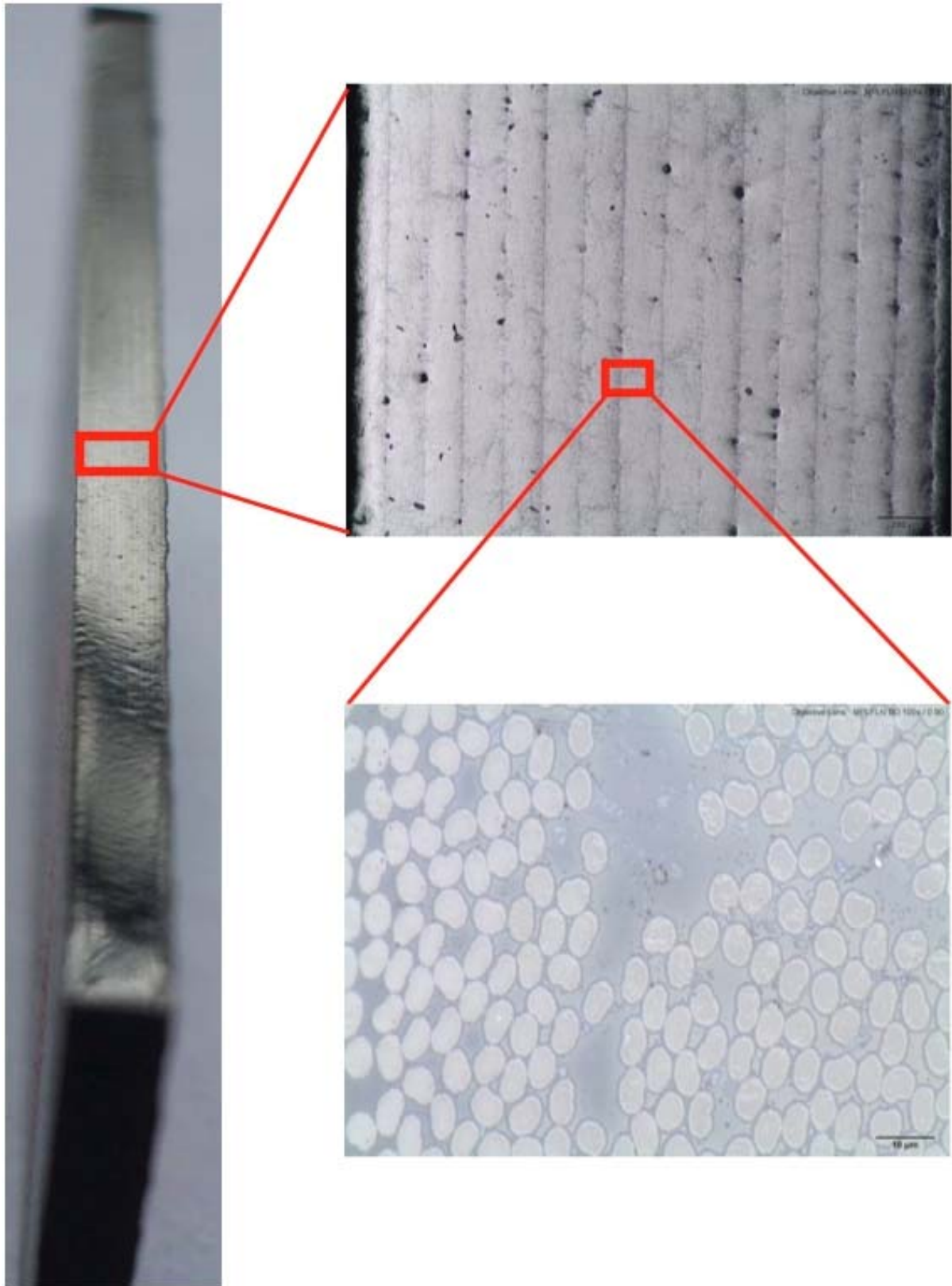**Figure A-5: Pre-Preg Panel T (As-Produced) Microscopy**

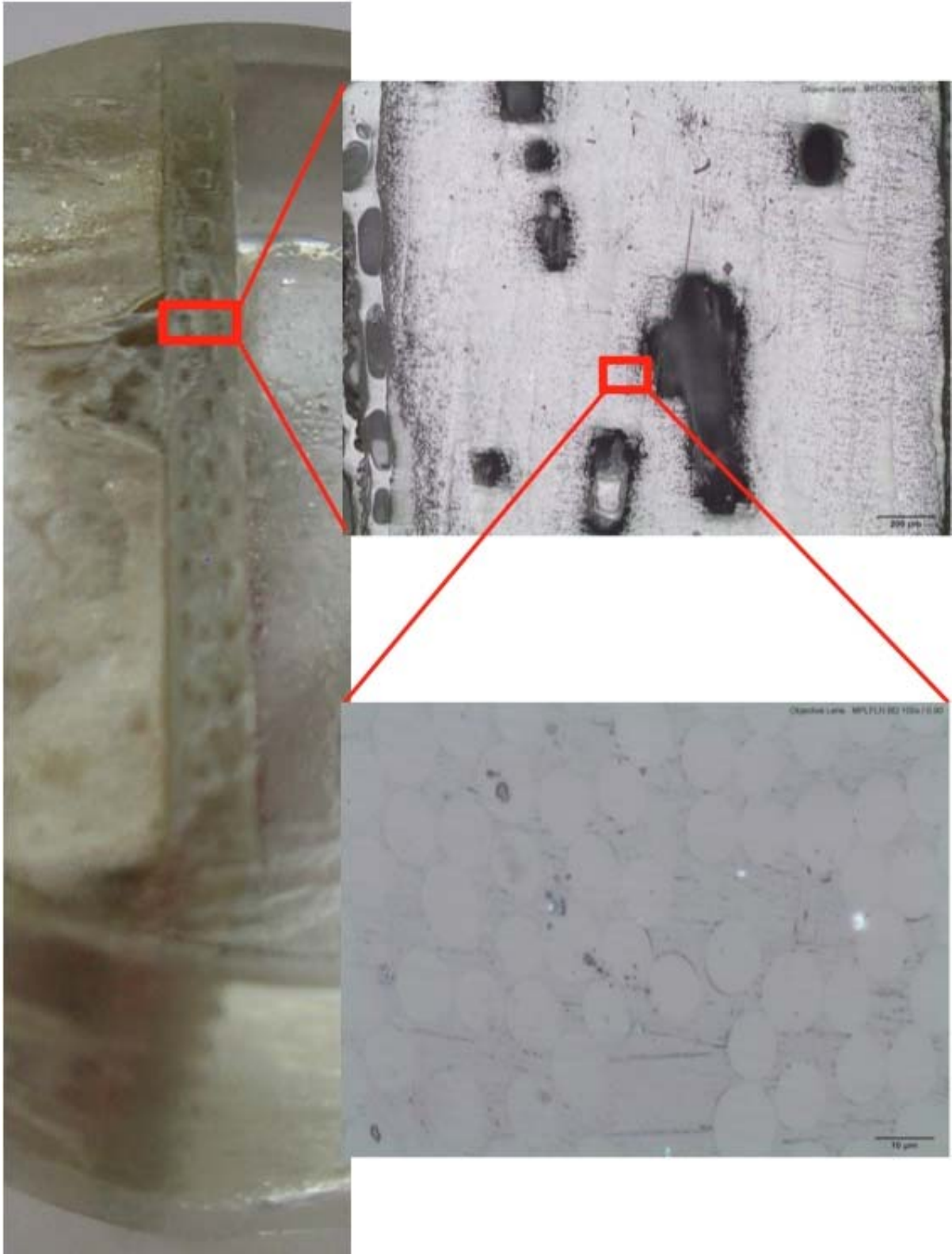**Figure A-6: Pre-Preg Panel U (Exposed 6 Months) Microscopy**

Figure A-7: GFRV Panel M (Exposed 9 Months) Microscopy

Figure A-8: GFRV Panels Q,R,X and Y Macro Photographs
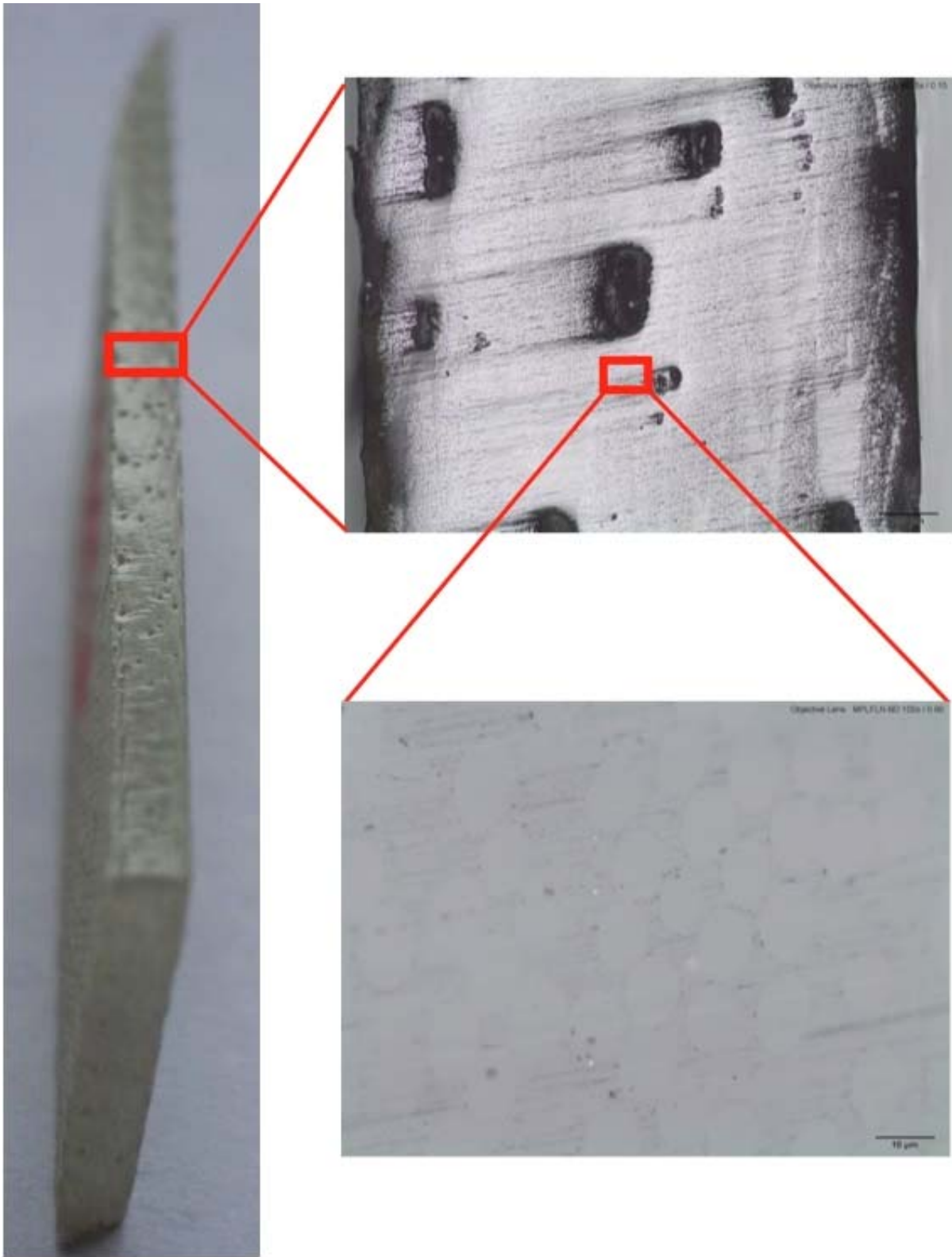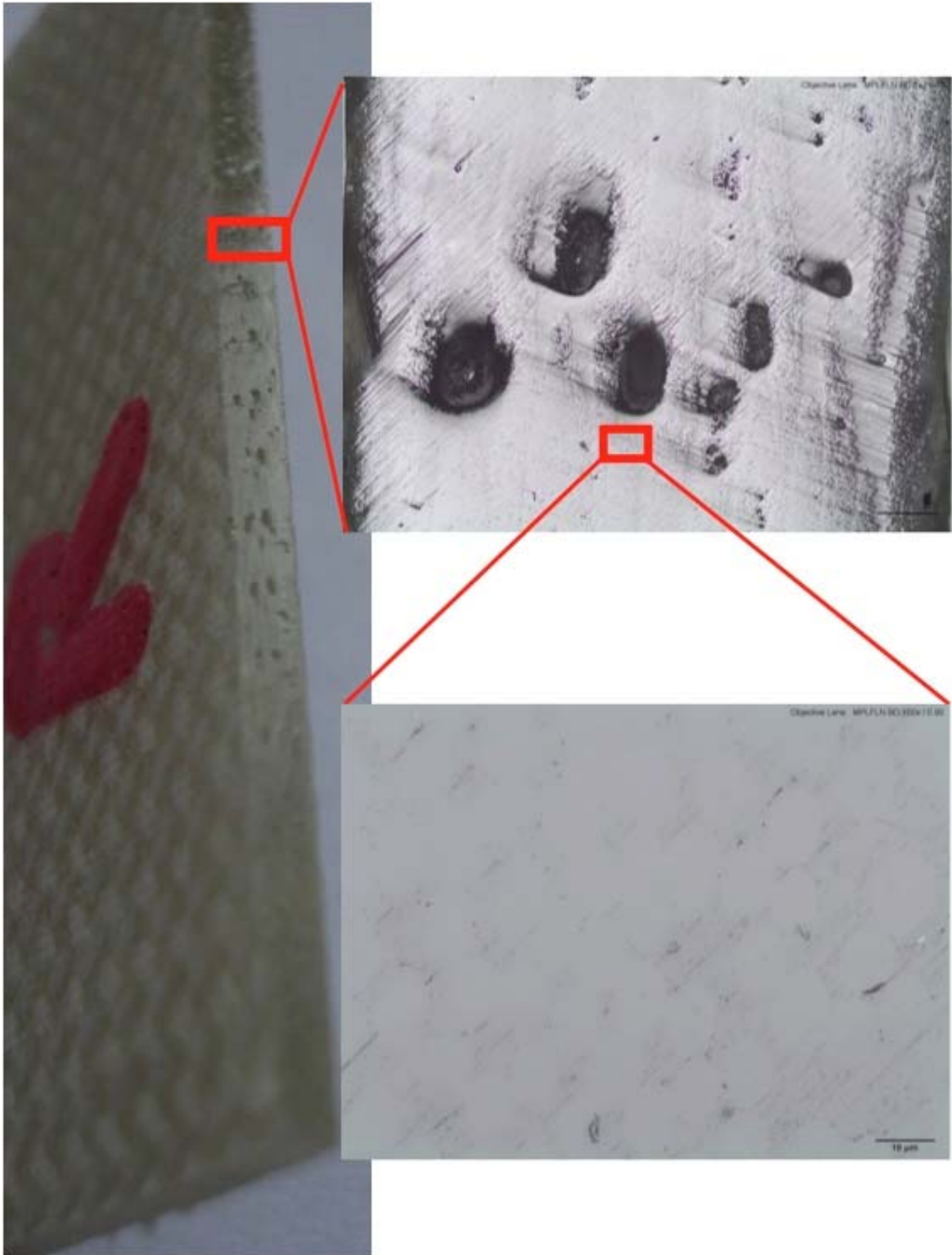
Figure A-9: GFRV Panel Q (Accelerated at 30°C) Microscopy

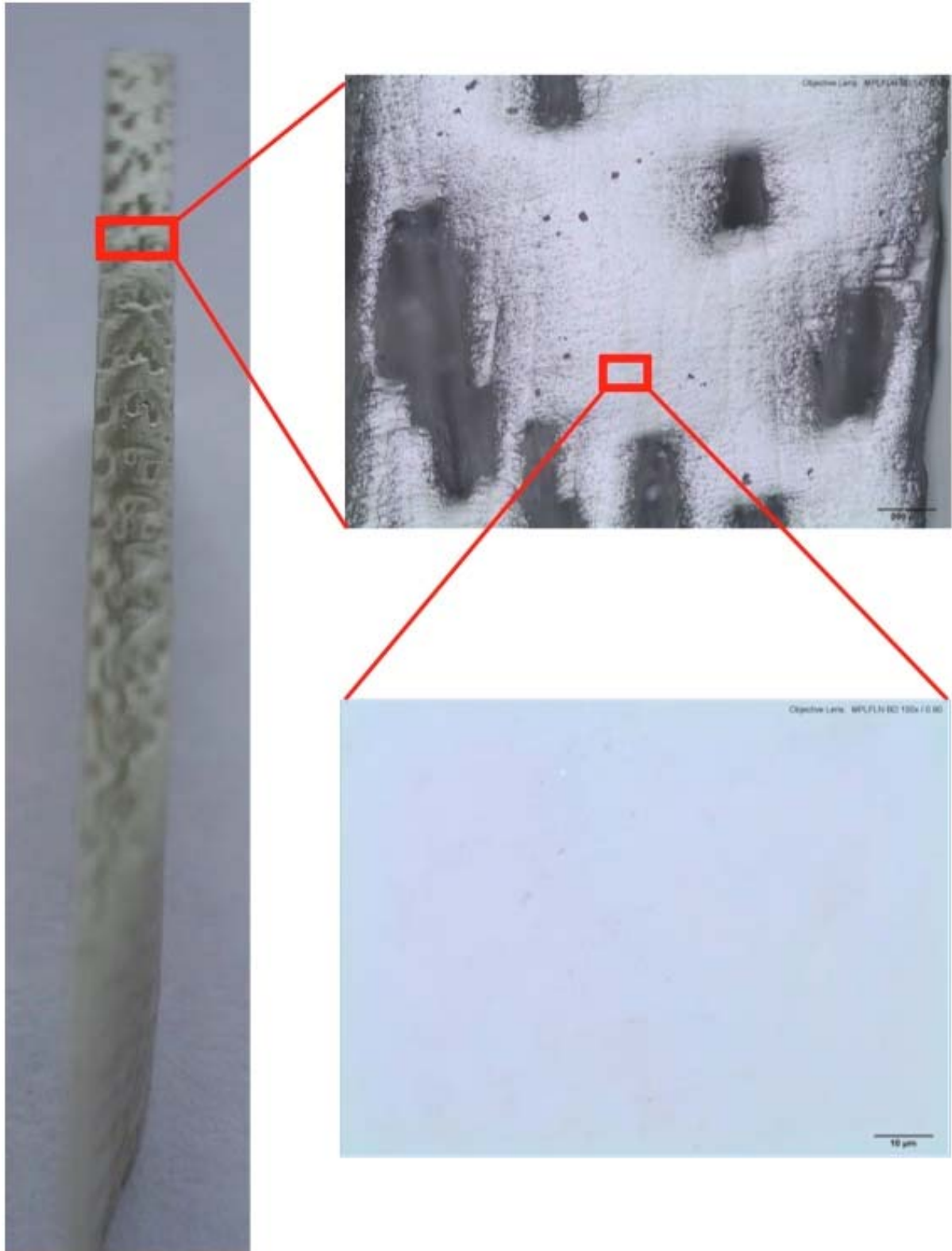**Figure A-10: GFRV Panel R (Accelerated at 40°C) Microscopy**
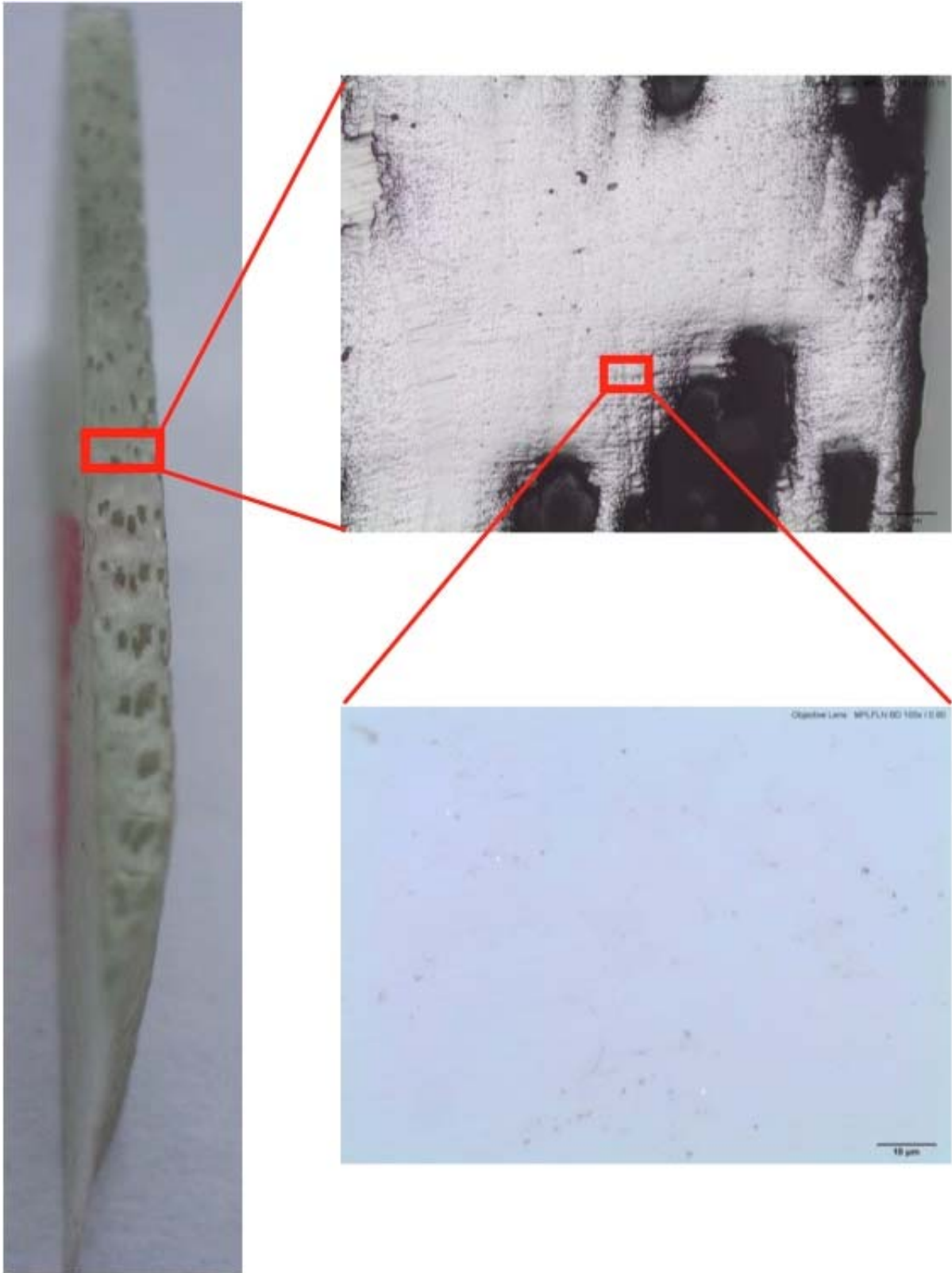
Figure A-11: GFRV Panel X (Accelerated at 50°C) Microscopy

Figure A-12: GFRV Panel Y (As-Produced) Microscopy